the ENERGY lab

DOE/NETL-2011/1478

A Comparative Study of the Mississippian Barnett Shale, Fort Worth Basin, and Devonian Marcellus Shale, Appalachian Basin

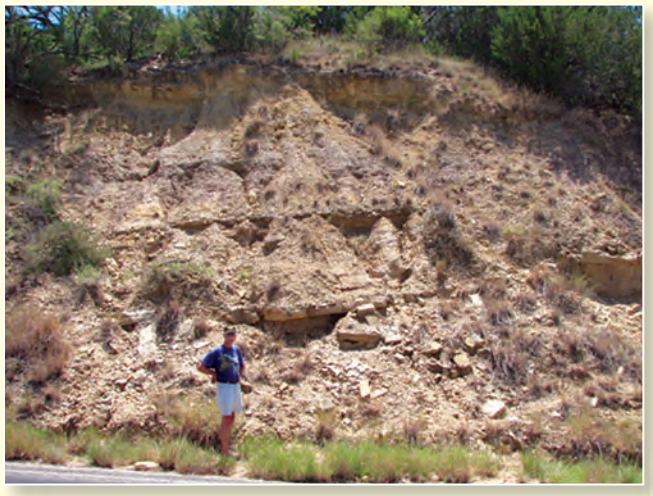

NATIONAL ENERGY TECHNOLOGY LABORATORY

U.S. DEPARTMENT OF ENERGY

DISCLAIMER

ACKNOWLEDGMENTS

The authors greatly thank Daniel J. Soeder (U.S. Department of Energy) who kindly reviewed the manuscript. His criticisms, suggestions, and support significantly improved the content, and we are deeply grateful.

Cover. **Top left:** The Barnett Shale exposed on the Llano uplift near San Saba, Texas. **Top right:** The Marcellus Shale exposed in the Valley and Ridge Province near Keyser, West Virginia. Photographs by Kathy R. Bruner, U.S. Department of Energy (USDOE), National Energy Technology Laboratory (NETL). **Bottom:** Horizontal Marcellus Shale well in Greene County, Pennsylvania producing gas at 10 million cubic feet per day at about 3,000 pounds per square inch. Photograph by Tom Mroz, USDOE, NETL, February 2010.

A Comparative Study of the Mississippian Barnett Shale, Fort Worth Basin, and Devonian Marcellus Shale, Appalachian Basin

By Kathy R. Bruner and Richard Smosna
(URS Corporation)

April 2011

DOE/NETL-2011/1478

U.S. Department of Energy

Contents

Figures

Tables

Abbreviations Used in this Report

bbl/min	barrels per minute
bcfg	billion cubic feet gas
BTU	British Thermal Unit
EUR	estimated ultimate reserves
GIP	gas in place
GOR	gas/oil ratio
HC	hydrocarbons
HI	hydrogen index (Rock-Eval)
IP	initial potential
Mcfg	thousand cubic feet gas
Mcfge	thousand cubic feet gas equivalent
MMcfg	million cubic feet gas
MMcfge	million cubic feet gas equivalent
NGL	natural gas liquids
ppt	parts per thousand
R_o	vitrinite reflectance value (in %)
S_1	thermally extractable petroleum (Rock-Eval)
S_2	petroleum generated by pyrolysis (Rock-Eval)
scfg/t	standard cubic feet gas per ton rock
tcfg	trillion cubic feet gas
TD	total depth
TFHL	theoretical fracture half-length
Tmax	maximum temperature S_2 (Rock-Eval)
TOC	total organic carbon

A Comparative Study of the Mississippian Barnett Shale, Fort Worth Basin, and Devonian Marcellus Shale, Appalachian Basin

By Kathy R. Bruner and Richard Smosna
(URS Corporation)

1.0 EXECUTIVE SUMMARY

1.1 Purpose

Many exploration and production programs are based on analogy with known successful plays. For example, the 1981 Barnett discovery well was tested only because of its encouraging well-log character compared to the Devonian Shale play of the Appalachian Basin (Steward, 2007). Some drilling programs, on the other hand, emphasize the individuality of any particular play. In this vein, the distinctive mineral composition, organic content, maturity, and mechanical properties of the Marcellus may make this reservoir unique among gas shales (Wells and Gognat, 2009; Berman, 2009). Perhaps to be expected, a review of the published literature indicates that the Barnett and Marcellus Shales share a number of critical geological and engineering features, but they also exhibit several important differences. And within each play there exists a large variability in drilling results, from one geographic area to another and from one company to another. In truth, a thorough knowledge of key characteristics of the two formations—such as similarities and/or dissimilarities in rock type, hydrocarbon potential, ability to fracture the shale, and sweet spots—will aid operators in both the Fort Worth and Appalachian Basins.

This present study compares and contrasts critical geological characteristics of the Barnett and Marcellus Shales and successful engineering practices used in drilling and stimulation. Specific topics include stratigraphy, structure, and lithofacies; organic carbon content, thermal maturity, and reservoir characteristics; fracture stimulation, horizontal drilling, and well performance. With this knowledge, producers in both regions should better understand the controls on gas volumes and distribution, those reservoir properties that influence gas production, and how drilling and stimulation techniques can be more effective in the future.

1.2 Summary

In terms of geology, the Barnett and Marcellus are remarkably alike. Both shales accumulated in a foreland basin created along the convergent margin of tectonic plates. The basins are bordered by a prominent thrust belt (Ouachita/Appalachian), structural arch (Bend/Cincinnati), and Precambrian uplift (Llano/Adirondack). They have an asymmetrical form, in that the structurally deepest axis lies immediately adjacent to the thrust front, and the strata shallow gently toward the opposite arch. A number of basement structures were reactivated during orogenic deformation, including major faults (Mineral Wells and Newark East/Rome and Clarendon-Linden) and arches (Bend and Lampasas/Cincinnati and Waverly) that influenced thickness patterns of the shale and overlying formations. After shale deposition, each basin filled with approximately 10,000 feet of post-orogenic sediments.

The stratigraphic composition of both units consists of organic-rich shale and limestone, and the formations are divided into a lower shale member, a middle limestone (perhaps two in the Marcellus), and an upper

shale member. Specific rock types of the Barnett Shale are dense, organic-rich, soft, thin-bedded, petroliferous, fossiliferous shale and hard, black, finely crystalline, petroliferous, fossiliferous limestone. Similar rock types of the Marcellus include splintery, soft to moderately soft, gray to brownish black to black, carbonaceous, highly radioactive shale with beds of limestone and carbonate concretions. The mineral composition, too, is reportedly similar (Table 1). Geologists in both basins routinely identify rock types, and particularly the black shale, by well-log values, such as a gamma-ray reading of greater than 150–200 API units or a bulk density less than 2.40–2.50 g/cm^3.

Both foreland basins were occupied by a narrow, restricted seaway bordered on the foreland side by a shallow-water carbonate platform (Chappel Limestone/Delaware Limestone). Marine upwelling contributed to algal blooms (radiolarians/*Tasmanites*) in the biologically-productive surface water. In the deep ocean, however, circulation was poor, the water column stratified, and bottom water was anaerobic to dysaerobic. Increased tectonic loading in the nearby thrust belt led to a rapid deepening of the basin, and water depth reached 550–700 feet/ft (Barnett) or 300–1,000 ft (Marcellus). In this environment hemipelagic mud and pelagic skeletal tests—the black-shale facies—accumulated on the sea floor. Sometime after deposition of the Barnett (following the Marble Falls Formation) and immediately after deposition of the Marcellus, coarser-grained deltaic sediments (Bend Formation/Mahantango Formation) prograded across the basin from the orogenic belt and buried these black shales.

Geological differences are limited but significant. The Fort Worth Basin was bordered on its outboard side by an island-arc system which supplied very little coarse-grained sediment to the Barnett Shale. On the other hand, the Appalachian Basin was bordered on its outboard side by a newly raised tectonic highland. Thus, in that direction the Marcellus Shale contains coarse-grained clastics of nearshore environments: gray, silty and calcareous shale and sandstone. Contemporary volcanic eruptions deposited the Tioga Ash at or near the base of the Marcellus. Limestone interbeds in the Barnett (including the middle Forestburg Member) formed as mass-gravity or turbidity flows of skeletal material derived from surrounding carbonate platforms. Immediately after black-shale deposition, a temporary expansion of the western carbonate produced the overlying Marble Falls Formation. Limestone interbeds in the Marcellus (such as the Purcell and Cherry Valley Members) were produced by a fall of sea level and temporary aerobic conditions.

Only one set of natural fractures (strike 100–120°) is recognized in the Barnett. Fractures tend to be mineralized, especially near major faults, and may be wider and more common in limestone interbeds. They formed by tectonic movements associated with the Ouachita Orogeny. In contrast, an orthogonal set of natural fractures (striking 60–75° and 315–345°) occur in the Marcellus. In outcrop the fractures are generally open, and they do not penetrate carbonate beds or concretions. They are thought to have formed by natural hydraulic fracturing when the shale was buried 4–5 km deep and generating hydrocarbons.

The presence of karst in the underlying Ellenburger Group results in high-angle normal faults, karst fault-chimneys, and local subsidence features in the Barnett Shale. The karst fault-chimneys occur at a spacing of about one per sq mi, range from 20–200 acres in size, and commonly extend through the stratigraphic section from the underlying unconformity up to the Bend Formation. Similar karst-influenced structures are absent in the Marcellus.

The Appalachian Basin may have contained several subbasins during the time of Marcellus Shale accumulation, leading to discontinuous deposits across the central basin area. Because of the subsequent Allegheny Orogeny, the Marcellus experienced extensive post-depositional deformation, such as the development of pencil cleavage, cleavage duplexes, and complex folding that is not present in the Barnett.

Table 1. Typical mineral composition for the Barnett and Marcellus Shales.

Mineral	Barnett (percent)	Marcellus (percent)
Quartz	35-50	10-60
Clays, primarily illite	10-50	10-35
Calcite, dolomite, siderite	0-30	3-50
Feldspars	7	0-4
Pyrite	5	5-13
Phosphate, gypsum	trace	trace
Mica	0	5-30

In terms of basic reservoir characteristics, the Barnett and Marcellus are practically identical.

- porosity approximately 6%.
- permeability measured in microdarcies to nanodarcies, affected by the presence of liquid hydrocarbons.
- water saturation around 20–30%, water bound to clay minerals, no free water.
- gas saturation around 70–80%, gas stored in interstitial pores and microfractures and adsorbed onto solid organic matter and kerogen.
- adsorbed gas as low as 20–25% or as high as 40–60%.
- normally pressured to slightly overpressured (0.46–0.52 psi/ft) although the Marcellus is underpressured in a large area of the play (0.10–0.35 psi/ft).
- formation pressure 3,000 to 4,000 psi where the gradient is normal.
- drilling depth 4,000–8,500 ft (Barnett) and 2,000–10,000 ft (Marcellus).

In terms of hydrocarbon generation, differences between the Barnett and Marcellus are more pronounced. Gas in place (GIP) is estimated at 140–200 billion cubic feet of gas per square mile (bcfg/sq mi) or 170–250 standard cubic feet of gas per ton (scfg/t) for the Barnett Shale, and 20–150 bcfg/sq mi or 60–100 scfg/t for the Marcellus.

Total GIP for the play is perhaps 390 trillion cubic feet of gas (tcfg) for the Barnett and 500 tcfg for the Marcellus. Regardless, the underlying principle of exploration and drilling programs in both basins is that critical geological-petroleum characteristics parallel the regional trends of depositional environment, basin structure, thermal maturity, and subcropping formations.

On the basis of unit surface area of the play (bcfg/sq mi), the Barnett has an in-place gas volume 30 to 100 % greater than that of the Marcellus. Gas volume is a function of several shale attributes including organic richness, kerogen type, thermal maturity, gas expulsion, and formation thickness, and in an overall sense conditions were more favorable in the Barnett.

1. The total organic carbon (TOC) content varies from 2–12% in both formations and is greater in the lower member. Typical TOC values, however, are 2–6% for the Barnett and 2–10% for the Marcellus, that is, in general the Marcellus is organically richer.

2. Barnett kerogen is type II with a minor admixture of type III, whereas Marcellus kerogen has a slightly greater mixture of type III. Because type II kerogen generates a greater quantity of hydrocarbons and at a lower temperature, the conversion of Barnett organic matter to natural gas was probably a more effective process.

3. Thermal maturity of the shale in both the Fort Worth and Appalachian Basins is attributed to post-depositional burial beneath Upper Paleozoic strata (which increases more-or-less uniformly across each basin) and to hydrothermal heating in and around deep-seated faults (which causes local highs around the fault). The Barnett vitrinite reflectance value (R_o) marking the beginning of dry gas ($R_o = 1.2$) is considerably lower than usual (Marcellus $R_o = 1.6$), and attributed to chemical interactions between petroleum, kerogen, and clay minerals in the shale or to a slow geological heating rate. Although maximum vitrinite reflectance values for the Marcellus are higher (1.7/3.5), reflecting a higher paleotemperature, the transformation ratio (amount of kerogen converted to hydrocarbons) is about the same: Barnett—32% where immature to 93% where late mature to post mature, and Marcellus—over 90% where post mature.

4. Calculations of hydrocarbon expulsion from the two shale formations encompass a great uncertainty, but estimates of gas loss by primary migration are less for the Barnett (20–60%) than for the Marcellus (54% or more).

5. The Barnett's thickness ranges from 50–1,000 ft whereas that of the Marcellus, from a feather edge to 660 ft. In summary GIP seems to be greater in the Barnett because it contains more type II kerogen, is thicker, and has lost less gas to expulsion.

The core area of the Barnett Shale is delineated by $R_o \geq 1.1$ and the presence of underlying and overlying frac barriers (Viola-Simpson and Marble Falls Formations). The entire gas-shale play is defined by the geographic extent of the shale to the east and north and a minimum thickness of 100 ft to the west. The core area of the Marcellus is marked by $R_o \geq 1.6$, the presence of an underlying frac barrier (Onondaga Limestone), and a minimum thickness of 50 ft. The entire gas play is defined by the geographic extent of the shale. Total gas in place for the Marcellus play may be 25% greater (390 tcfg/500 tcfg). This reversal from a higher Barnett GIP based on unit surface area is because of the very much larger area of the Marcellus gas-shale play (9,000 sq mi/75,000 sq mi). Vitrinite reflectance values, which in large part establish a most important border of the core area in both basins, can be suppressed; that is, they may underestimate the degree of thermal maturity and maximum paleotemperature (suppression is seemingly related to kerogen type, amount, and diagenesis). Suppression would mean that the core's boundary line for dry gas in both plays would shift to the west some considerable distance.

Many of the drilling and stimulation techniques applied in the Marcellus play, primarily slickwater fracture treatment and horizontal drilling, were first developed and then perfected in the Barnett.

The Barnett and Marcellus plays have become so very successful because their beds of siliceous shales behave in a brittle fashion and fracture easily. Fractures drain a very small volume of rock, apparently just a few feet; hence, a long and wide fairway must be established between natural and artificial fractures. Well stimulation generates geometrically complex fairways (with many fractures in multiple orientations) which can be mapped by tilt meters and microseismic geophysics. Fairways in the Barnett Shale are characteristically square to rectangular in shape, 1,500–3,000 ft long, and 400–1,000 ft wide. The artificial fractures orient themselves with today's natural stress system and are generally perpendicular to the set of prominent natural fractures.

A typical slickwater frac in the Barnett Shale consists of 500,000–6,000,000 gal fresh water (higher volumes in horizontal wells) with friction-reducing additives, 80,000–1,000,000 lb sand proppant (greater weights in horizontal wells), and a pumping rate of 50–100 barrels per minute (bbl/min). 20–70% of the injected frac fluid is returned over 2–3 days or more up to the life of the well (shorter period reflects better completion technique). Lower and upper shale members of the Barnett are treated either in combination or individually (however a longer fracture fairway develops with the latter). Re-stimulation by slickwater treatment is accomplished after several years of production, connecting additional reservoir rock to the borehole and sometimes exceeding the original initial production.

A typical slickwater frac in the Marcellus Shale consists of 100,000–850,000 to as much as 4,000,000 gal water (higher volumes in horizontal wells), 250,000–750,000 lbs sand proppant, and a pumping rate of 30–100 bbl/min. About half of the frac fluid remains in the reservoir after cleanup. Refracture treatment can use 25% more frac fluid than the original stimulation.

The role of natural fractures is highly debated in both basins. Do natural fractures contribute significantly to gas production? What are their height, aperture size, and density in the subsurface? What specific rock properties control fracture density? Do open natural fractures exist in the subsurface, or are they mostly healed? Are natural fractures open and unmineralized away from major faults? Do open natural fractures inhibit the growth of induced fractures? Do natural fractures in the middle limestone connect upper and lower shale members? Are healed fractures unresponsive to well stimulation, or do they serve as zones of weakness during treatment? Answers to these important questions are often contradictory.

Fracture barriers are necessary in the stratigraphic section to control the height of the fracture so that stimulation energy is not conducted away from the shale (which would reduce the efficiency of well stimulation) and to keep the induced fractures from intersecting any nearby water-bearing unit (water entering the shale formation from adjacent stratigraphic units would severely decrease gas production). Water encroachment into the Barnett from the underlying Ellenburger Group can be a significant problem, but water movement into the Marcellus from the Oriskany-Huntersville Formations is poorly understood at present. Dense limestones typically have a higher fracture threshold than the shale; these rocks are not prone to fracture at the gradients required to fracture the shale, and with proper stimulation design they should serve as an excellent fracture barrier. Suitable limestone barriers exist beneath the Barnett and Marcellus (Viola-Simpson Formations/Onondaga-Selinsgrove Limestones) and above (Marble Falls Formation/Tully Limestone). Thick siltstones and limestones in the Mahantango Formation may also be a barrier above the Marcellus. Additionally middle limestone members (Forestburg/Purcell and Cherry Valley) can serve as a frac barrier within the formation, effectively separating the upper and lower shale members. The sweet spot of gas production is identified in part by the presence of these barriers, and where they are absent, the drilling risk is considered to be higher.

Horizontal wells are drilled for a number of reasons: to increase reservoir exposure to the borehole, to drain several parallel sections of the reservoir thus increasing the overall drainage area, to reduce the chance of fractures breaking into an adjacent water-bearing formation, and to minimize disturbance to surface structures. In addition such wells generally yield a higher initial potential and estimated ultimate recovery

In the Barnett Shale wells are commonly drilled normal to the expected propagation direction of the hydraulically induced fractures. The length of horizontal laterals can reach 5,000 ft although the optimum is about 2,500–3,500 ft. At a close well spacing (30 acres), fracture treatments overlap and per-well reserves fall. Wells with a shorter lateral require a single stimulation and the casing is uncemented; however unstimulated gaps may remain in the reservoir. Wells with greater lateral length require multiple-stage stimulation and the casing is cemented; however problems may develop with fracture initiation. If the spacing of perforation clusters in a multiple-stage stimulation is too close, a stress shadow can restrict fracture growth in the middle cluster; fracture growth will then be disproportionately higher in the heel and toe. The optimal cluster spacing to reduce fracture interference is 1.5 times the fracture height (which is typically 300–400 ft). To reduce the probability of creating multiple competing fractures, the cluster length should be less than 4 times the wellbore diameter (that is, less than 4 ft). A cement system (preferably acid-soluble) isolates the annulus between perforation clusters and facilitates the creation of independent hydraulic fractures at each cluster. Utilizing a cross-linked gel and 100-mesh sand in the pad stage of treatment produces fewer and wider dominant fractures, which improves the ability to disperse later proppants in the region around the borehole.

In the Marcellus Shale horizontals are oriented to intersect permeable natural fractures with either the borehole or the induced fracture network. Laterals are usually drilled with an inhibited, water-based mud although some operators use oil-based mud for its compatibility with the shale and to increase the penetration rate. Laterals extend for 2,000 to 6,000 ft. Multiple stages with cemented production casing are required to fracture-perforate the shale (generally 4 to 8 stages) because sufficient pressure cannot be maintained to induce fractures over the complete lateral. One variation involves an open hole with isolation by mechanical packer in conjunction with fracture-stimulation-initiation sleeve. An example of a sequenced hydraulic fracture treatment is: *acid treatment* to clean drilling mud from around the borehole and initiate the fracturing process; *slickwater pad* to fill the borehole and open the formation for friction-reduction purposes and to facilitate the flow and placement of the proppant farther into the fracture network; *fine-proppant succession* with an increasing concentration of proppant to carry fine sand deep into the induced fractures; *coarse-proppant succession*; and finally *flushing* with fresh water to remove excess proppants. Simultaneous fracs and zipper fracs between neighboring horizontals have proven successful in preventing communication between the fracture fairways and to maximize borehole contact with the reservoir.

Increasingly, horizontal wells are drilled to the Barnett and Marcellus because of their higher initial potential, higher estimated ultimate recovery, lower finding-and-development cost, shallower decline curve, and better rate of return (Table 2). The plain attraction is that a horizontal well may cost approximately 2–3 times that of a vertical, but the initial potential can be 3–4 times as much. Moreover, complete development of a property may require 4 or more vertical wells compared to 1 horizontal, or 16 vertical wells compared to one multiwell pad for horizontals. Good horizontal wells tend to be very good.

Table 2. Comparison of gas volumes and well costs between a vertical and horizontal well in the Barnett and Marcellus Shales[1].

[tcfg, trillion cubic feet of gas; bcfg, billion cubic feet of gas; Mcfg/d, thousand cubic feet of gas per day; %, percent; <, less than; --, no data available]

	Barnett		Marcellus	
	Vertical well	Horizontal well	Vertical well	Horizontal well
Undiscovered, technically recoverable gas, tcfg	39		50	
Well spacing	27-55 acres		40 acres	160 acres
Initial potential (IP), Mcfg/d	700-1,000	1,600-2,500	<1,000	1,400-9,000
Estimated ultimate reserves (EUR), bcfg	0.7-1.0	2.4-3.5	0.2-0.4	0.6-3.5
Recovery efficiency	7-12%; 12-20% with closer well spacing and shorter laterals; up to 20% with refrac		10%; 18-20% with refrac	
Production decline	60-65% first year	50-55% first year	--	67% first 105 days
Well cost	$1,000,000	$2,000,000	$800,000 to $1,800,000	$3,000,000 to $4,000,000
Finding and development cost, per Mcfg	$1.71	$1.06	--	$1.34

[1] From various sources.

1.3 Outcrop Photographs of Barnett and Marcellus Shales

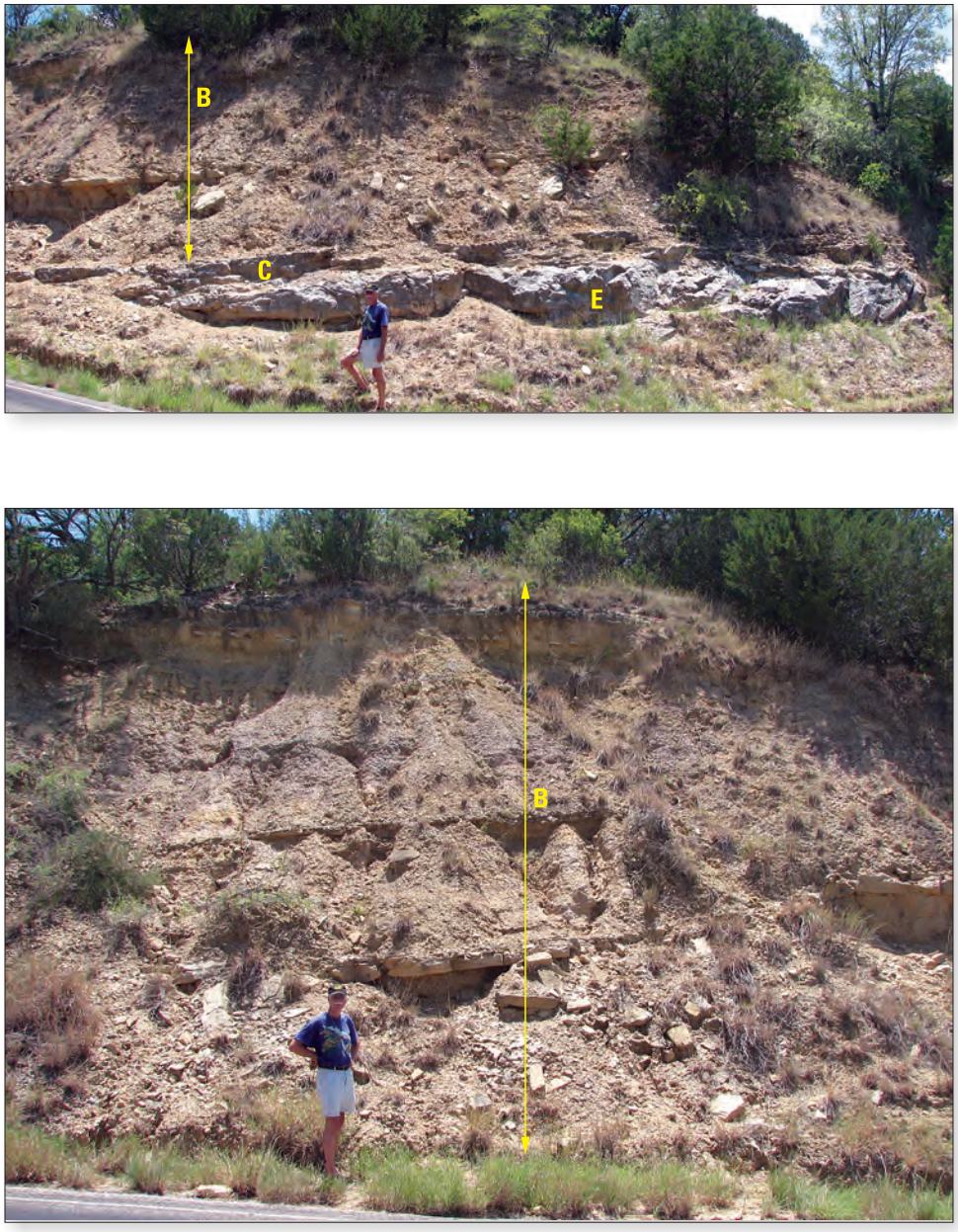

The Barnett Shale exposed on the Llano uplift near San Saba, Texas. Barnett Shale (B), Chappel Limestone (C), and dolomite of the Ellenburger Group (E).

Chappel Limestone (C) separated from Ellenburger Group (E) by unconformity.

Overlying limestone and shale of the Marble Falls Formation.

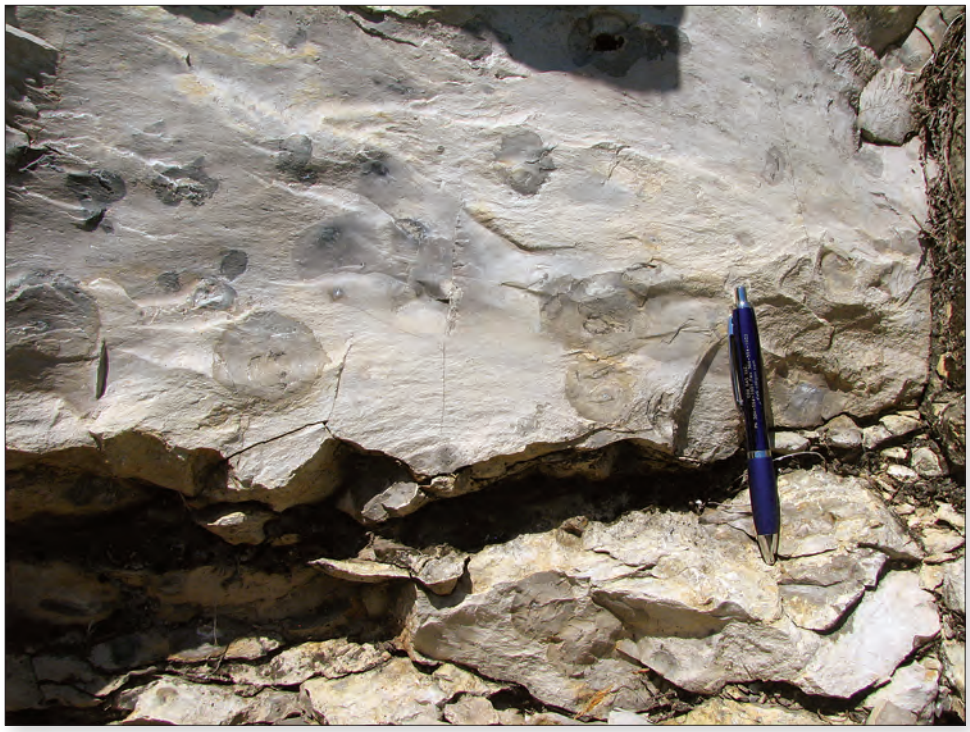

Overlying cherty limestone and shale of the Marble Falls Formation.

The Marcellus Shale exposed in the Valley and Ridge Province near Keyser, West Virginia. Vertical black shale with few limestone interbeds.

Kathy Bruner on Marcellus Shale outcrop near Bedford, Pennsylvania. Photograph by Daniel J. Soeder, DOE.

Richard Smosna examining Marcellus Shale outcrop near Bedford, Pennsylvania. Photograph by Daniel J. Soeder, DOE.

Type section of the Marcellus Shale, 1 mile south of Marcellus, New York. Photograph by Daniel J. Soeder, DOE.

Geologists swarm over Marcellus Shale exposed on a rock face in the Hanson Aggregates quarry in Oriskany Falls, New York. The flat area in the foreground where several geologists are standing is the top of Onondaga Limestone below the Marcellus Shale. Above the Onondaga, the lower, organic-rich Union Springs Member of the Marcellus Shale is about 20 feet thick in this quarry. The blocky, meter-thick Cherry Valley Limestone is visible above it. The Oatka Creek Member above the Cherry Valley has more clay and is more fissile than the Union Springs. Most of the upper part of the Oatka Creek Member is missing here. The cobble and gravelly material at the top of the exposure is glacial till from the last Ice Age, and is much younger than these rocks. Photograph by Daniel J. Soeder, DOE.

2.0 INTRODUCTION

In recent decades the production of natural gas from unconventional reservoirs in the U.S. has increased significantly. Unconventional resources include gas from tight sand, coalbed methane, and shale gas. In 2006 production of natural gas from unconventional reservoirs accounted for 43 percent of domestic gas production (8.5 trillion cubic feet of a total 18.6 tcfg), a dramatic increase from 16 percent in 1990 (2.8 tcfg of a total 17.2 tcfg; Energy Information Administration, 2008).

Of particular interest to this study are the unconventional organic-rich shales of the Fort Worth and Appalachian basins, the Barnett and Marcellus Shales respectively (Figure 1). Recent studies estimate that the two formations together may hold as much as 89 tcfg of undiscovered, technically recoverable gas—39 tcfg in the Barnett and 50 tcfg in the Marcellus (Powell, 2008; Engelder and Lash, 2008). These shale-gas systems are a continuous-type accumulation characterized by widespread gas saturation (areally extensive and charged with gas throughout), subtle trapping mechanism, a seal of variable lithology, and relatively short hydrocarbon migration distance (Roen, 1993; Curtis, 2002). Gas in these reservoirs is stored in three states: free gas in natural fractures and interparticle porosity, adsorbed gas on kerogen and clay particles, and gas dissolved in kerogen and bitumen (Schettler and Parmely, 1990; Martini and others, 1998).

Producing gas economically from shale reservoirs is challenging. In contrast to conventional reservoirs, very few shale wells can achieve commercial production without stimulation. (Those wells with unstimulated production almost always intercept well developed fracture systems.) Shale reservoirs with commercial production exhibit a wide variation in five key parameters: 1) reservoir thickness, 2) total organic carbon, 3) thermal maturity, 4) volume of gas in place, and 5) fraction of adsorbed gas. Such reservoirs, however, share the common characteristics of very low permeability and some degree of natural-fracture development, which are both controlling factors in gas producibility (Curtis, 2002). In addition, the shale serves as source rock, reservoir, and seal for the gas.

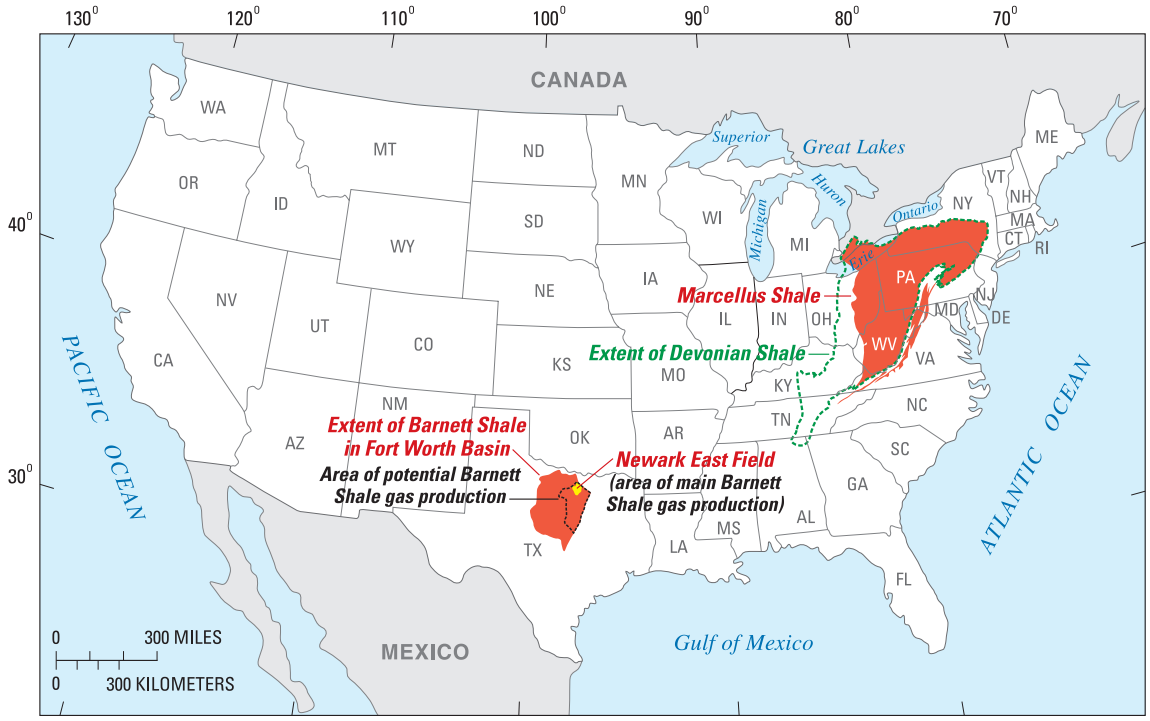

Figure 1. Location of Mississippian Barnett Shale, Fort Worth Basin, and Devonian Marcellus Shale, Appalachian Basin.

Gas exploration and production in the Barnett Shale of the Fort Worth Basin, Texas, has been ongoing for almost 30 years. Rapid growth in the play began in the mid-late 1990s with the application of economical slickwater-fracture stimulation combined with improved technology in horizontal drilling (Johnston, 2004a). Activity in the Marcellus Shale of the Appalachian Basin of Pennsylvania, New York, and West Virginia is much more recent, spanning just over 5 years. Following the proven success of slickwater-fracture stimulation in Texas, producers in the Appalachian Basin are now using the same technology for successful completions in the Marcellus.

This study describes significant geological and engineering features of the Barnett and Marcellus Shales as reported in the published literature. Many of these characteristics are well known, others are only poorly understood, and some are quite controversial. Nevertheless, with this knowledge producers in both regions should better comprehend the controls on gas volumes and distribution, reservoir properties that influence production, and how drilling and stimulation techniques can be more effective in the future.

3.0 BARNETT SHALE, FORT WORTH BASIN, TEXAS

3.1 Location

The Barnett Shale is present across the Fort Worth Basin and adjoining Bend Arch in north-central Texas (Figure 2), extending over a total area of 28,000 sq miles. The formation outcrops on the Llano Uplift at the southern margin of the basin and dips northward into the deep subsurface near the Texas/Oklahoma border. Geographic limits of the Barnett include the Ouachita Thrust front to the east, the Muenster and Red River Arches to the north, and the Eastern shelf and Concho Arch to the west (Montgomery and others, 2005; Pollastro, 2007). The gas-shale play covers roughly the eastern third (approaching 9,000 sq miles) of the entire geographic area of the Barnett.

Most Barnett production is from a limited area in the northern part of the basin where the shale is relatively thick (Montgomery and others, 2005). The Newark East field, the sweet spot of shale-gas production, covers parts of Denton, Wise, and Tarrant Counties although the entire three-county area comprises the core of the play (Hayden and Pursell, 2005). The Newark East field is currently the largest gas field in Texas covering 500 sq miles, with over 2,400 producing wells and 2.7 tcfg of proven reserves (Durham, 2005; Montgomery and others, 2005).

The play has expanded from the core area northward into Montague and Cooke Counties and immediately southward into Parker and Johnson Counties (Figure 3). Operators are also exploring in Clay, Jack, Palo Pinto, Erath, Hood, Somervell, Hamilton, Bosque, Dallas, Ellis, and Hill Counties to the west, south, and east (Johnston, 2004a; Powell, 2008). Hayden and Pursell (2005) divided the non-core area into Tier 1 counties (Johnson, Parker, and Hood) and Tier 2 (counties to the west and south) based on the present level of development and assessed risk. The biggest risks involve estimating an initial production rate, decline rate, and thermal maturity.

The core area approximately corresponds to the Greater Newark East Fracture-Barrier Continuous Barnett Shale Gas Assessment Unit (1,800 sq miles) of the U.S. Geological Survey, and Tier 1 and 2 counties approximately correspond to the Extended Continuous Barnett Shale Gas Assessment Unit (7,000 sq miles) (Montgomery and others, 2005; Pollastro, 2007).

3.2 Geological Setting

3.2.1 Fort Worth Basin

The Fort Worth Basin is one of several that formed during the late Paleozoic Ouachita Orogeny, generated by convergence of Laurussia and Gondwana (Figures 4 and 5). It was part of the foreland basin situated on the southern leading edge of Laurussia. Paleogeographic reconstructions by Gutschick and Sandburg (1983), Arbenz (1989), and Blakely (2005) depict the Fort Worth Basin as a narrow, restricted, inland seaway.

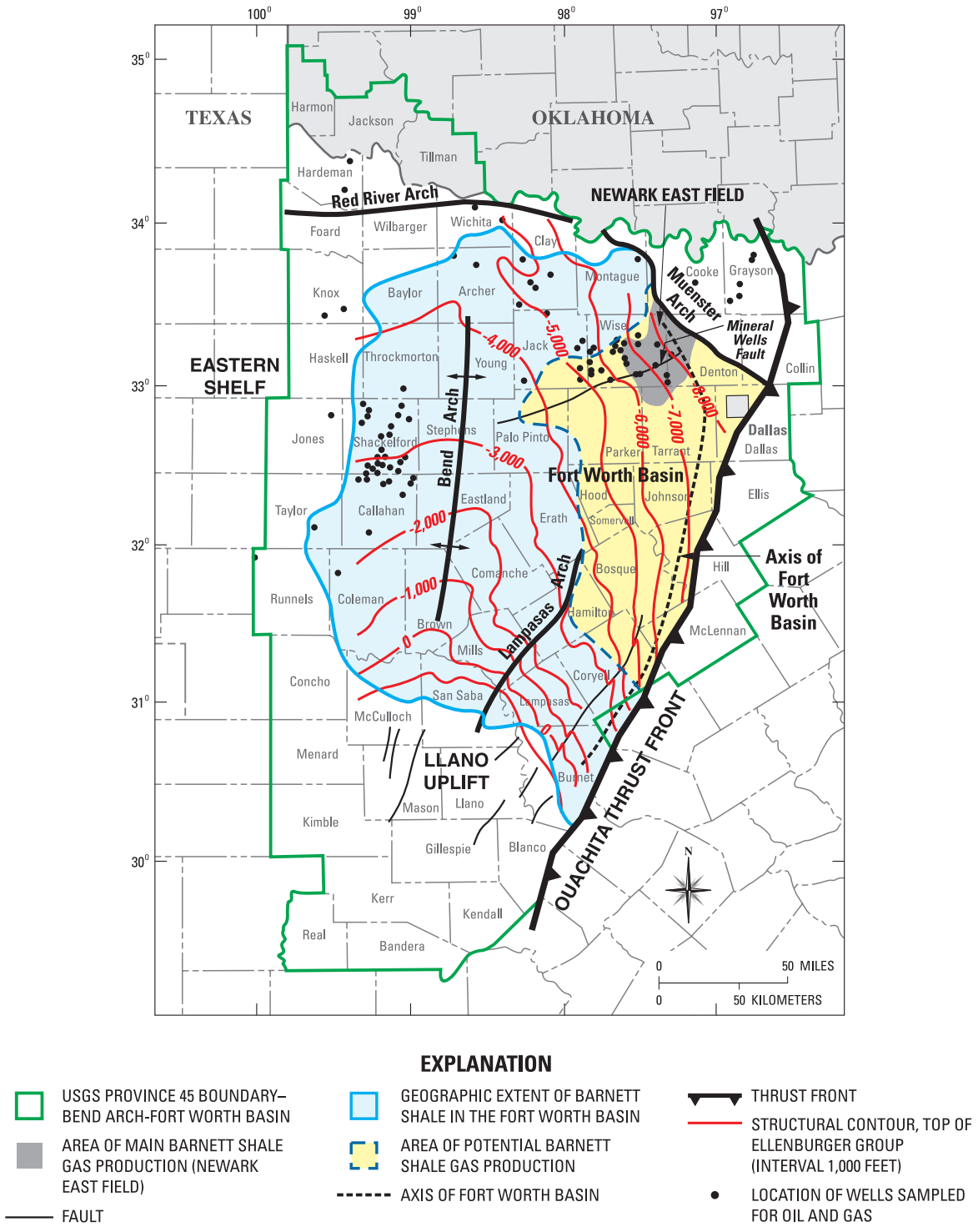

Figure 2. Fort Worth Basin showing the major geological features that influence the Barnett Shale and structural contours. The main producing area of the Newark East field is indicated by darker shading. Contours are drawn on top of the Ordovician Ellenburger Group; contour intervals equal 1,000 feet. Modified from Hill and others, 2007a, and Montgomery and others, 2005.

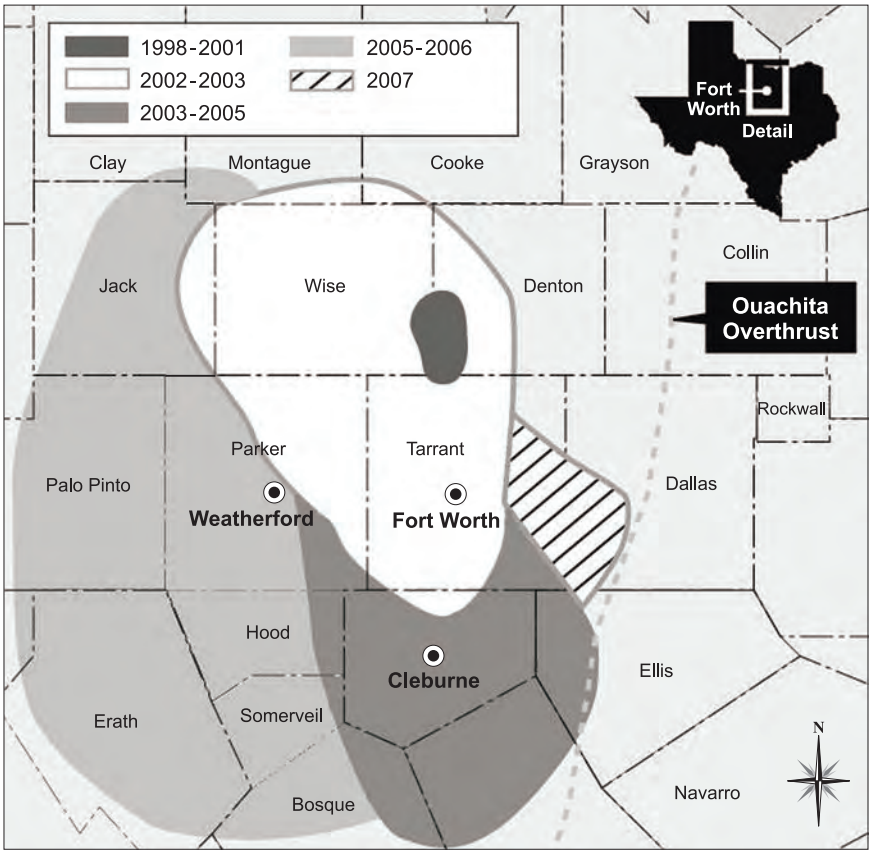

Figure 3. Stages of exploration in the Barnett Shale, 1998–2007. Modified from Barnett Shale Maps, 2007.

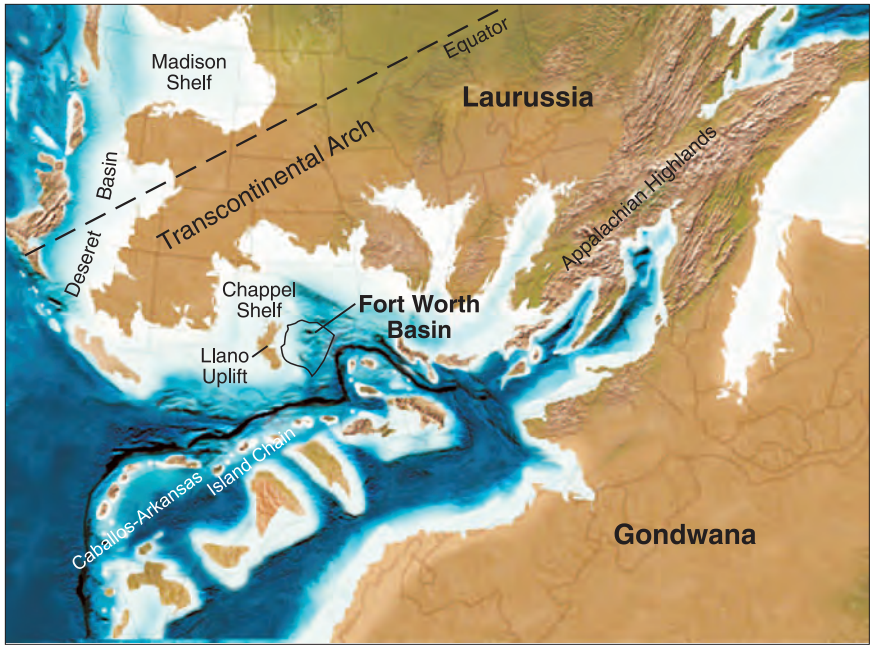

Figure 4. Regional paleogeography of the southern mid-continent region during the Late Mississippian (325 Ma), showing the approximate position of the Fort Worth Basin. Modified from Blakey, 2005; Loucks and Ruppel, 2007.

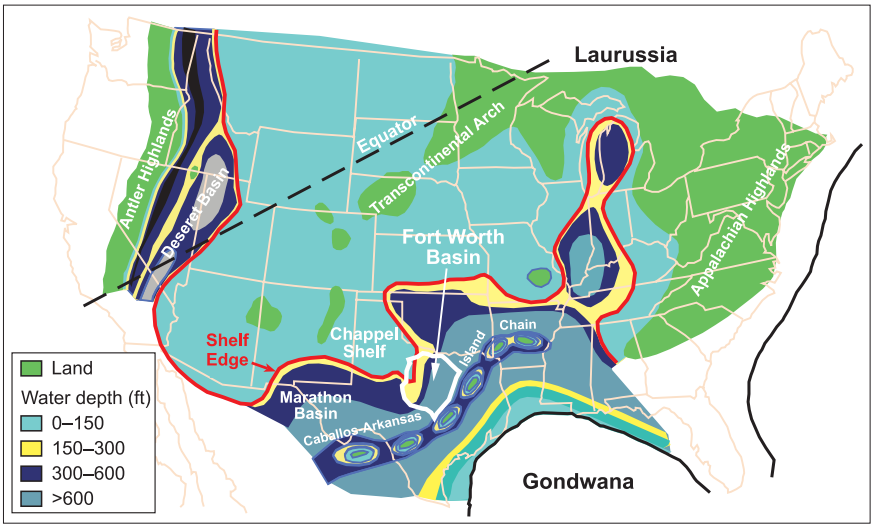

Figure 5. Middle Mississippian paleogeographic map of the United States indicating that the Fort Worth Basin was relatively deep. Modified from Gutschick and Sandberg, 1983; Loucks and Ruppel, 2007.

Today the basin is a shallow, asymmetric feature with a north-south structural axis that parallels the Ouachita Thrust front (Figure 2) (Lancaster and others, 1993). This front marks the boundary between the Ouachita thrust-and-fold deformation belt to the east and the Fort Worth Basin. The basin axis lies immediately adjacent to this thrust front, and the basin is structurally deepest in the northeast (Montgomery and others, 2005). The basin shallows gently toward positive features in the west (Bend Arch) and southwest (Llano Uplift). The Bend Arch is a shallow structural feature, whereas the Llano Uplift is a dome that exposes Precambrian and Paleozoic rocks. Farther to the west are the Eastern (carbonate) shelf and Concho Arch. To the north are two fault-bounded basement uplifts, the Muenster and Red River Arches (Loucks and Ruppel, 2007).

3.2.2 Stratigraphy

The Mississippian stratigraphic section in the Fort Worth Basin consists of limestone and organic-rich shale (Figure 6). The Barnett Shale, in particular, consists of dense, organic-rich, soft, thin-bedded, petroliferous, fossiliferous shale and hard, black, finely crystalline, petroliferous, fossiliferous limestone (Lancaster and others, 1993). It is mostly Late Mississippian in age, ranging from Osagean through Chesterian (Hayden and Pursell, 2005; Montgomery and others, 2005).

In the northeastern portion of the basin, the Barnett is divided into informal upper and lower shale members by the presence of the intervening Forestburg Limestone Member (Hayden and Pursell, 2005; Loucks and Ruppel, 2007). In addition, the shale members themselves contain a significant volume of interbedded limestone and minor dolomite in the north. The lower member can be subdivided into five distinct shale units separated by limestone beds 10–30 ft thick (Figure 7) (Johnston, 2004a), but these subdivisions are only local in extent (Kuuskraa and others, 1998). Over the Bend Arch the lower Barnett passes laterally into the Chappel Limestone (Figure 6), a crinoidal limestone with local buildups up to 300 ft (Montgomery and others, 2005). The upper shale is usually thinner than the lower member and not divided. Two typical well logs from the Newark East field (Figure 8) illustrate the general stratigraphy. The middle Forestburg Member ranges up to 300 ft (Loucks and Ruppel, 2007), but thins to a feather edge in southernmost Wise and Denton Counties (Figure 9) (Montgomery and others, 2005; Barnett Shale Maps, 2007). Where the Forestburg is absent, the Barnett is treated as a single, undifferentiated formation.

An isopach map of the Barnett (Figure 10) shows it to be less than 50 ft thick to the southwest along the Llano Uplift (Barnett Shale Maps, 2007). Because thickness-contour lines parallel the trend of the uplift, the edge of the Barnett there seems to be its depositional limit. The formation thickens to the northeast across the basin to a maximum of 800 ft near the Muenster Arch; however, several authors cite a maximum of 1,000 ft

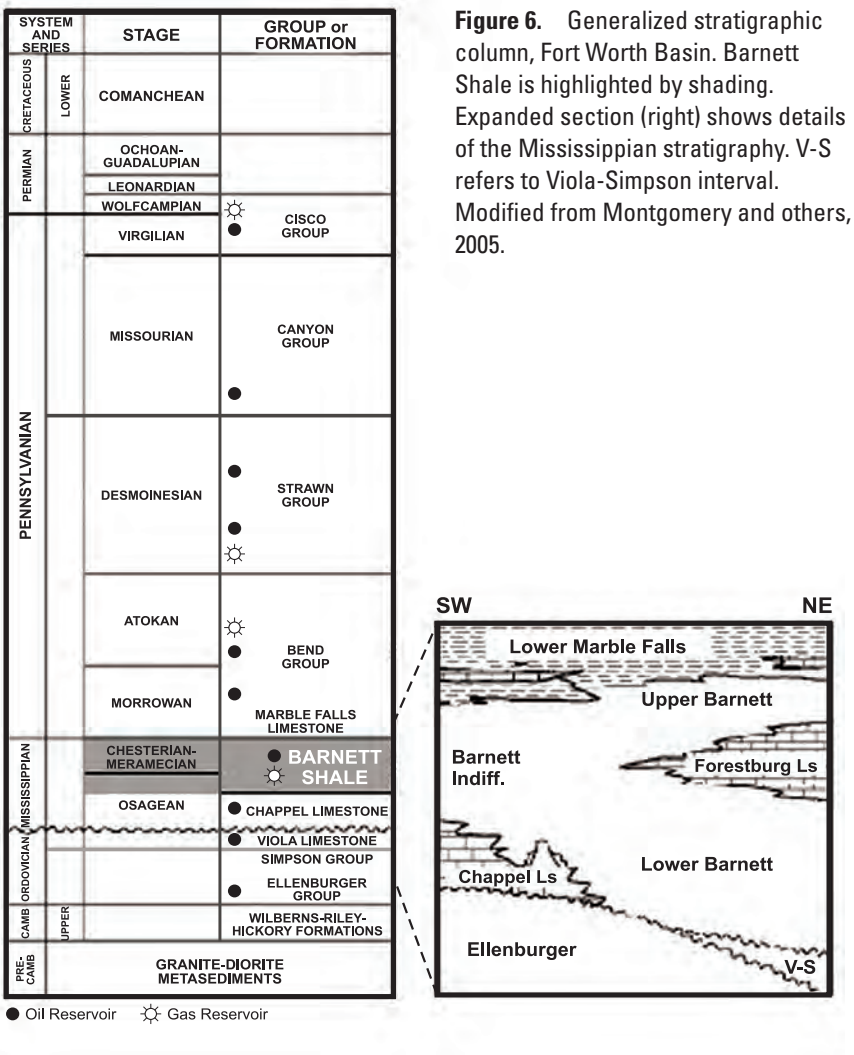

Figure 6. Generalized stratigraphic column, Fort Worth Basin. Barnett Shale is highlighted by shading. Expanded section (right) shows details of the Mississippian stratigraphy. V-S refers to Viola-Simpson interval. Modified from Montgomery and others, 2005.

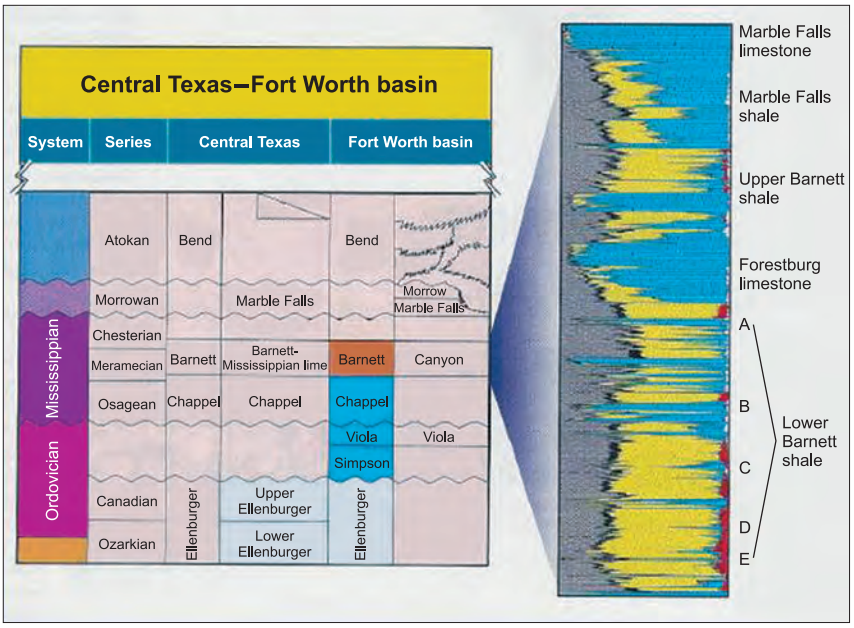

Figure 7. Lower Barnett member locally divided into 5 unit (A through E) packages of shale interbedded with limestone. Modified from Johnston, 2004a.

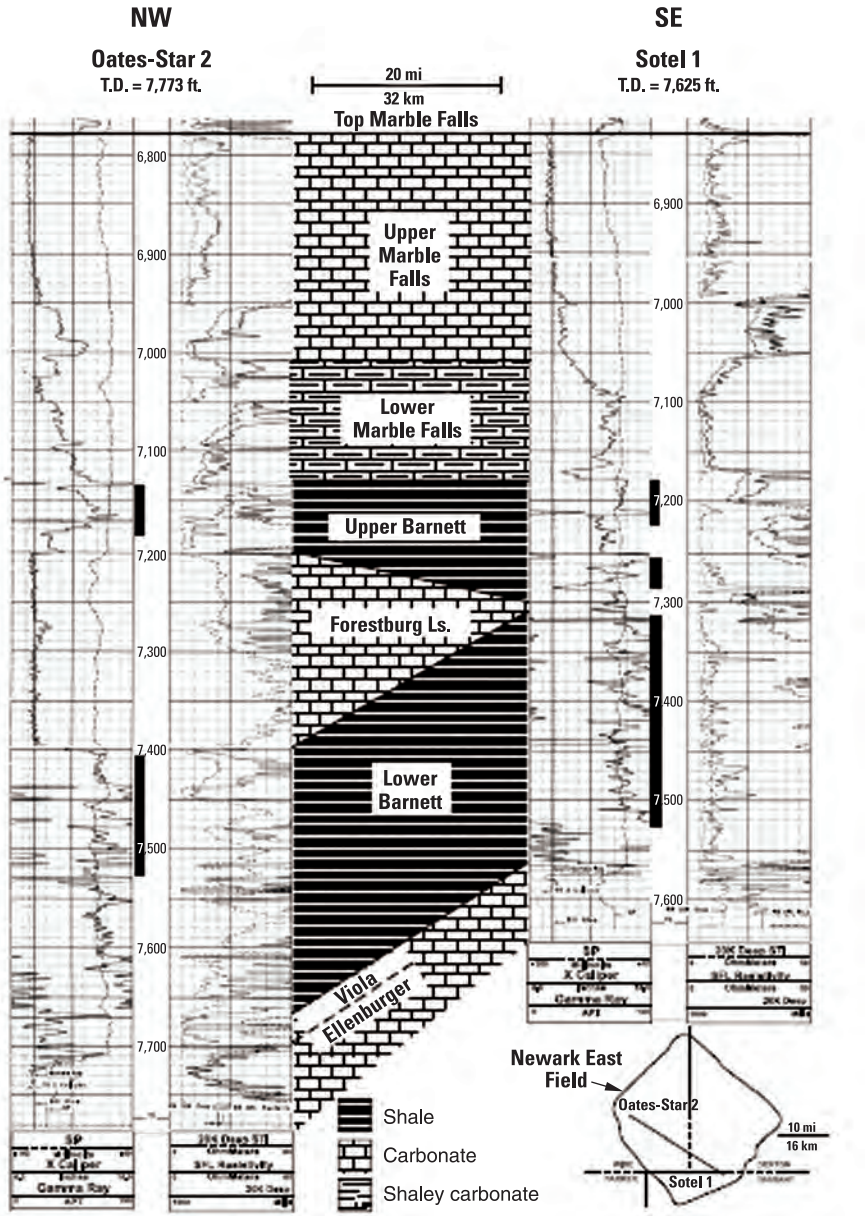

Figure 8. Two well logs in the Newark East Field. Modified from Montgomery and others, 2005.

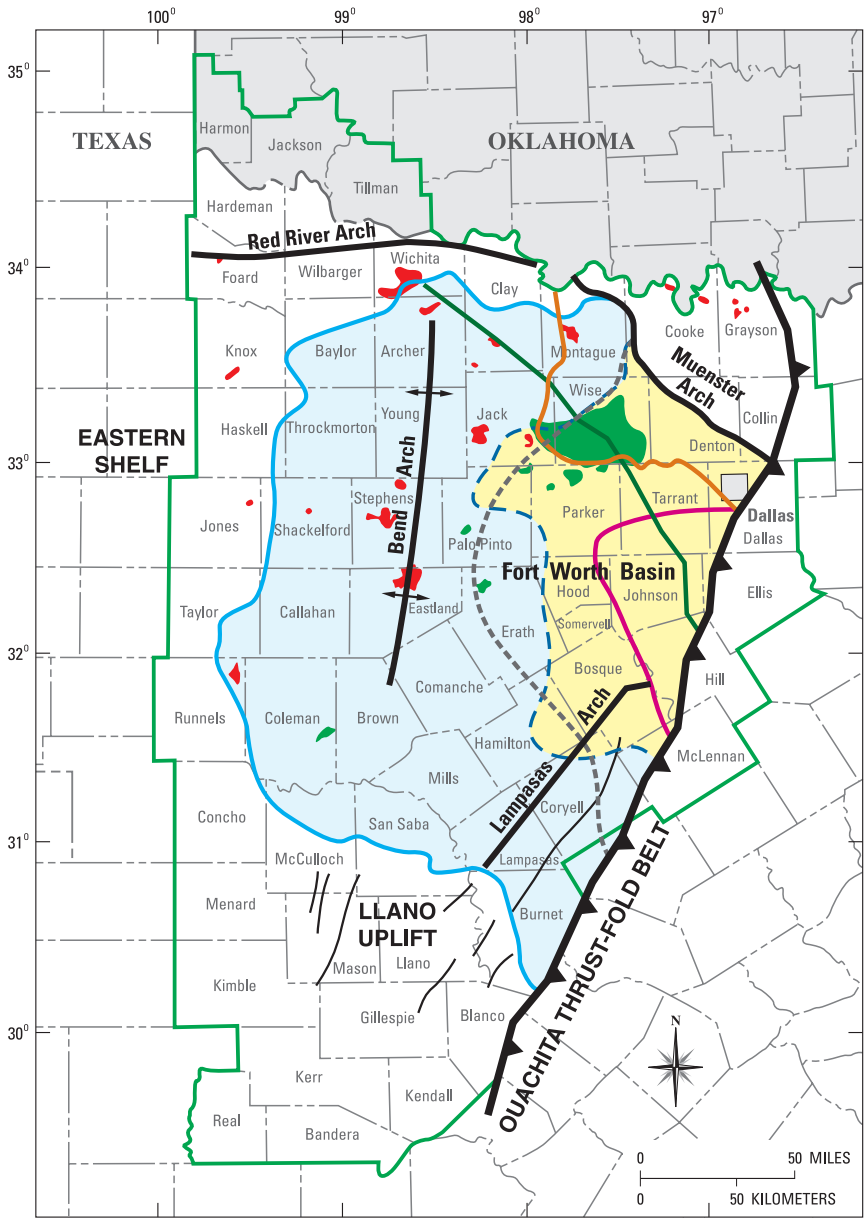

Note: Forestburg limit modified from Givens and Zhao (2005); all others modified from Montgomery and others (2005); major oil and gas reserves from Galloway and others (1983) and Kosters and others (1989). The Major Gas and Oil Reserves refer to non-Barnett production.

EXPLANATION

- USGS PROVINCE 45 BOUNDARY–BEND ARCH-FORT WORTH BASIN
- BARNETT SHALE EXTENT
- GAS WINDOW AREA (Montgomery and others, 2005)
- MAJOR GAS RESERVES
- MAJOR OIL RESERVES
- THRUST-FOLD BELT
- GAS MATURATION LINE (Givens and Zhao, 2005)
- VIOLA-SIMPSON FORMATION (absent west of this line)
- MARBLE FALLS FORMATION (absent east of this line)
- FORESTBURG LIMESTONE (absent west of this line)

Figure 9. Extent of Barnett Shale in the Fort Worth Basin and (a) pinch-out line of middle Forestburg Limestone Member in orange, (b) pinch-out line of underlying Viola-Simpson Formations in dark green, and (c) pinch-out line of overlying Marble Falls Formation in purple. Modified from Barnett Shale Maps, 2007.

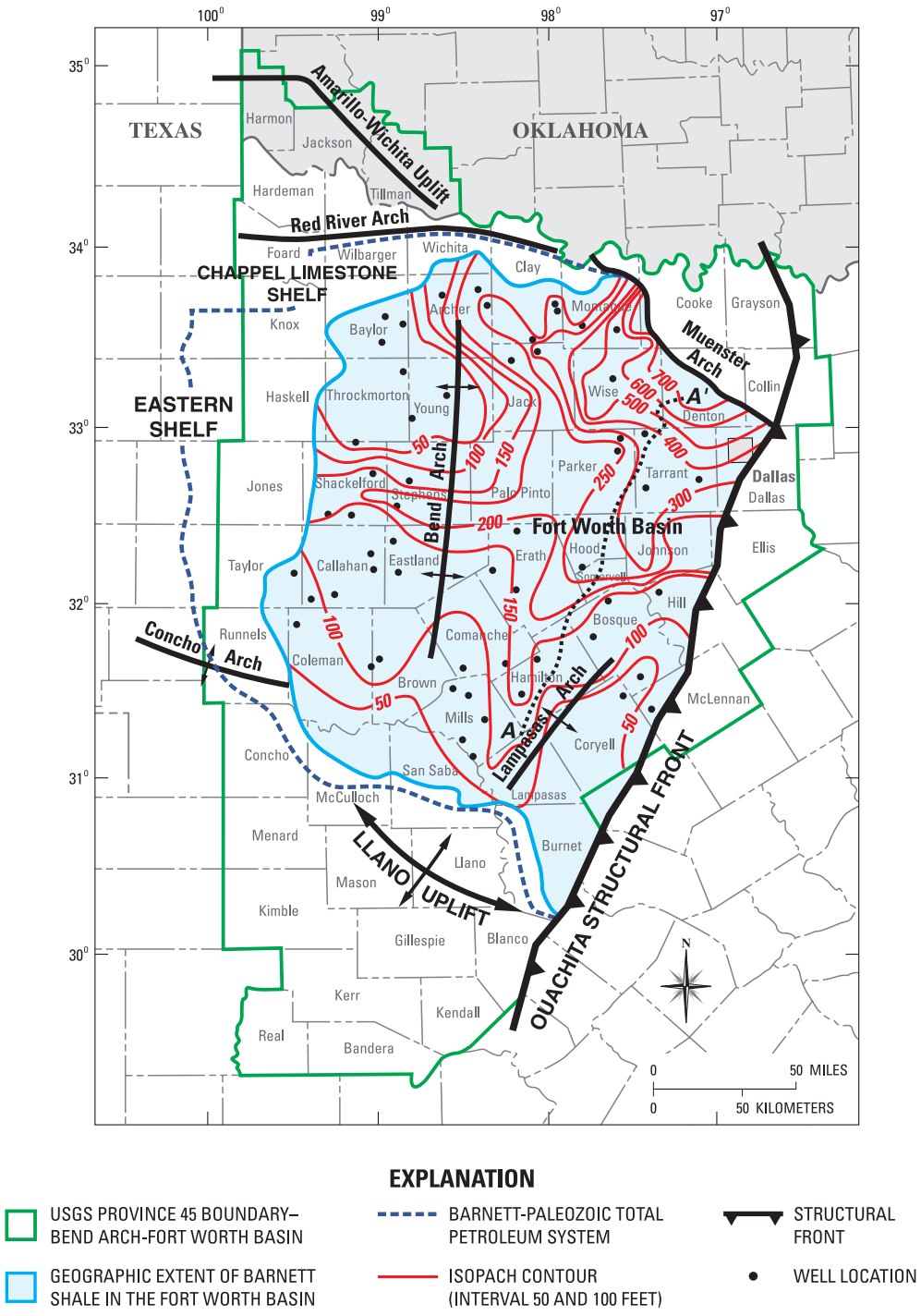

Figure 10. Thickness of Barnett Shale, isopach lines in red, contour interval equals 50 and 100 ft. Line A-A′ marks the approximate axis of deposition. Modified from Barnett Shale Maps, 2007.

(Johnston, 2004a; Montgomery and others, 2005; Loucks and Ruppel, 2007). The truncation of thickness-contour lines to the north and west by a line marking the maximum extent of the Barnett suggests that these edges must be erosional in nature (Lancaster and others, 1993). Furthermore, local thinning of the formation along the axis of the Bend and Lampasas Arches (because of erosion, nondeposition, or lateral facies change) hints that such structures were active during the time of Barnett deposition. The Barnett may also extend beneath the Ouachita Thrust belt to the east where its character is unknown (Loucks and Ruppel, 2007). A northeast-southwest line through the area of thickest Barnett (from the Llano Uplift to the Muenster Arch) marks the approximate axis of deposition (Pollastro and others, 2003).

Silurian and Devonian-age rocks are absent in the Fort Worth Basin, and the Barnett unconformably overlies Ordovician carbonate rocks. The Middle to Upper Ordovician Viola-Simpson Formations consist of dense, coarsely crystalline to micritic limestone and dolomitic limestone. The Viola also contains sandstone, anhydrite, and halite (Cheney, 1929). These strata are confined to the northeastern part of the basin (Figure 9), disappearing along an erosional pinch-out that trends northwest-southeast through Wise, Tarrant, and Johnson Counties (Figure 11) (Montgomery and others, 2005). The Lower Ordovician Ellenburger Group comprises porous dolomite and limestone with abundant chert. Everywhere its upper surface is an erosional unconformity characterized by karst, solution-collapse, and brecciated structures (Loucks, 2003). The Ellenburger occurs below the Viola-Simpson limestones in the area of the Newark East field, or directly below the Barnett Shale southwest of the Viola-Simpson pinch-out, or below the Chappel Limestone to the west along the Bend Arch (Figure 6).

Conformably overlying the Barnett is the Marble Falls Formation, mostly Pennsylvanian in age although the lowest strata may be Late Mississippian (Montgomery and others, 2005). The Marble Falls consists of a lower member of interbedded dark limestone and gray-black shale (also called the Comyn Formation) and an upper member of white to gray, crystalline limestone. The lower shale is less radioactive and contains less organic matter than that of the underlying Barnett (Montgomery and others, 2005). The Marble Falls Formation thins to the east and is locally absent around Johnson County (Figures 9 and 11) (Montgomery and others, 2005). There, the younger Pennsylvanian Bend Formation, consisting of porous sandstone and conglomerate, overlies the Barnett (Hentz and others, 2006).

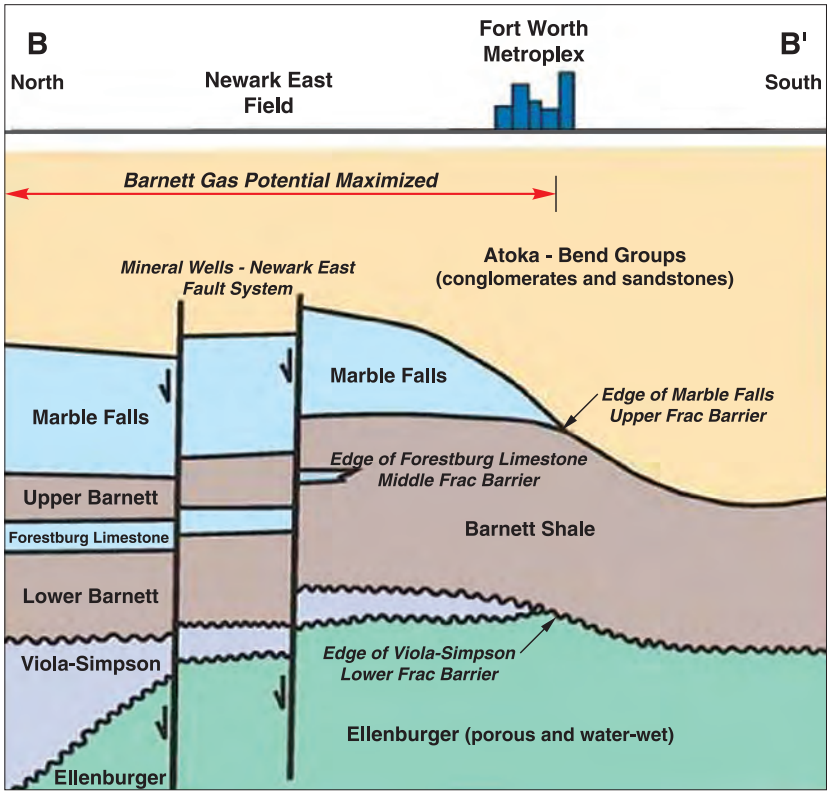

Figure 11. North-south structural cross section through the Newark East Field, showing the pinch out of stratigraphic units above and below the Barnett Shale. Modified from Barnett Shale Maps, 2007.

3.2.3 Tectonics and Structure

Geological mapping and seismic studies show that the Barnett Shale extends northward from outcrops on the Llano uplift at the southern margin of the Fort Worth Basin into the deep subsurface near the Texas/Oklahoma border (refer back to Figure 10). Figure 2 is a structural-contour map on the top of the underlying Ellenburger Group (approximately the base of the Barnett). The maximum depth of the Barnett is about 8,000 ft below sea level (drilling depth of 8,500 ft) near the Muenster Arch.

The asymmetrical, wedge-shaped Fort Worth Basin (refer back to Figure 2) is a peripheral foreland basin containing up to 12,000 feet of Paleozoic strata (Hill and others, 2007a). The Ouachita structural front to the east was created as the orogenic belt advanced westward onto the margin of Laurussia (North America). Emplacement of this deformation belt caused a gradual down warping of the pre-existing Ellenburger carbonate platform in Middle to Late Mississippian time, and the Barnett was deposited during this initial stage of basin deepening. Continued migration of the structural front through Early to Middle Pennsylvanian time resulted in the westward shift of the depocenter (Figure 12) (Thompson, 1982). Ouachita Thrust sheets may have been obstructed locally by pre-existing positive areas on the craton, such as the Llano Uplift (Thompson, 1982). Erosion of the Barnett Shale occurred around the basin margins perhaps in the Early Pennsylvanian.

Large-scale structures in and around the basin formed in conjunction with Ouachita thrusting (Figure 2). The Muenster and Red River Arches, which had formed as part of the Precambrian-Cambrian Southern Oklahoma aulacogen (Keller, 2005), were reactivated during the Ouachita Orogeny. Major basement faults define the southern margin of these two arches (Flawn and others, 1961; Montgomery and others, 2005). In particular, the flanking fault along the Muenster Arch is a down-to-the-southwest normal fault with an estimated 5,000 ft of displacement (Figure 12) (Flawn and others, 1961). The Bend Arch is a broad, north-plunging positive structure that marks the western hinge line of basin subsidence—the peripheral bulge of the Ouachita thrust-and-fold belt (Flippen, 1982). Periodic uplift of this arch from Middle Ordovician through Early Pennsylvanian time resulted in several erosional unconformities (Flippen, 1982; Pollastro and others, 2003).

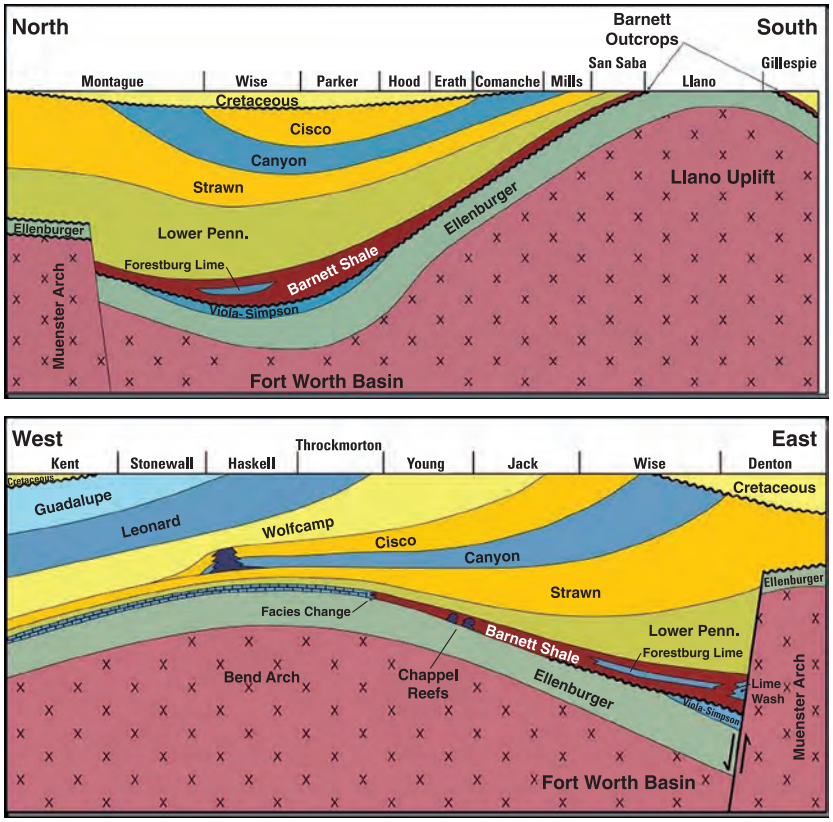

Figure 12. North-south and west-east cross sections through the Fort Worth Basin, illustrating the structural position of the Barnett Shale between the Muenster Arch, Bend Arch, and Llano Uplift. Modified from Barnett Shale Maps, 2007.

The Mineral Wells Fault and Lampasas Arch are smaller structures that lie within the Fort Worth Basin (Figure 2). The Mineral Wells Fault, which bisects the Newark East field where it joins with the Newark East fault system, is another basement structure that underwent reactivation during the Ouachita Orogeny. It is thought to have influenced thickness patterns of the Barnett Shale and overlying Bend Formation as well as the thermal history and hydrocarbon migration in the northern part of the basin (Thompson, 1982; Pollastro and others, 2003). The Lampasas Arch may be related to development of the Llano Uplift (Browning and Martin, 1982).

Also present are high-angle normal and graben faults of various orientations throughout the basin (often associated with either the Ouachita Thrust front, Llano Uplift, or Mineral Wells Fault) and minor thrust-fold structures along the eastern basin margin (Walper, 1982; Montgomery and others, 2005). Faulting and local subsidence may also be associated with karst and solution-collapse features on top of the Ellenburger Group (Gale and others, 2007). Rarely faults exhibit slickensides and calcite-cemented breccia.

Small-scale structures include natural fractures (which, if open and intersected by a well, increase gas deliverability) and microfractures. Natural fractures in the producing area, as observed in core and formation microimager (FMI) logs, range in width from 0.02–0.2 mm and have a strike of 100–120° (mean 114°) and dip of 74–80° SW (Lancaster and others, 1993; Kuuskraa and others, 1998; Johnston, 2004a). Fractures tend to be wider in the carbonate rocks (up to 2 mm), and fractures may or may not be more common in interbedded limestones (Gale and others, 2007; Jarvie and others, 2007). Natural fractures in the northern part of the basin parallel the axis of the Muenster Arch (Montgomery and others, 2005). Hydraulically induced fractures, on the other hand, have an orientation that reflects today's stress field, striking 45–80° (mean 60°) and dipping 81° NW. The natural fractures are of limited vertical extent, generally terminating within the cored section (0.5–32 in long) (Lancaster and others, 1993; Bowker, 2007b), and they have almost always been mineralized by calcite (or less commonly quartz, albite, pyrite, barite, and dolomite; Gale and others, 2007). Near major fault planes, 75–80% of the fractures are mineralized (Johnston and others, 2004a; Montgomery and others, 2005; Givens and Zhao, 2009). Gale and others (2007) speculated on the possibility of large open fractures in the Barnett Shale, but Bowker (2007a) argued that open natural fractures cannot exist in areas where the formation is overpressured. Microfractures, though seldom studied, are attributed to the generation of hydrocarbons in organic-rich facies of the Barnett Shale.

3.2.4 Lithology and Lithofacies

The Barnett Shale, as determined by core and outcrop studies, is dominated by clay- and silt-size sediment with occasional beds of skeletal debris. Lithologically the formation consists of black siliceous shale, limestone, and minor dolomite (Papazis, 2005; Montgomery and others, 2005; Loucks and Ruppel, 2007). The lithologic log of a typical Barnett core is depicted in Figure 13.

Silica makes up approximately 35–50% of the formation by volume and clay minerals less than 35%. As reported by Bowker (2002), the mean composition is: 45% quartz (primarily altered radiolarian tests), 27% illite with minor smectite, 8% calcite and dolomite, 7% feldspars, 5% organic matter, 5% pyrite, 3% siderite, and traces of native copper and phosphate material. Givens and Zhao (2009) reported a similar mineral content except for significantly more calcite and dolomite (15–19%). Jarvie and others (2007) presented mineral data from a Barnett well with 40–60% quartz, 40–60% clay minerals, and a highly variable calcite content (Figure 14a). Loucks and Ruppel (2007) offered the following averages for their siliceous-mudstone lithofacies: 41% quartz, 29% clays, 9% pyrite, 8% feldspar, 6% calcite, 4% dolomite, and 3% phosphate. Ternary diagrams (Figure 14b) show relative proportions of clay, carbonate (calcite, dolomite, siderite, and ankerite), and other minerals (quartz, plagioclase and K-spar, pyrite, and phosphate) by stratigraphic member and by lithofacies (Loucks and Ruppel, 2007). A basal zone (10 ft thick) in the east-central part of the basin contains abundant apatite (phosphate mineral). The shale's relative brittleness can be appraised by the ratio of quartz/(quartz + calcite + clays) (Figure 14a; Jarvie and others, 2007).

Hickey and Henk (2007) recognized two major lithofacies—organic shale and fossiliferous shale—and four additional facies produced by diagenetic alteration—dolomite rhomb shale, dolomitic shale, concretionary carbonate (skeletal wackestone and mudstone), and phosphorite (phosphatized pellets, ooids, shells, and shale matrix). Total organic carbon content is highest (mean near 5%) in the organic shale and phosphorite.

Based on detailed petrologic analysis, Loucks and Ruppel (2007) recognized three lithofacies. (1) Laminated siliceous mudstone is the predominant rock type in the lower and upper members. Major components include silt-sized peloids (fecal pellets and flocculated clay particles) and fragmented skeletal material (radiolarians, sponges, mollusks, foraminifera, conodonts, calcareous algae, and echinoderms; mostly

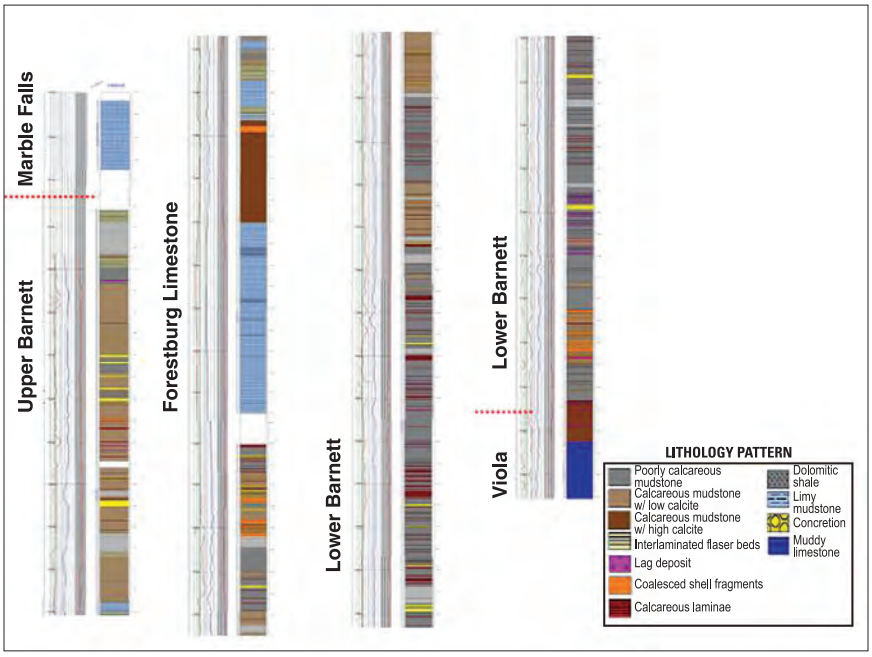

Figure 13. The lithologic log of a typical Barnett core. Modified from Slatt and others, 2009.

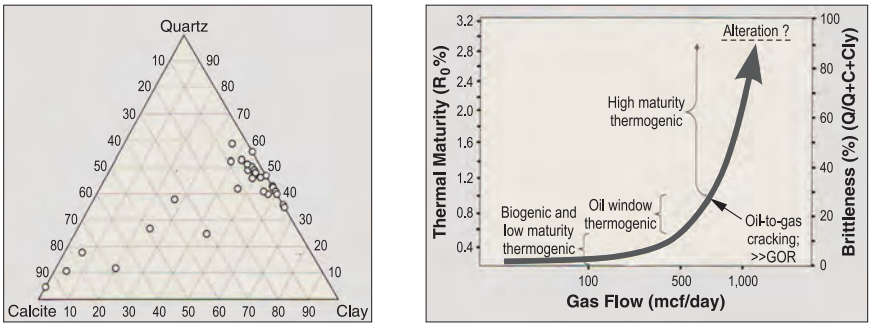

Figure 14a. Left: mineral content of the Barnett Shale in terms of quartz, clay minerals, and calcite. Right: relationship between gas flow and thermal maturity and shale brittleness (Q/(Q+C+Cl). Modified from Jarvie and others, 2007.

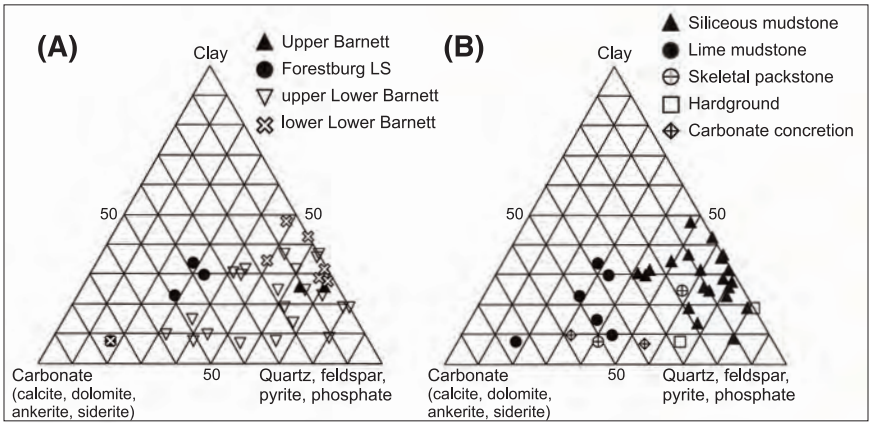

Figure 14b. Ternary diagrams of Barnett mineral content by member (A) and by lithofacies (B). Modified from Loucks and Ruppel, 2007.

transported). Silt-sized detrital quartz, plagioclase, and potassium feldspar are also present. The mudstone ranges from calcareous to noncalcareous. (2) Laminated argillaceous lime mudstone is the predominant rock type in the middle Forestburg Limestone Member. Calcite (lime mud and silt-sized particles) and dolomite (30-micron crystals) are the main constituents, but clay minerals, quartz, feldspars, and pyrite are common. Fossils include radiolarians, sponge spicules, and mollusks. The laminated structure results from the alternation of clay-poor and clay-rich limestone layers. (3) Skeletal argillaceous lime packstone is present in the lower and upper members. Thin beds of physically compacted shells (mollusks, brachiopods, sponges, and radiolarians) and transported phosphate debris (peloids, intraclasts, and coated grains) are separated by thin laminae of organic-rich skeletal siliceous mudstone. In addition, Loucks and Ruppel (2007) identified large calcareous concretions, smaller phosphate and pyrite concretions, and phosphate-pyrite hardgrounds.

Rock type has been linked to the well logs by Jarvie (2004) and Hickey and Henk (2007). Black shale is identified by a high gamma-ray reading and separation of the neutron and density logs. Phosphatic shale has a gamma-ray value of greater than 150 API units, calcareous black shale 130–140 API units, and grainstone limestone 100–120 API units. Dolomitic black shale has a gamma-ray value of 100–120 API units and shows crossover of the neutron and density logs. Bulk density increases with a greater carbonate and phosphate content and a reduced organic content.

3.2.5 Depositional Environment

Mississippian paleogeographic reconstructions by Gutschick and Sandberg (1983), Blakey (2005), and Loucks and Ruppel (2007) depict the Fort Worth Basin to have been occupied by a narrow seaway (Figures 4 and 5). This seaway was bordered by an island-arc chain to the east-southeast and the Eastern (Chappel) carbonate platform to the west. Barnett deposition occurred during an early stage of foreland-basin development.

Although some authors (for example, Lancaster and others, 1993, and Fisher and others, 2002) considered the Barnett to be a normal-marine shelf deposit, presumably because of its limestone interbeds and contained fossils, Loucks and Ruppel (2007) interpreted the formation as having originated in a deep-water slope-to-basin setting (Figure 15). The lithofacies (described previously in section 3.2.4) suggest that the sea floor was below storm wave base and the oxygen-minimum zone. Oceanic circulation was restricted and the water column stratified, accounting for the dysaerobic to anaerobic conditions of deposition. Marine upwelling contributed to blooms of planktonic radiolarians and the production of phosphate grains (Gutschick and Sandberg, 1983). Maximum water depth was estimated to have been greater than 600 feet by Gutschick and Sandberg (1983) and 700 feet by Loucks and Ruppel (2007). Deposition began during a second-order highstand of sea level, but eustatic sea level fell 150 feet by the end of Barnett time (Ross and Ross, 1987; Loucks and Rupple, 2007). Superimposed on this overall fall were numerous third-order fluctuations (parasequences) of relative sea level (Loucks and Ruppel, 2007; Slatt and others, 2009).

Terrigenous clay minerals, fine quartz, and silt-sized feldspars were sourced in the Caballos Arkansas island arc chain (Figures 4 and 5), a low-lying land area to the southeast that contributed little coarse-grained sediment (Lancaster and others, 1993; Loucks and Ruppel, 2007). The fine sediment settled from hemipelagic plumes that originated near the island arc chain, along with pelagic skeletal tests from the oxygenated surface waters. Coarser carbonate sediment, mostly fragmented shell material, was transported from the Eastern (Chappel) carbonate platform. The platform was dominated by crinoidal lime sediment and pinnacle reefs, and shell material moved down slope into the basin as hemipelagic plumes, dilute turbidity currents, and debris flows (Henry, 1982; Montgomery and others, 2005; Loucks and Ruppel, 2007). Some carbonate debris flows entered from a northern source as well (Bowker, 2007a), perhaps eroded from exposed Ellenburger carbonate rocks on or beyond the Muenster Arch. Such mass-gravity flows may have introduced—infrequently and temporarily—oxygenated water into the deep basin, accounting for a limited benthonic fauna of foraminifera and burrowers (Hickey and Henk, 2007). Once deposited on the basin floor, the sediment was occasionally reworked by contour currents.

Characteristics of the depositional facies have also been inferred by geochemical analyses of Barnett oils (Hill and others, 2007a). The analyses include pristane/phytane ratio, hopane/sterane ratio, C_{19}/C_{23} tricyclic terpane ratio, C_{35}/C_{34} and C_{33}/C_{32} homohopane ratio, and gammacerane/hopane ratio. Collectively this evidence suggests that the shale source rock formed from type II kerogen (mainly marine algae) under normal-marine salinity and dysaerobic conditions.

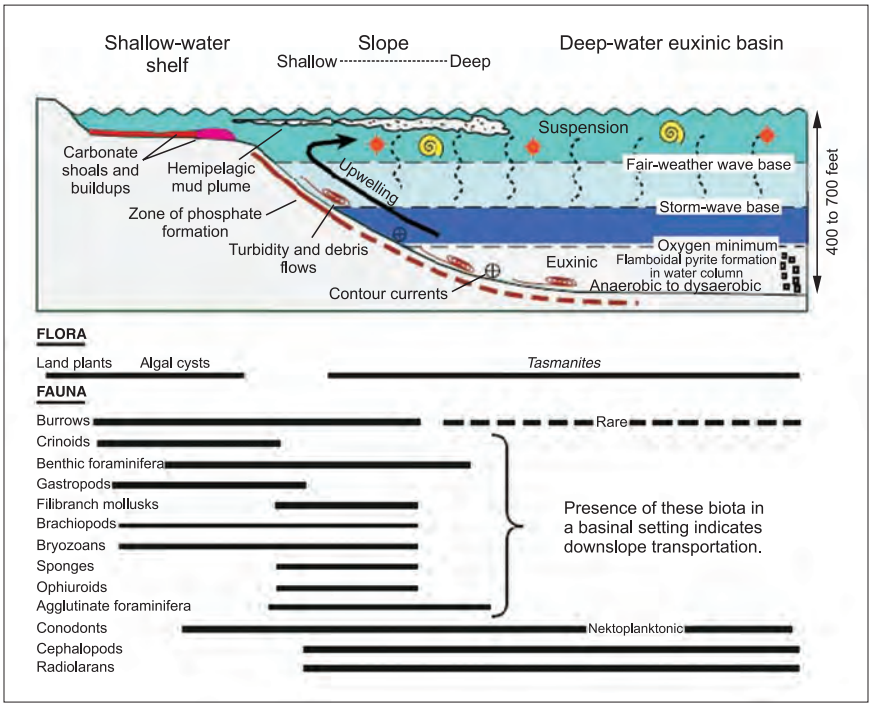

Figure 15. Generalized model for the Barnett Shale showing depositional profile, sedimentary processes, and distribution of biota. Modified from Loucks and Ruppel, 2007.

3.3 Petroleum Geology

3.3.1 Organic Carbon Content

The total organic carbon (TOC) content by weight in the Barnett Shale is reported to average 3.16–3.26 by Jarvie (2004), 3.3–4.5% by Montgomery and others (2005), and 2.4–5.1% by Jarvie and others (2007). These values were measured in cores and well cuttings taken from the north-central part of the basin where the rocks are thermally mature. Pollastro and others (2003) suggested that highest average TOC values in the Fort Worth Basin follow the northeast-southwest axis of deposition (Figure 10). According to the classification scheme of Peters and Cassa (1994), the Barnett is a very good (TOC = 2–4%) to excellent (TOC > 4%) source rock in terms of its organic richness. The organic content is generally highest in the silica-rich and phosphatic beds (lowest in the dolomitic and calcitic beds), mostly in the lower shale member but also in the upper Barnett. The TOC in the middle Forestburg Limestone Member averages only 1.8% (Montgomery and others, 2005), perhaps because higher oxygen levels associated with carbonate deposition led to greater degradation of the contained organic matter.

In contrast, values of TOC reach 11–13% in Barnett outcrop samples from near the Llano Uplift, where the rocks are thermally immature (Jarvie and others, 2001; Hayden and Pursell, 2005). This regional difference reflects the partial conversion of organic matter to petroleum where the rock is thermally mature; the TOC is thought to have decreased 36–50% with increasing maturity from immature to postmature (Pollastro and others, 2003; Jarvie and others, 2007). Back-calculations of geochemical data suggest that when originally deposited, the shale contained as much as 20% total organic carbon in the southern basin (Bowker, 2003) and 5–12% in the central basin (Montgomery and others, 2005).

Hill and others (2007b) provided the following maceral composition for two Barnett samples: amorphous kerogen 91–93% (with occasional algal *Tasmanites*), vitrinite 3–5%, inertinite 1–5%, and exinite 1%. Amorphous kerogen is unrecognizable organic matter, but frequently assumed to originate from marine algae.

Vitrinite is derived from lignin and cellulose in the cell walls of land plants and humic peat. Exinite represents the casings of pollen and spores, and inertinite is fossilized charcoal. The kerogen is classified as Type II (with minor admixture of Type III) and oil-prone when immature (1.41 hydrogen/carbon ratio and 0.10 oxygen/carbon ratio). Pollastro and others (2003) and Jarvie and others (2007) reported an original hydrogen index (HI measured by Rock-Eval) of 350–475 milligrams hydrocarbon per gram of TOC.

Hickey and Henk (2007) recognized that a good linear correlation exists between TOC and grain density measured in the lab: TOC (wt %) = 85.9 – 30.8 x grain density (g/cc). They speculated that a similar correlation exists between TOC and wire-line bulk density. Resistivity readings on Barnett well logs range from 10–1,000 ohms, and density porosity ranges from 0–16 porosity units (Johnston, 2004a). Neutron-porosity values read slightly to much higher than density-porosity values.

3.3.2 Thermal Maturity and Burial History

Vitrinite reflectance (R_o) is the measure most commonly cited to assess the thermal maturity of the Barnett Shale. An increasing value of R_o reflects a greater thermal maturity of the source rock, which in turn influences the expected hydrocarbons generated (Table 3). However, Hill and others (2007b) cautioned that the rate of heating can influence the temperature required for a particular value of R_o.

A map of R_o (isoreflectance) values for the Barnett Shale across the basin indicates a general trend of increasing thermal maturity toward the east-northeast (Figure 16a and 16b) (Montgomery and others, 2005). Values range from a minimum of less than 0.7 near the Llano Uplift and near the Red River Arch, to a maximum of greater than 1.7 along the Ouachita Thrust belt.

R_o does not change uniformly across the area; rather, local increases and decreases from the regional trend reflect the presence of intrabasinal structures. Values are locally higher adjacent to the Ouachita Thrust front, the Mineral Wells-Newark East fault system, and Lampasas Arch and locally lower over the Bend Arch (Figure 16). Pollastro and others (2003) and Montgomery and others (2005) attributed these anomalies to a complex burial history with multiple thermal events and to hydrothermal heating in and around deep-seated faults. Bowker (2007a) thought that thermal maturity was controlled exclusively by proximity to the Ouachita Thrust front and associated hot brines. A burial-history diagram (Figure 17) illustrates three stages to the thermal history of the Barnett Shale (Montgomery and others, 2005). Following deposition in the Late Mississippian, an initial stage of rapid burial occurred in the Pennsylvanian and Permian. Jarvie and others (2001) postulated that primary oil and gas were generated during this first stage, possibly with some secondary cracking of oil. The second stage occurred while the Barnett remained at an elevated temperature (240–285°F) from the Late Permian through the Early Cretaceous. Gas was generated at that time by the cracking of oil, bitumen, and kerogen. The third stage, extending from the Late Cretaceous to Tertiary, was one of uplift and erosion of the overburden. Montgomery and others (2005) hinted that oil may also have been generated during this last stage when the pressure and temperature dropped.

Paralleling the general trend of R_o is a regional change in reported hydrocarbon production (Figure 18) (Montgomery and others, 2005). (1) Oil production roughly follows the isoreflectance line R_o = 0.9, occurring to the west over the Bend Arch and Eastern shelf and extending along the northern margin of the basin. In Brown County (R_o = 0.6–0.7%) the Barnett yields oil of 38° API gravity (Pollastro and others, 2003).

Table 3. Relationship between vitrinite-reflectance value (% R_o), stage of thermal maturity, and generated hydrocarbons in the Barnett Shale.

R_o (percent)	Maturity	Thermogenic hydrocarbons
0.20-0.60	Immature	none
0.60-0.70	Early Mature	top of oil window
0.70-1.00	Peak Mature	peak oil
1.00-1.40		oil and wet gas
1.00-1.10	Late Mature	top of gas window
1.20-1.30		peak wet gas
1.40-2.10	Post Mature	peak dry gas

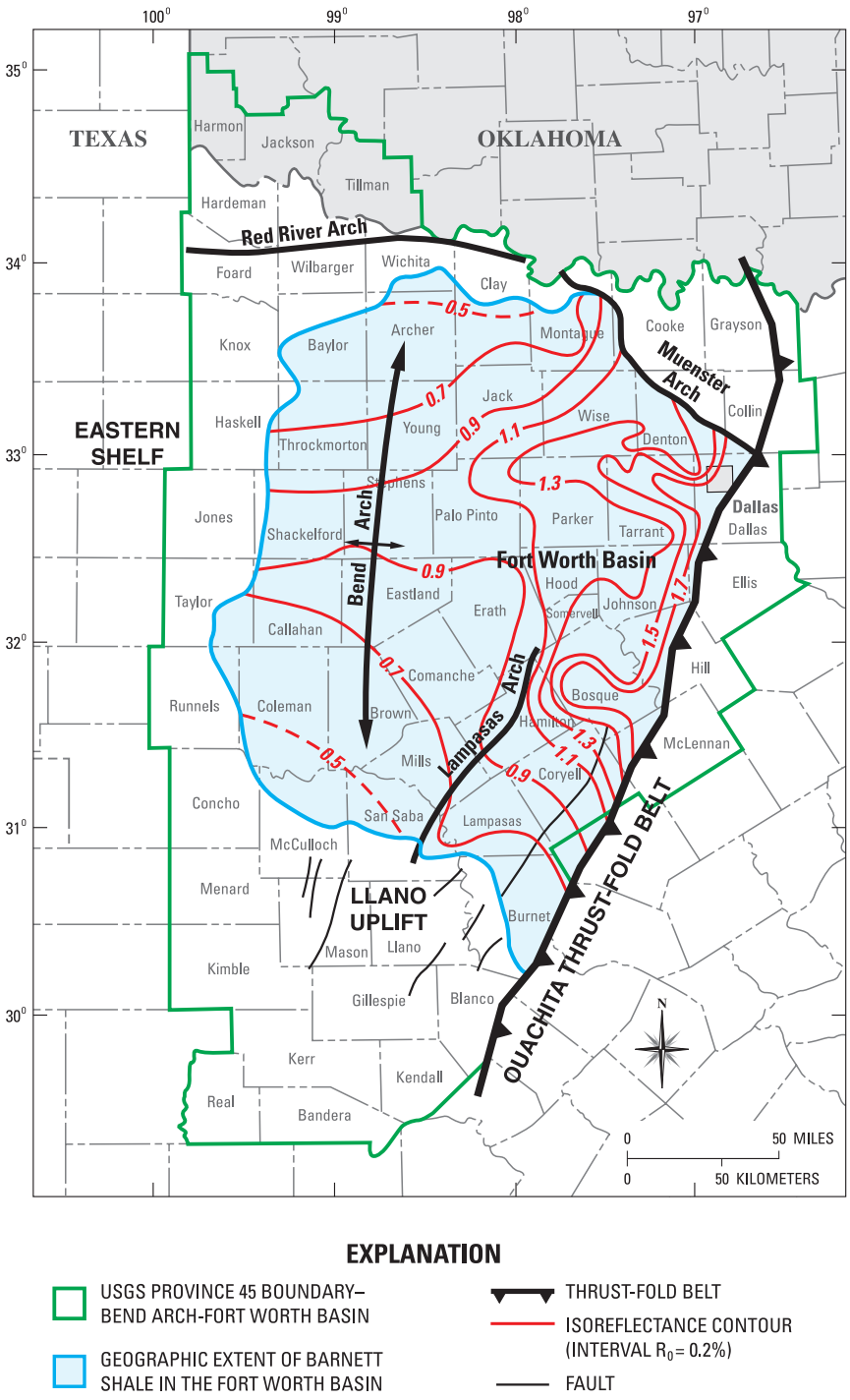

Figure 16a. Isoreflectance map, Fort Worth Basin and Bend Arch. Contour interval R_o = 0.2%. Modified from Montgomery and others, 2005.

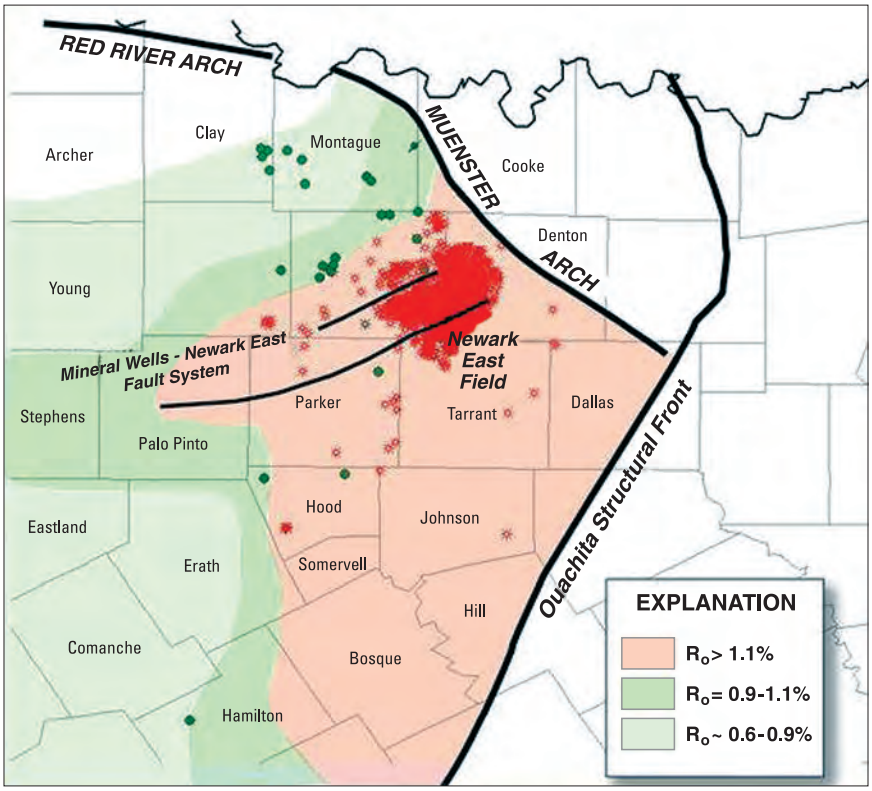

Figure 16b. Detailed map showing reflectance values in vicinity of Newark East Field. Modified from Montgomery and others, 2005.

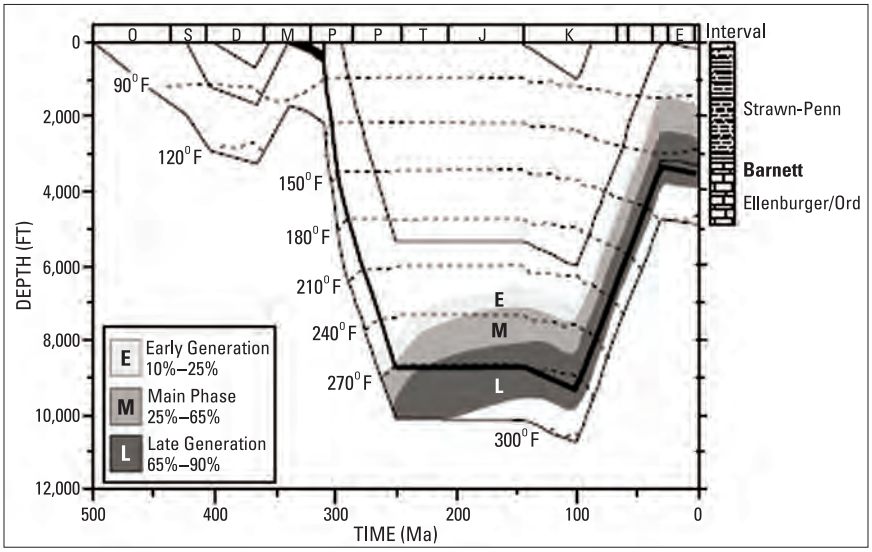

Figure 17. Burial-history diagram for Barnett Shale in southwestern Fort Worth Basin. Modified from Montgomery and others, 2005.

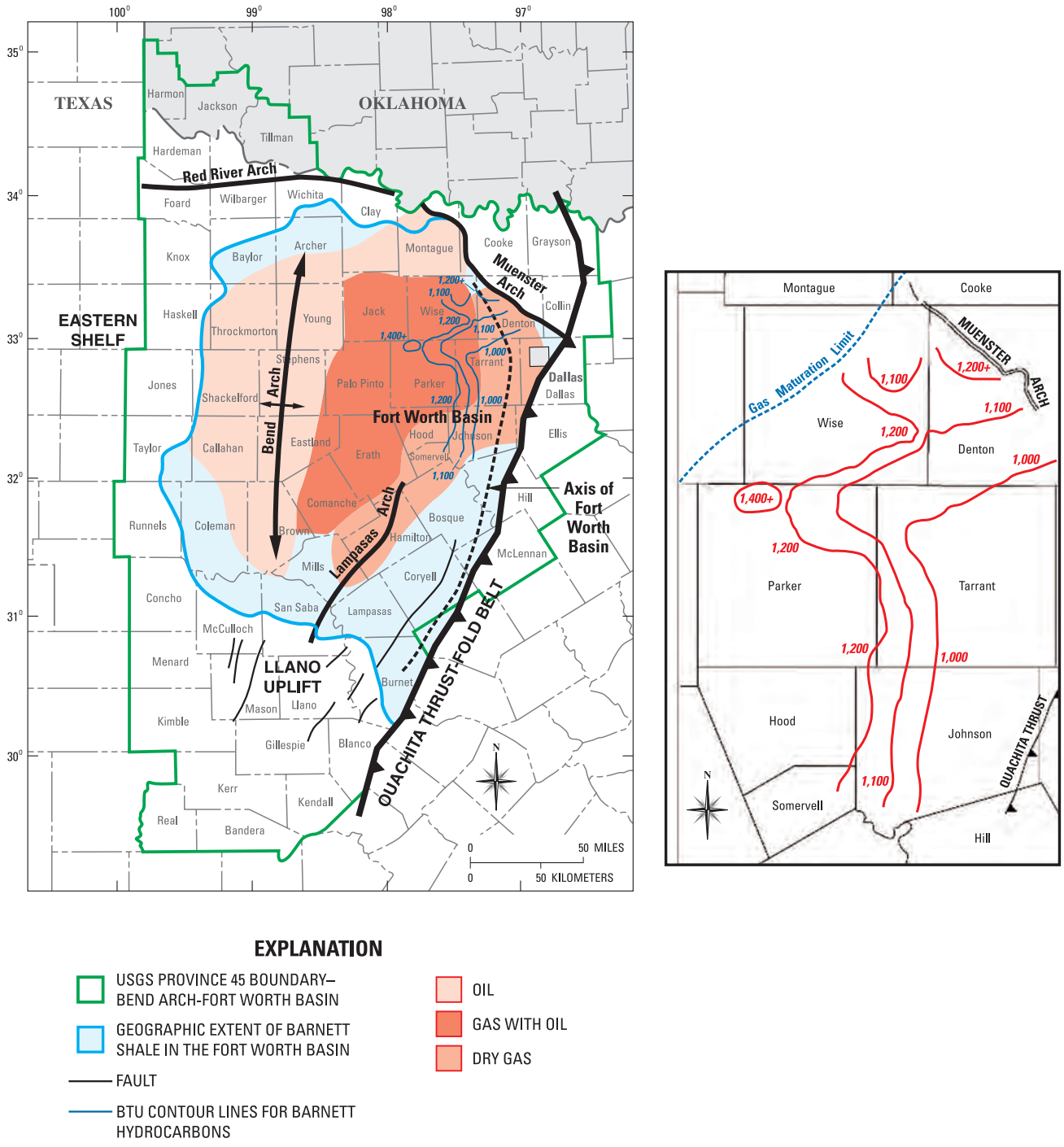

Figure 18. Left: Regional trend in reported production from the Barnett Shale; modified from Montgomery and others, 2005. Right: Contour lines of BTU data for Barnett hydrocarbons; modified from Givens and Zhao, 2009.

(2) Production of dry gas roughly follows the isoreflectance line R_o = 1.2 along the Ouachita Thrust front to the east, the bounding fault of the Muenster Arch, and the structural axis of the basin. (3) Production of gas with oil occurs in the intervening area where R_o = 0.9–1.2. The onset of oil cracking seems to begin near R_o = 1.3 (Hill and others, 2007b). Moreover, within the gas window the eastward increase in maturity is accompanied by a decrease in gas wetness and in heating content (BTU >1,400 in oil-prone area, BTU = 1,050–1,380 in gas-prone area; Givens and Zhao, 2009). Where vitrinite-reflectance data are lacking, some geologists use the gas BTU content as an indicator of thermal maturity (Figure 18).

Thermal maturity of the Barnett Shale can also be derived from TOC and Rock-Eval (Tmax and HI) measurements. For example, Jarvie (2004) found that Tmax ranges between 430–465°C in samples from the oil window and between 465–580°C in the gas window. Pollastro and others (2003) reported well cuttings of low-maturity samples with an average 3.2% TOC to have a Tmax of less than 435°C. Moreover, Pollastro and others (2003) reported samples from the wet-gas/dry-gas window to have a hydrogen index (HI) of less than 100 (equivalent R_o value > 3.1%; TOC = 4.5%). Interestingly, Jarvie and others (2007) suggested that the thermal-maturity boundary of the Barnett (and hence its potential gas production) based on chemical assessment may extend farther westward in the basin compared to assessment made by vitrinite reflectance.

3.3.3 Reservoir Characteristics

The Barnett Shale is in effect a single, very large (continuous) gas resource that underlies thousands of square miles. It is a stratigraphic trap within a fault-bounded basin, occupying a structural low and straddling the axis of the Fort Worth Basin.

The average porosity in productive portions of the formation ranges from 3 to 6%, whereas porosity in nonproductive portions is as low as 1% (Johnston and others, 2004a). Slatt and others (2009) presented SEM photomicrographs of Barnett interparticle pores approximately 3 micrometers in diameter (Figure 19). As determined by mercury-porosimetry analysis (Figure 20), most pore throats have a radius of less than 0.005 micrometer, about 50 times the radius of a methane molecule (Bowker, 2007b), and perhaps less than 0.0001 micrometer (Jarvie and others, 2007). Much of the interparticle (matrix) porosity may have resulted from thermal decomposition of kerogen to petroleum. Jarvie and others (2007) calculated that the thermal decomposition of organic matter in the shale (original TOC = 6.41%) in the dry-gas window (R_o = 1.4) creates 4.3% matrix porosity. Matrix porosity adjacent to major faults is partially occluded by calcite cement (Bowker, 2007a).

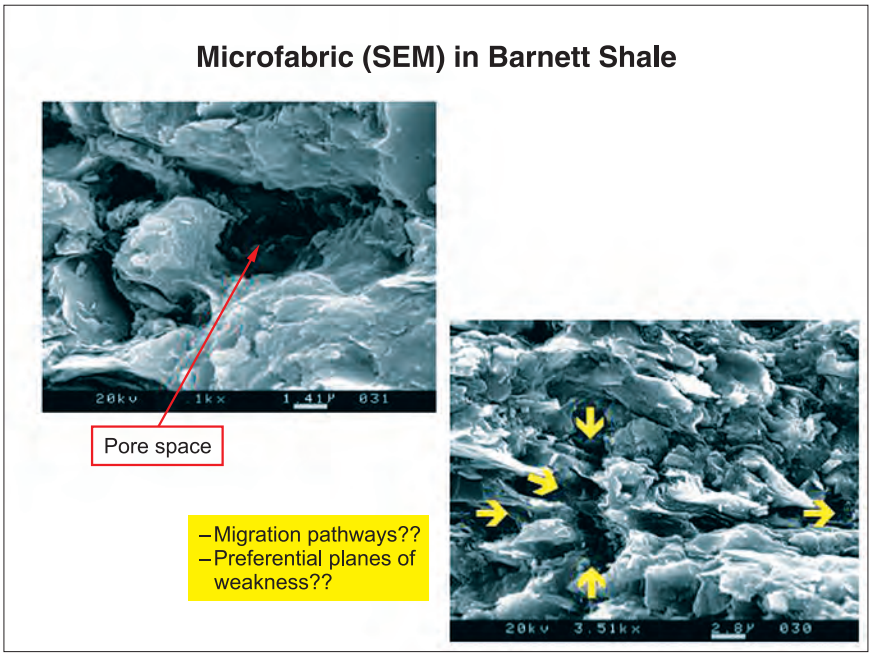

Figure 19. SEM view of pores and porosity pathways in the Barnett Shale. Modified from Slatt and others, 2009.

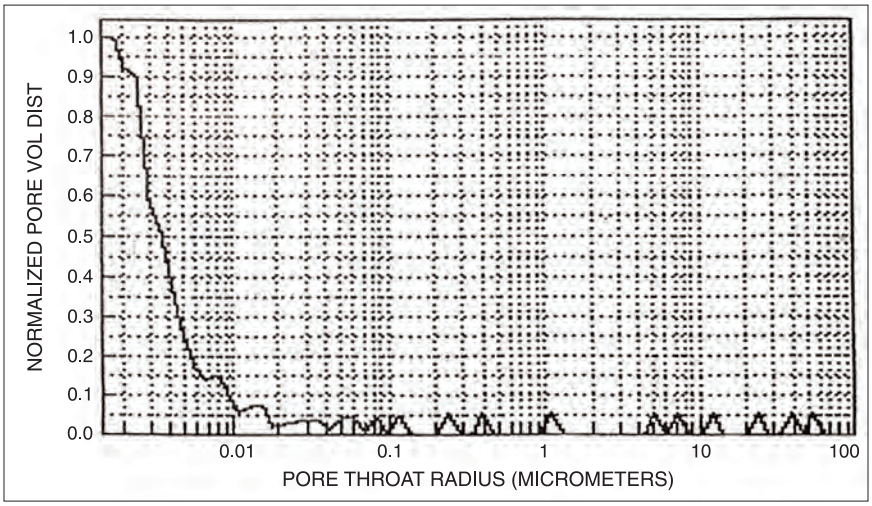

Figure 20. Results of mercury-porosimetery analysis of the Barnett Shale. Eighty percent of the pore throats have a radius of less than 0.005 micrometer. Sample from 8,094 ft in Enre Corporation (Chevron), Mildred Atlas #1, Johnson County. Modified from Bowker, 2007b.

Published values for average matrix permeability have variously been reported to be 0.02–0.10 millidarcies (Jarvie and others, 2004), less than 0.01 millidarcies (Montgomery and others, 2005), 0.0005–0.00007 millidarcies (Ketter and others, 2008), or in the range of microdarcies to nanodarcies (Johnston, 2004a; Bowker, 2007b). Geographical variation in the formation's permeability is complex and depends on the local interplay of fractures, faults, and stress (Kuuskraa and others, 1998).

Productive, organic-rich portions of the Barnett Shale average 25–43% water saturation (Lancaster and others, 1993; Hayden and Pursell, 2005; Bowker, 2007b). Water saturation increases greatly in parts of the formation with less organic matter (more calcareous), suggesting that generation of hydrocarbons in the organic-rich beds also resulted in a loss of water (drying of the reservoir; Montgomery and others, 2005). The water is bound to clay minerals and/or capillary-bound in micropores and natural fractures, but there is no free water (Johnston and others, 2004a; Bowker, 2007b). The rock is generally assumed to be slightly oil wet because of the high organic content and the unusually high percent of fracture-stimulation water recovered during well completions (60–70% in some areas of the Newark East field).

In the dry-gas window, gas saturation equals 75% (Montgomery and others, 2005). Natural gas is stored within interstitial pores and microfractures and adsorbed onto solid organic matter and kerogen. Generation of hydrocarbons produced the microfractures in the shale as well as a slight overpressuring (about 0.52 psi/ft in the gas-saturated portion of the play; Bowker, 2007a); however, microfractures have subsequently been healed by residual oil and pyrobitumen. The volume of adsorbed gas may be as high as 40–60% (fully saturated; Jarvie and others, 2004; Montgomery and others, 2005) or as low as 20–25% (Lancaster and others, 1993; Kuuskraa and others, 1998; Hayden and Pursell, 2005), and adsorption sites must be filled or saturated before expulsion/production can proceed. At a subsurface pressure of 4,000 psi (typical initial pressure 3,000–4,000 psi; Hayden and Pursell, 2005), an estimated 80% of the Barnett gas is free and stored in open pores, but that at a pressure below 1,000 psi, desorption of methane can play an important role in gas production (Lancaster and others, 1993).

3.3.4 Generation of Hydrocarbons

Hydrocarbon gas in the Barnett Shale is approximately 90% methane and primarily thermogenic. Hill and others (2007b) modeled the processes of gas generation by laboratory simulation, reporting that gas volume was a function of organic richness (a threefold increase in original TOC may triple the gas yield), thermal maturity (gas yield may increase by a factor of 25 between R_o = 1.3 and 2.0), oil volume retained in the shale (oil cracking is the source of some gas), and formation thickness. Carbon dioxide accounts for less than 2% of the gas volume (perhaps related to cracking of labile oxygenated functional groups, such as decarboxylation of carboxylic groups). Nitrogen and hydrogen sulfide usually occur in trace amounts (Johnston, 2004a).

Gas may be generated in small amounts at the beginning of thermal degradation of the kerogen, R_o = 0.5–0.6; however, mostly low-sulfur, low-gravity oil and some condensate are generated at $R_o < 1.0$ (Pollastro, 2007). At R_o = 1.1, oil in the shale begins to crack to gas and condensate (Hill and others, 2007b). This level of maturity is lower than expected from theoretical calculation and may be due to an interaction of the oil with kerogen or clay minerals (acting as a catalyst) in the source rock. At R_o = 1.6, however, only a small volume of the oil has cracked (15%), suggesting that gas in the Barnett at R_o = 1.0–1.6 is predominantly produced by cracking of kerogen and bitumen. The gas, therefore, appears to be mostly cogenerated with oil (Hill and others, 2007a). At R_o = 1.86 half of the oil has cracked, and at R_o = 2.2 nearly 90 percent of the oil has cracked.

Jarvie and others (2007) calculated that a Barnett shale with original TOC = 6.41 wt % contains 2.32 wt % convertible carbon (convertible to hydrocarbon with increasing thermal maturity) and 4.09 wt % residual organic carbon (not reactive because of insufficient hydrogen).

Rock-Eval analysis of an immature outcrop sample (TOC = 11.47% and R_o = 0.48) yields a value for S_2 (hydrocarbon-generation potential) of 54.43 mg HC/g rock. Analysis of a mature Barnett sample (TOC = 4.51% and R_o = 1.15) provides the following data (Hill and others, 2007b): S_1 (thermally extractable petroleum) 1.73 mg HC/g rock, S_2 (petroleum generated by pyrolysis) 3.07 mg HC/g rock, and HI (hydrogen index, S_2/TOC x 100) 68 mg HC/g TOC. The production index ($S_1/S_1 + S_2$) equals 0.36, meaning that 36 percent of the potential hydrocarbons had already been generated. Rock-Eval analysis of a sample (TOC = 5.21%) subjected to progressive simulated maturation (R_o increasing from 0.62 to 1.30) provides the following data (Montgomery and others, 2005): S_2 1.36 mg HC/g rock, HI 41 mg HC/g TOC, and transformation ratio 93%.

Calculated generated-gas potential (total gas yield) is 7.4 scfg/t of reservoir rock at R_o = 1.3 and 184 scfg/t at R_o = 2.0 (Hill and others, 2007b). Expressed in a different manner, the total original generation potential for immature Barnett source rock is about 820 bcfg/sq mi, ignoring any migration (Jarvie and others, 2007). Estimates of average gas-in-place range from 25–42 bcfg/sq mi (Kuuskraa and others, 1998) to 100 bcfg/sq mi (Johnston, 2004a) to 142.5 bcfg/sq mi (Montgomery and others, 2005) to 204 bcfg/sq mi (Jarvie and others, 2007). The increase in GIP estimates over these ten years probably reflects improvements in analytic techniques and mass-balance calculations. The volume of adsorbed gas in place is 60–125 scfg/ton rock at a reservoir pressure of 3,800 psi (Montgomery and others, 2005), which is released as the formation pressure is lowered and contributes to the long life of Barnett wells (Lancaster and others, 1993). The volume of free gas in place is around 105 scfg/t, and the total GIP (free plus adsorbed) varies from 170–350 scfg/t (Johnston, 2004a; Hayden and Pursell, 2005; Montgomery and others, 2005; Arthur and others, 2008a). Reservoir modeling shows that, with a matrix porosity of 6% and pressure of 3,800 psi, gas-storage capacity can be 159 scfg/t or more (Jarvie and others, 2007).

The low-porosity, low-permeability character of the source rock itself provides the seal. In addition, adsorbed petroleum is trapped in the shale by surface chemistry. However, Hill and others (2007b) calculated that 20% of the total gas yield (comparing immature and mature samples) was lost by migration to conventional reservoirs in the basin or to fractures. Jarvie and others (2007) estimated 60% expulsion. Dissolution-precipitation diagenesis of minerals in the shale may have decreased the porosity and permeability so that the source rock cannot retain as much gas at high temperatures (Hill and others 2007b). Geochemical analyses of biomarkers and light hydrocarbons confirm that large-scale migration has occurred episodically from the Barnett to conventional reservoirs in the Ellenburger and Viola (Ordovician) and Bend, Strawn, and Canyon (Pennsylvanian) (Montgomery and others, 2005; Hill and others, 2007a).

3.3.5 Delineation of the Barnett Play

Historically, the vast majority of Barnett Shale production comes from the core area (sweet spot) in and around the Newark East field of Denton, Wise, and Tarrant Counties (refer back to Figures 2 and 3). Much of the initial development by Mitchell Energy Corporation (now part of Devon Energy) took place here. The core

area was most commonly drilled with vertical wells and treated with large hydraulic fractures ((Hayden and Pursell, 2005). In this area the Barnett is thickest (300–700 ft), deepest (7,000–8,000 ft), and exceptionally organic rich (original TOC = 5–12%). The Barnett here is most thermally mature (R_o > 1.1) which corresponds to the highest calculated gas-in-place volumes. Moreover, the Barnett is overlain and underlain by lithological barriers that facilitate large fracture treatments (see section 3.4.2).

The play has expanded in all directions from the core area, but primarily to the south and west (Johnston, 2004a; Powell, 2008). The rationale is that critical geological characteristics of the core area must parallel the regional northeast-southwest trends of depositional environment, basin structure, thermal maturity, and subcropping formations and—it is hoped—key geological characteristics may even extend updip (shelfward) to the west (Kuuskraa and others, 1998). Hayden and Pursell (2005) divided the non-core area into Tier 1 counties (Johnson, Parker, and Hood) and Tier 2 (counties to the west and south) based on the present level of development and assessed risk. Tier 1 counties generally lack the underlying lithological barrier (Viola-Simpson limestone), but this problem can be solved by horizontal drilling and smaller, multiple fracture treatments. Gas-in-place calculated for the core area and Tier 1 counties is 140–145 bcfg/mi^2 (Hayden and Pursell, 2005). Tier 2 counties comprise the least developed area. This area may be within the oil window (R_o <1.0, Figure 16) where the only production would be uneconomic volumes of oil (Hayden and Pursell, 2005). In addition, the highest TOC values in the Fort Worth Basin follow the northeast-southwest axis of deposition (Figure 10) (Pollastro and others, 2003), meaning that counties to the west would be less organic rich. Some geologists arbitrarily choose the -5,250 ft structural-contour line of the Ellenburger Group (approximately equal to the base of the Barnett) as a western limit to the Barnett Shale play (Figure 2) (Kuuskraa and others, 1998).

Kuuskraa and others (1998) provided an early quantitative assessment of the continuous Barnett gas play. They based their assessment on (1) geographical extent of untested areas within the play (minimum, intermediate, and maximum areas akin to core and Tiers 1 and 2), (2) well spacing (320 acres per well), (3) success ratio in and around core area (86%), (4) liquids/gas ratio (in order to include volumes of natural gas liquids), (5) recovery percent (7–20%), and (6) reservoir drainage area (10–30 acres per well). Values for porosity, permeability, water saturation, and the efficiency of well treatments are indirectly included in these six input parameters, but consideration of future improvement in technology and development practices is excluded from their assessment. Using these input data, Kuuskraa and others (1998) calculated the mean, technically recoverable gas resources to be 10.0 tcfg.

Pollastro and others (2003) first assessed the continuous Barnett play in terms of the USGS Total Petroleum System concept. Their assessment included (1) areal extent and thickness of the source rock, (2) organic richness (TOC), kerogen type (II) and maturity (measured by R_o and Rock-Eval analysis), and (3) reservoir character, seal rock, and traps. They too identified three assessment units. The Barnett Shale in the Newark East sweet spot (Greater Newark East Fractured Siliceous Shale Gas Assessment Unit) is siliceous, thick, slightly overpressured, within the gas-generation window, and enclosed below and above by impermeable formations. They reported a mean Estimated Ultimate Recovery (EUR) in this assessment unit of 1.25 bcfg per well, and recompletion of a well after about five years of production commonly adds 0.75 bcfg to its EUR (Pollastro and others, 2003). An outlying area of Barnett Shale (Ellenburger Subcrop Fractured Barnett Shale Gas Assessment Unit) lies within the gas-generation window, but the underlying lithological barrier is absent and the overlying barrier may be absent. The area of least potential (North Basin and Arch Fractured Shale Gas and Oil Assessment Unit) is that where the formation produces both oil and gas, and the overlying and underlying lithological barriers may be absent.

Pollastro (2007) updated the USGS assessment of the Barnett Shale play (two gas assessment units only, excluding the oil unit), using the Total Petroleum System concept. Input variables include: number of cells (40-acre locations) that have been tested, number of cells that were successful, historical EUR of wells, total acreage of assessment unit based on geological uncertainty, the estimated drainage area, percent of area that is untested, percent of area that is untested that has potential to add to reserves, estimated future success rate, and EUR for untested area. Exploration and production histories were available for about 1,700 vertical wells that produced gas, and EUR values were available for 177 wells with multiple completions in the Greater Newark East Fracture-Barrier Continuous Barnett Shale Gas Assessment Unit (1,800 sq miles). Geological uncertainty and the uncertainty distribution for input variables are minimal for this assessment unit. Exploration and production histories were also established for just 134 vertical wells that produce gas and EUR values for 78 wells in the Extended Continuous Barnett Shale Gas Assessment Unit (7,000 sq miles). Geological uncertainty, therefore, is greater for this second assessment area (fewer wells drilled and shorter histories). Pollastro (2007) estimated a total volume of 14.6 ± 1.3 tcfg of undiscovered, technically recoverable gas in the Greater Newark

East Fracture-Barrier Continuous Barnett Shale Gas Assessment Unit and 11.6 ± 3.5 tcfg in the Extended Continuous Barnett Shale Gas Assessment Unit. In addition, the Barnett Shale has 3–4 tcfg of proved reserves and an estimated 1.0 billion barrels of natural gas liquids. Pollasto's (2007) estimates, however, are based on well histories dating from 1981–2003 and do not include recent data from horizontal drilling.

The two gas assessment units together (Figure 21) are bound and defined by geological features, namely

- the Ouachita Thrust front,
- the basement fault along the southern margin of the Muenster Arch,
- the line of thermal maturity R_o = 1.1, and
- the 100-ft isopach line of the Barnett Shale.

The Extended Continuous Barnett Shale Gas Assessment Unit is interpreted to contain the larger area of continuous-type gas accumulation in the Barnett, and the Greater Newark East Fracture-Barrier Continuous Barnett Shale Gas Assessment Unit is the area with highest potential given current technology (Montgomery and others, 2005). These assessment units are also bound and defined by geological features:

- the western limit of the Viola-Simpson Formations which serve as a competent lower-fracture barrier, and
- the southern limit of the Marble Falls Formation which serves as a competent upper-fracture barrier.

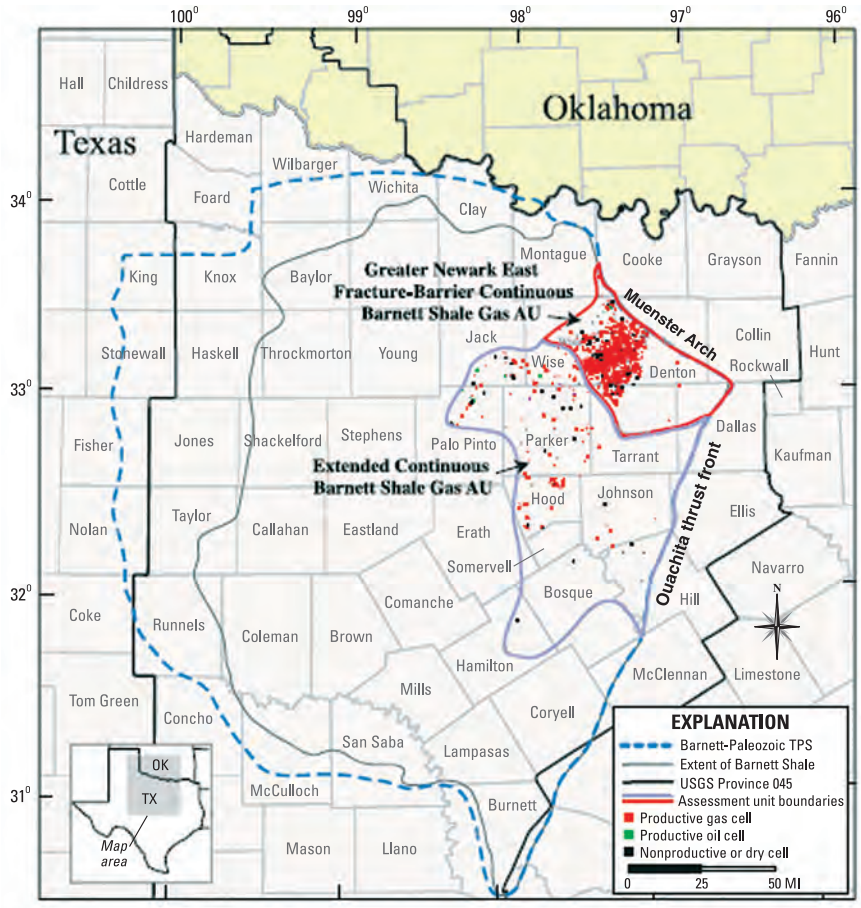

Figure 21. Extent of the Barnett-Paleozoic total petroleum system and boundaries of the Greater Newark East Fracture-Barrier Continuous Shale Gas Assessment Unit and Extended Continuous Barnett Shale Gas Assessment Unit. Modified from Pollastro, 2007.

4.0 MARCELLUS SHALE, APPALACHIAN BASIN

4.1 Location

The Middle Devonian Marcellus Shale extends for almost 600 miles through the central Appalachian Basin (Figure 22). It is present in Ontario, New York, Pennsylvania, Ohio, West Virginia, Maryland, and Virginia, an areal extent of some 75,000 sq mi. Although the shale has traditionally been regarded as the source rock for conventional Upper Devonian and Lower Mississippian reservoirs, it also has a history of gas production dating to 1821. However, the recent revival in Marcellus exploration began in 2004–2005 when Range Resources-Appalachia introduced two key drilling and treatment technologies that had previously been developed for the Barnett play of Texas: horizontal wells and slickwater fracturing. The initial reports announced a spectacular success in Pennsylvania, kicking off a new shale-gas play (Durham, 2008).

The Marcellus crops out on the eastern (Virginia to Pennsylvania) and northern (New York) margins of the basin where it has been studied in both proximal and distal geological areas. Approximate boundaries of the play include the Allegheny Structural Front to the east, the Adirondack Uplift to the northeast, and the Waverly or Cincinnati Arch to the west. The core area—where the formation exceeds 50 ft thick and is generally thought to have the best potential—includes Pennsylvania, West Virginia, and New York, an incredible 50,000 sq mi (Wrightstone, 2008; Engelder and Lash, 2008). Hence exploration, leasing, permit applications, drilling, and formation evaluation are concentrated in these three states (Figure 22) (Wrightstone, 2008; Sumi, 2008).

The core area comprises the Marcellus Shale Assessment Unit of the Devonian Shale-Middle and Upper Paleozoic Total Petroleum System of the U.S. Geological Survey (Milici and Swezey, 2006). The Assessment Unit may be divided into seven plays: Pittsburgh Basin, Eastern Rome Trough, New River, Portage Escarpment, Penn-York Plateau, Western Susquehanna, and Catskill.

4.2 Geological Setting

4.2.1 Appalachian Basin

The Appalachian Basin is an asymmetrical foreland basin (Figure 23). It formed over a period of approximately 200 million years and through three separate orogenies. The Middle-Late Ordovician Taconic Orogeny resulted from collision of the Laurentian or Laurussian plate (containing modern-day North America) and an oceanic island-arc system. The Middle Devonian to Lower Mississippian Acadian Orogeny was produced by the collision of Laurentia and a minor continental plate (Avalonia, Baltica, or Armorica). Finally the Pennsylvanian-Permian Allegheny Orogeny came about by the convergence of Laurentia and Gondwana and assembly of the supercontinent Pangaea.

Crustal thickening due to thrust faulting of the Acadian Orogeny created an elevated highland in the east, the principle source area for Devonian-Mississippian siliciclastic rocks of the Appalachian Basin (Figure 24). The leading continental margin of Laurentia flexed downward beneath the tectonic load, and eventually up to 7,000 ft and perhaps as much as 12,000 ft of mostly deltaic sedimentary rocks accumulated as the Acadian clastic wedge (Piotrowski and Harper, 1979; Milici and Swezey, 2006). Paleogeographic reconstruction shows that the basin was covered by an epeiric seaway that stretched from New York to Georgia, wide to the north but narrowing southward (Figure 24). Within this seaway accumulated several black shales, including the Geneseo, Middlesex, Rhinestreet, Huron, and Sunbury. The Marcellus is generally considered to be the oldest and deepest (although the black Needmore Shale locally underlies the Marcellus). Following deposition and burial, the Marcellus was subjected to extensive tectonic deformation during the succeeding Allegheny Orogeny.

Today the basin trends northeast-southwest. The structural axis (at -6,000 ft below sea level) lies slightly basinward of the Allegheny Structural Front, running through east-central West Virginia, south-central to northeastern Pennsylvania, and into southeastern New York (Figure 25) (Milici, 1996). The structural front marks the boundary between the Valley and Ridge Province with intensely deformed sedimentary rocks and the Allegheny Plateau Province with relatively undeformed rocks. Acadian thrust sheets may have been locally

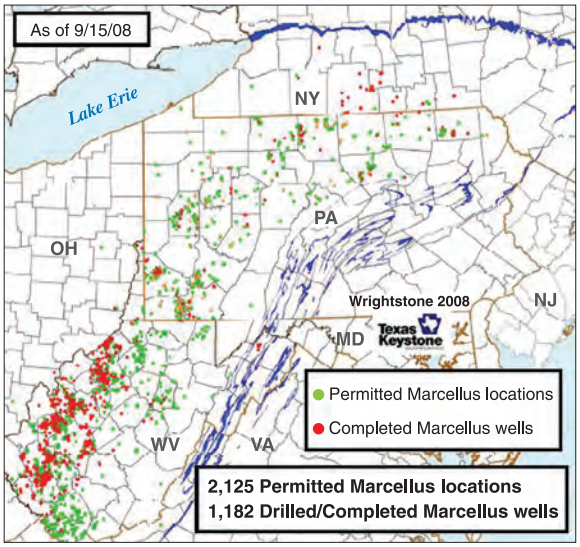

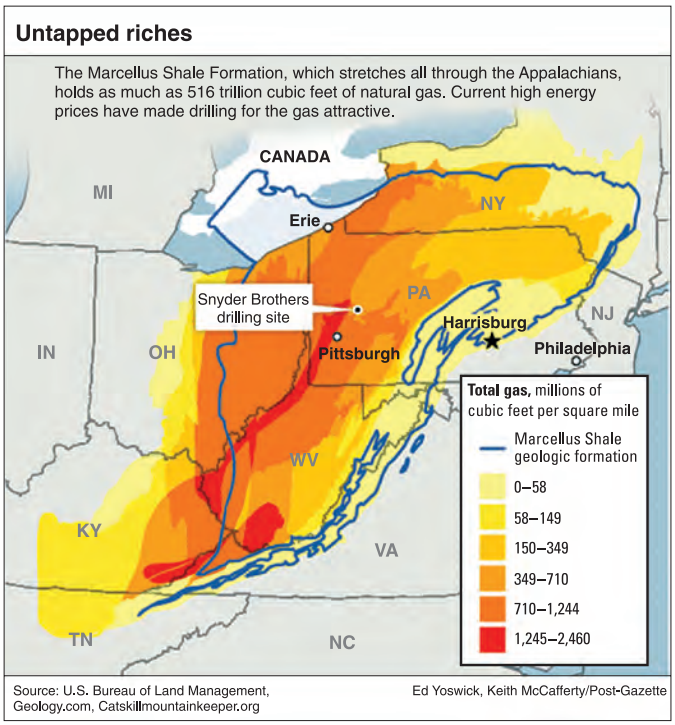

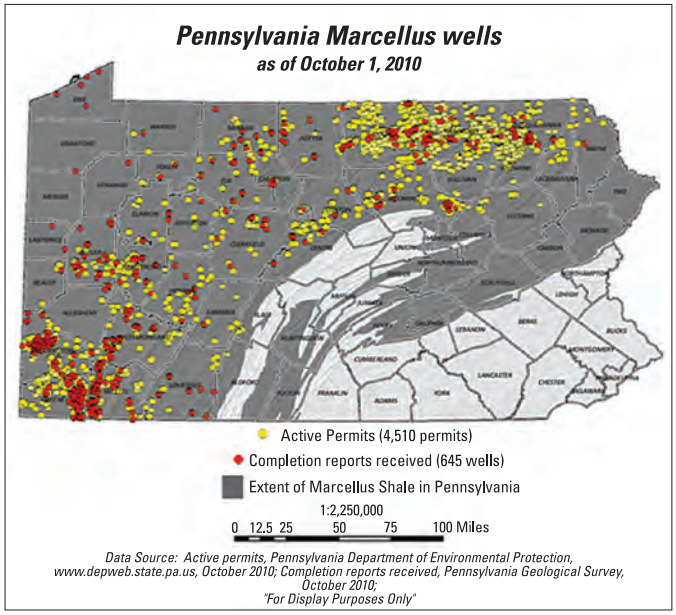

Figure 22. Top: recent drilling activity in the Marcellus Shale; modified from Wrightstone, 2008. Bottom left: Estimated gas in place (MMcfg/sq mi); modified from Marcellus Shale in New York, 2009. Bottom right: Marcellus Shale drilling activity in Pennsylvania as of October 2010, clearly showing the southwestern and north-central play areas. Map from Pennsylvania DEP.

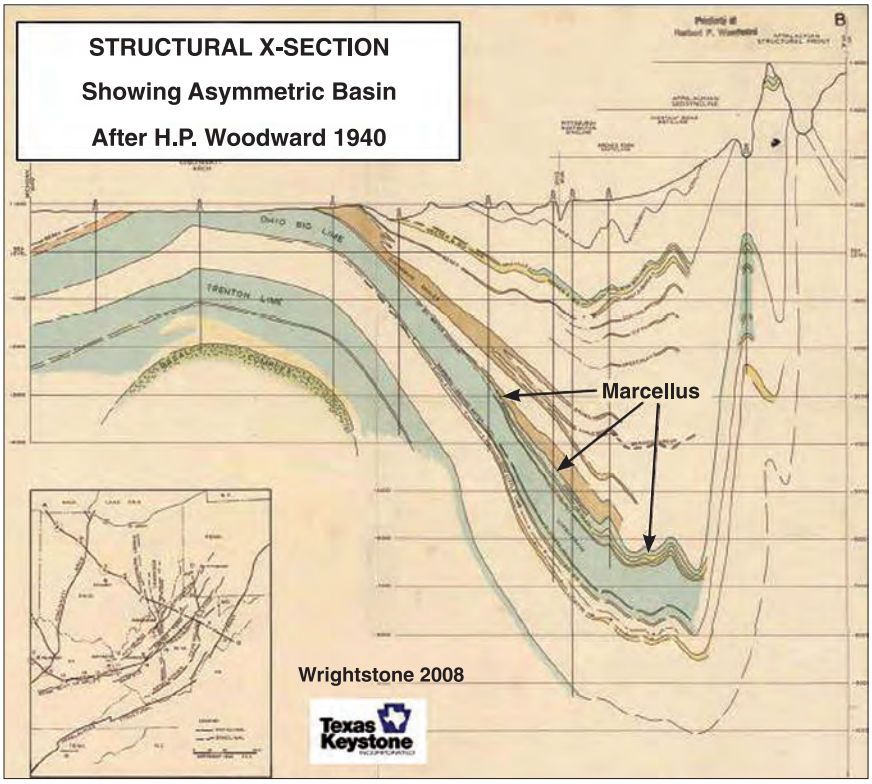

Figure 23. West-east structural cross section of Devonian section showing the asymmetrical shape of the Appalachian basin. Modified from Wrightstone, 2008.

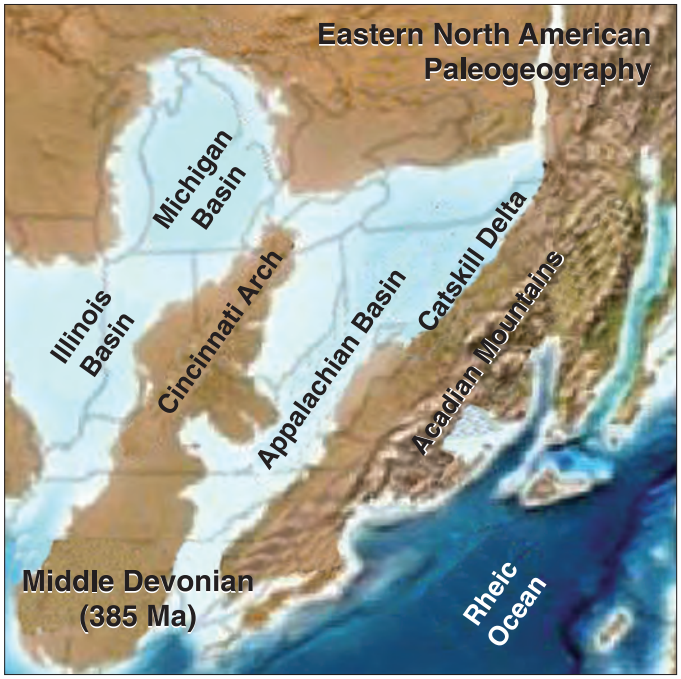

Figure 24. Paleogeography of eastern U.S. during Middle Devonian time. Modified from Geology.com, 2008.

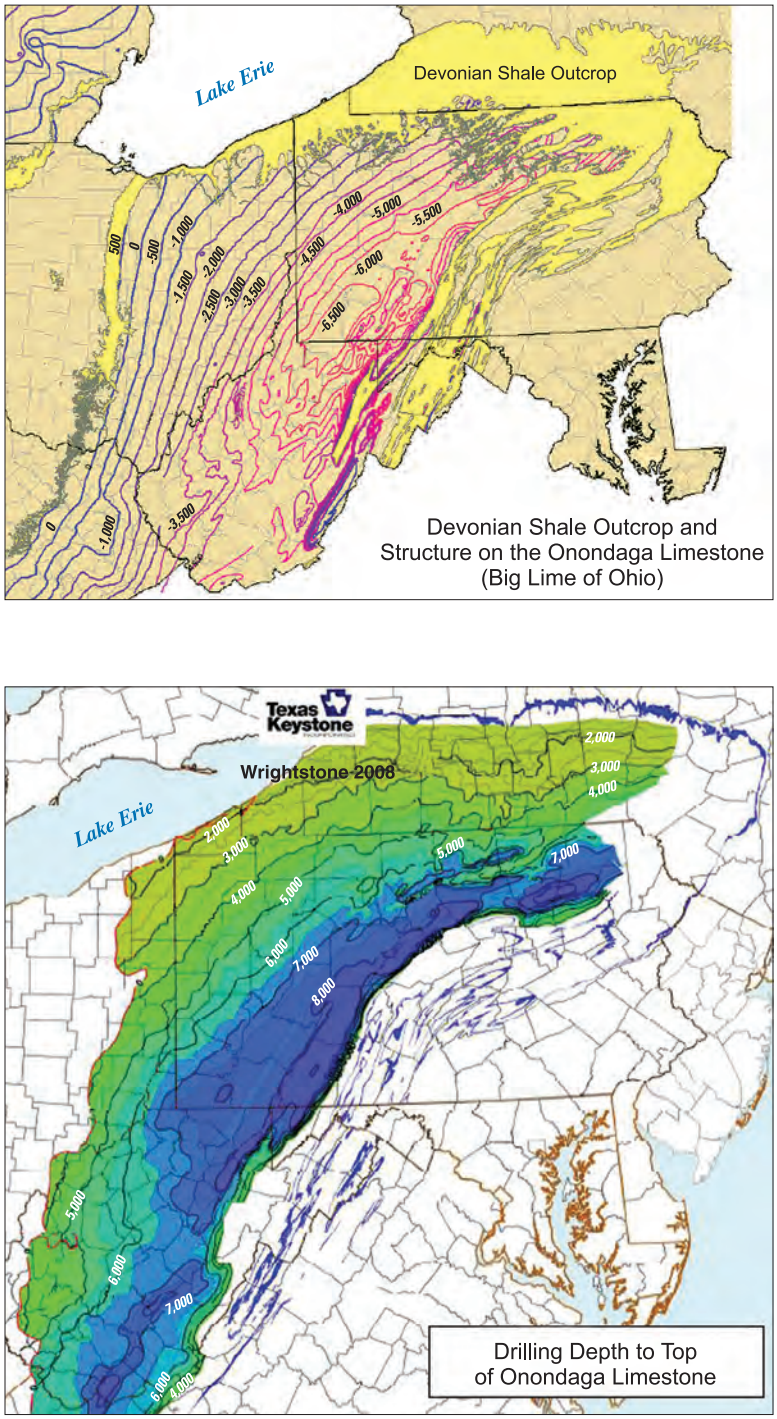

Figure 25. Top: structure map on top of Onondaga Limestone (base of Marcellus Shale); modified from Wickstrom and Carter, 2008. Bottom: drilling depth to top of Onondaga Limestone (base of Marcellus); modified from Wrightstone, 2008.

obstructed by Precambrian rocks of the Adirondack Uplift in New York. Across the basin is the Cincinnati Arch in Ohio, a crustal arch or peripheral bulge that developed on the foreland in response to tectonic and sedimentary loading at the plate margin (Figure 24) (Shumaker, 1996). Devonian strata dip eastward from the Cincinnati Arch at an average rate of 55 ft/mi so that the Marcellus now occurs at a subsurface depth of nearly 10,000 ft in central Pennsylvania.

4.2.2 Stratigraphy

The Marcellus Shale and the overlying Mahantango Formation constitute the Hamilton Group (Figures 26 and 27), belonging to the Eifelian and Givetian Stages of the Middle Devonian (Repetski and others, 2005). The Marcellus is a splintery, soft to moderately soft, gray to brownish black to black, carbonaceous, highly radioactive shale with beds of limestone and carbonate concretions (Figure 28). Pyrite is abundant, especially near the base, and fossils occur within the limestones. The formation thickness exceeds 660 ft in northeastern Pennsylvania (Figures 29 and 30), thinning dramatically in the west and southwest to 200 ft in central Pennsylvania, 140 ft in northern West Virginia, and eventually pinching out in eastern Ohio (Zielinski and McIver, 1982; Wrightstone, 2008; Boyce, 2009). Geographical limits of the Marcellus Shale seem to be erosional in all directions. The total thickness of radioactive black shale in the Hamilton Group, as determined by gamma-ray logs, parallels the thickness trend of the Marcellus, and this value is often mistakenly reported as that of the Marcellus itself (Figure 31) (Piotrowski and Harper, 1979; Roen, 1984; de Witt and others, 1993; Milici and Swezey, 2006; Geology.com, 2008).

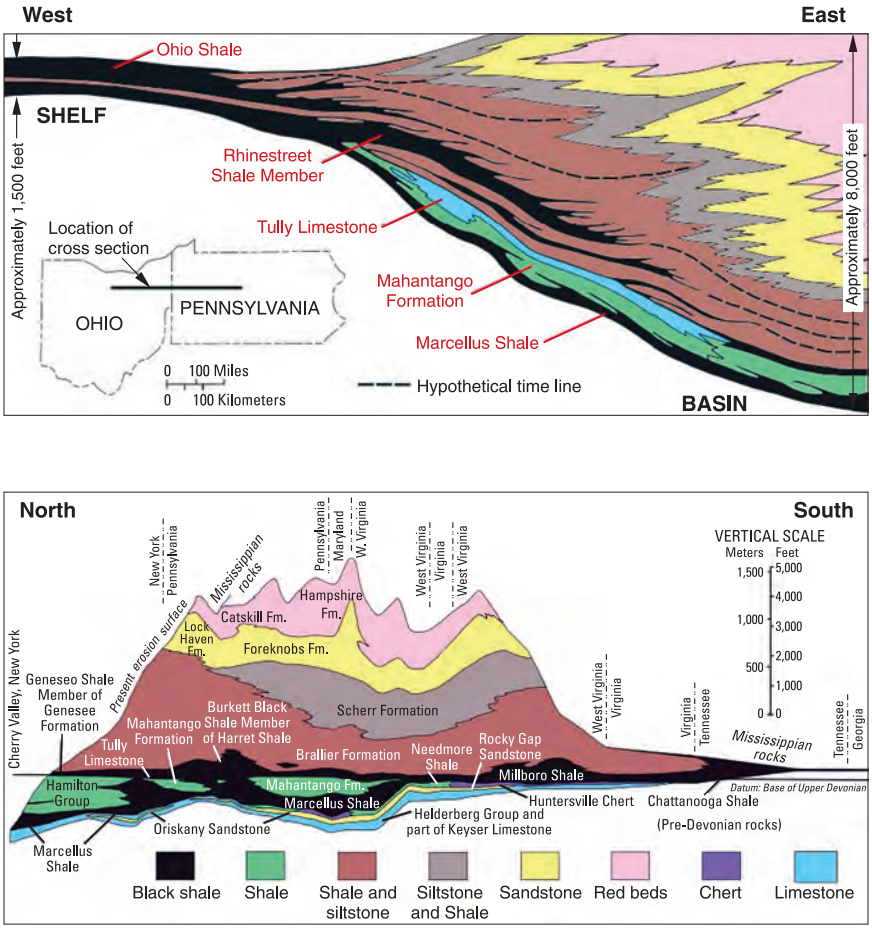

Figure 26. Stratigraphic cross sections illustrating relationships between Middle and Upper Devonian formations of central Appalachian basin. Top west-east; bottom north-south; modified from Wikipedia, Marcellus Formation, 2010.

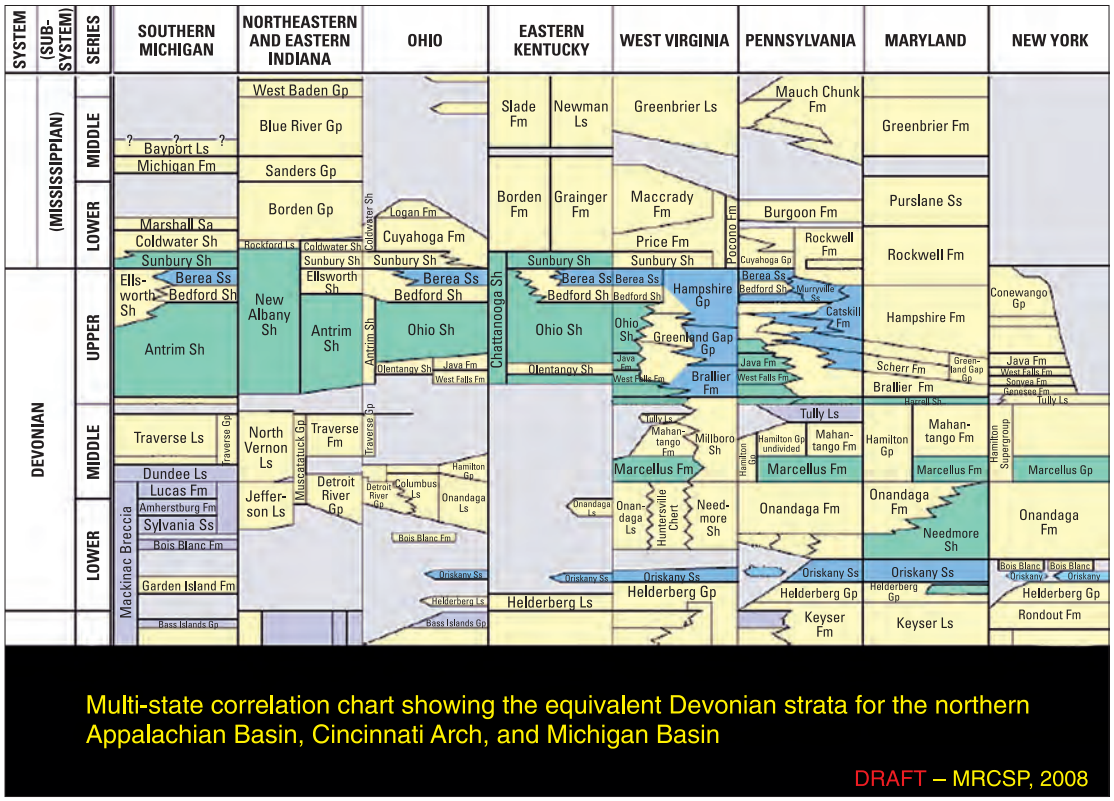

Figure 27. Multi-state correlation chart of Devonian strata in eastern U.S. The Middle-Upper Devonian Taghanic unconformity has removed much of the rock record in Ohio and adjoining states. Modified from Wickstrom and Carter, 2008.

In outcrops of western New York and the subsurface, the Marcellus is divided into three formal members. The Union Springs, the lower member, is thinly bedded, organic-rich, pyritiferous, blackish gray to black shale with lime-mudstone concretions. Interbeds of siltstone occur at its base. An isopach map shows that it reaches 60 ft (and possibly 150 ft) in northeastern Pennsylvania, pinches out to the west, but reappears in Ohio where it is less than 20 ft (Figure 32) (Zielinski and McIver, 1982; Lash, 2008; Wrightstone, 2008). The middle member, the Cherry Valley, is a skeletal limestone. In West Virginia the middle member is called the Purcell Limestone, a fine-grained limestone or an interbedding of limestone and calcitic shale (Dennison and Hasson, 1976). Barite nodules may be present. The Purcell varies in thickness from 50 to 100 ft, but disappears westward across the state. Most geologists consider the Cherry Valley and Purcell to be the same unit with different names; however, some geologists map the limestones in the subsurface as different units (Figure 33) (Barrett, no date). The upper member of the Marcellus, the Oatka Creek, comprises two units: a basal black shale resembling the Union Springs (and distinguishable on gamma-ray logs) and an upper unit of gray shale (Figure 34). An isopach map of the Oatka Creek shows that it reaches 270 ft (and possibly 570 ft) in eastern Pennsylvania and 120 ft in Ohio, but thins to 30 ft in central New York (Figure 32) (Zielinski and McIver, 1982; Lash, 2008; Wrightstone, 2008). This area of thinning is the same as where the Union Springs Member locally pinches out, suggesting the continued presence of a paleotopographic high (possible peripheral bulge) trending northeast-southwest in New York and Pennsylvania. In eastern New York and Pennsylvania, the Marcellus has been divided into a profusion of members (Nyahay and others, 2007; Ver Straeten, 2007). These members reflect a complex interbedding of organic-rich shale, gray or silty or calcareous shale, sandstone, and limestone. They include, among other members, Cardiff shale, Pecksport shale, Solsville sandstone, Bridgewater shale, Berne shale, Stony Hollow shale and limestone, and Bakovan black shale (Figure 34).

Immediately below the Marcellus lies a collection of formations of the Lower Devonian Onesquethaw Stage: Onondaga Limestone, Huntersville Chert, and Needmore Shale (Figure 35) (Dennison, 1961). The Onondaga is a cherty, argillaceous, calcarenitic limestone or an interbedding of medium-grained argillaceous

Top depth 7,496 feet

Bottom depth 7,505 feet

Top depth 7,451 feet

Bottom depth 7,463 feet

Figure 28. (Left) basal contact at 7,499.4 feet of calcareous black shale with the underlying limestone and gray calcareous shale of the Onondaga Limestone; (right) black, sooty, organic-rich Marcellus Shale; (bottom) close-up of organic-rich shale, MERC-1, Monongalia County, West Virginia.

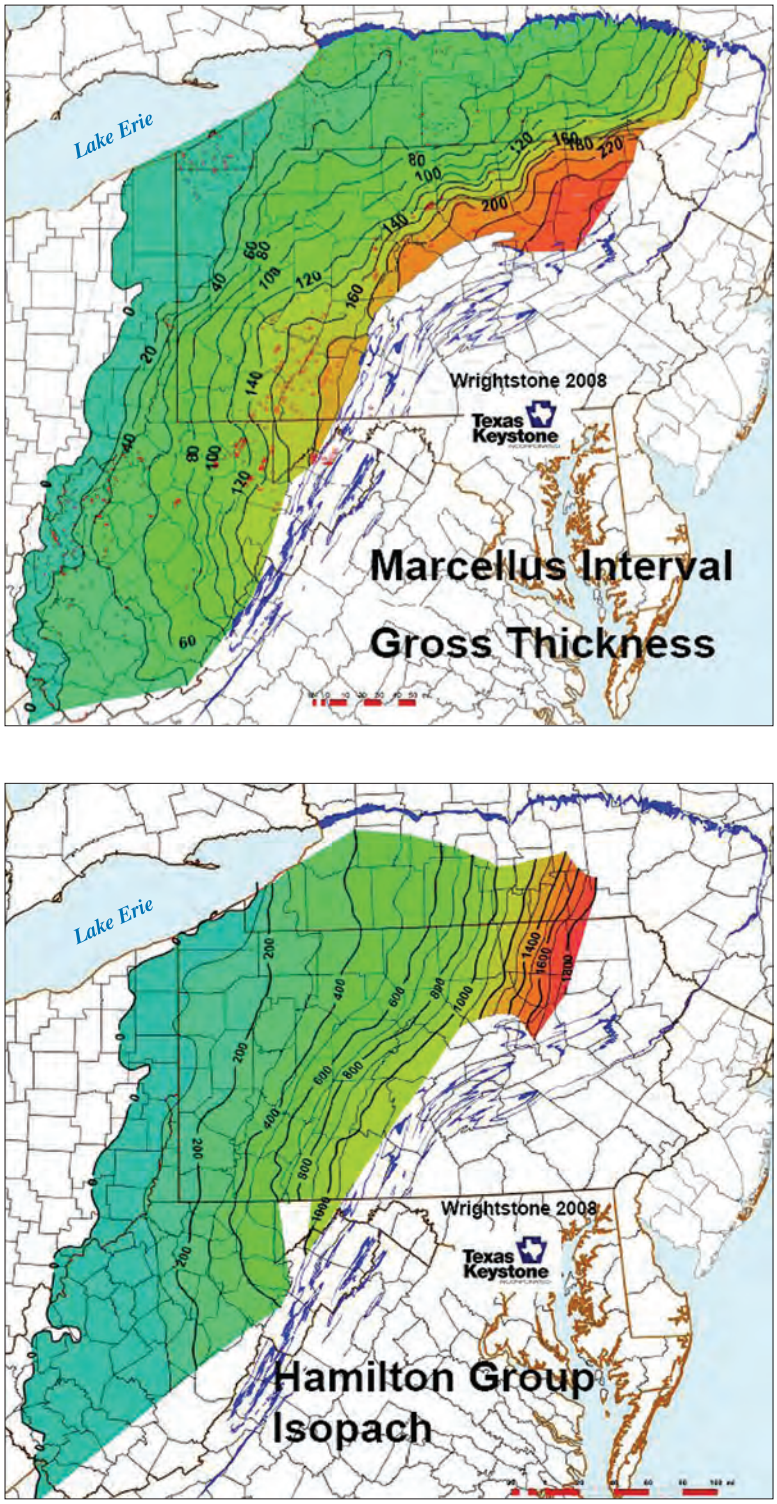

Figure 29. Isopach map of Marcellus Shale (above) and Hamilton Group, that is, Marcellus plus Mahantango (below). Modified from Wrightstone, 2008.

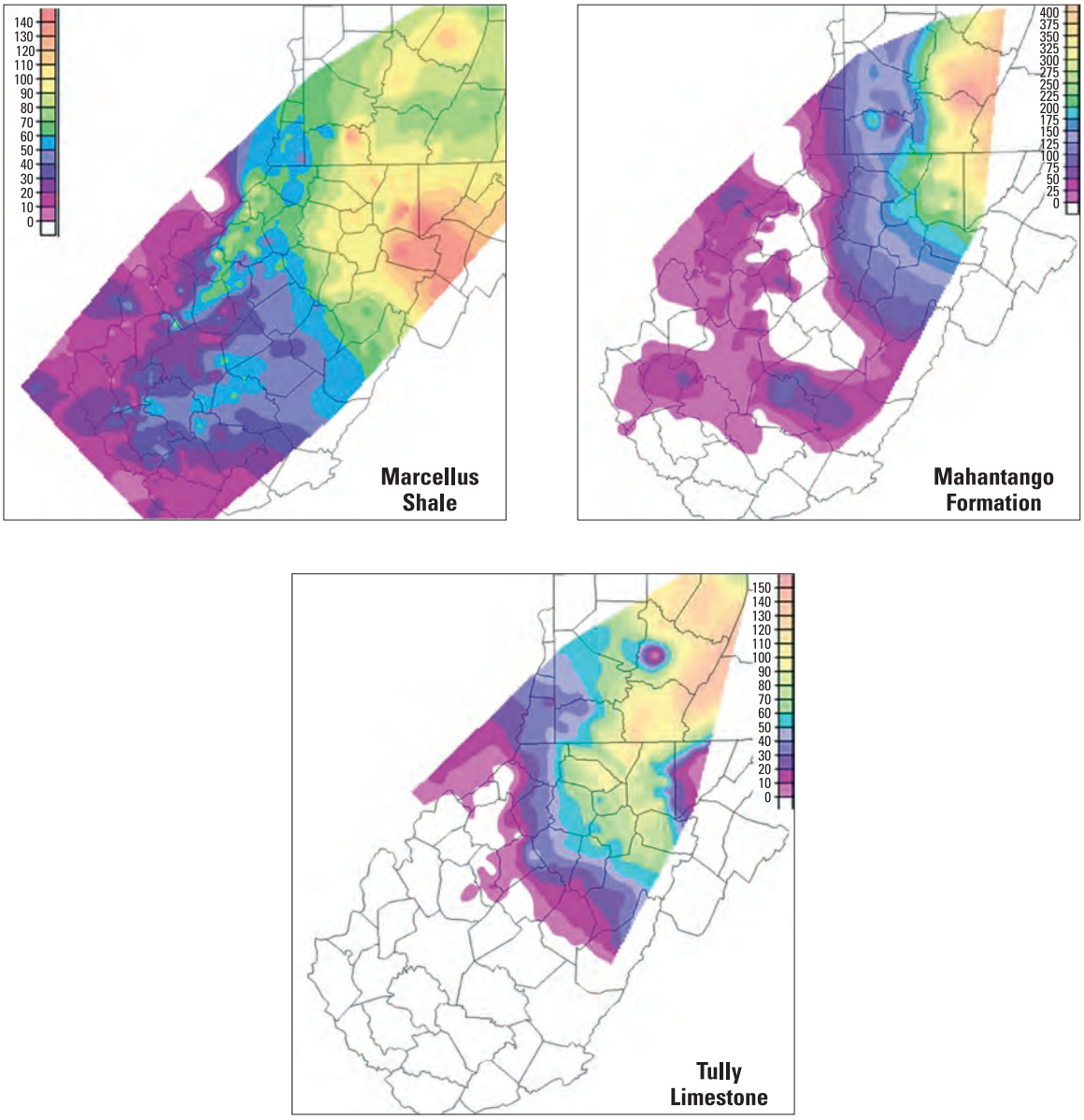

Figure 30. Isopach maps of Marcellus Shale (upper left), Mahantango Formation (upper right), and Tully Limestone (bottom) in West Virginia and southwestern Pennsylvania. Modified from Boyce, 2009 (scales in feet).

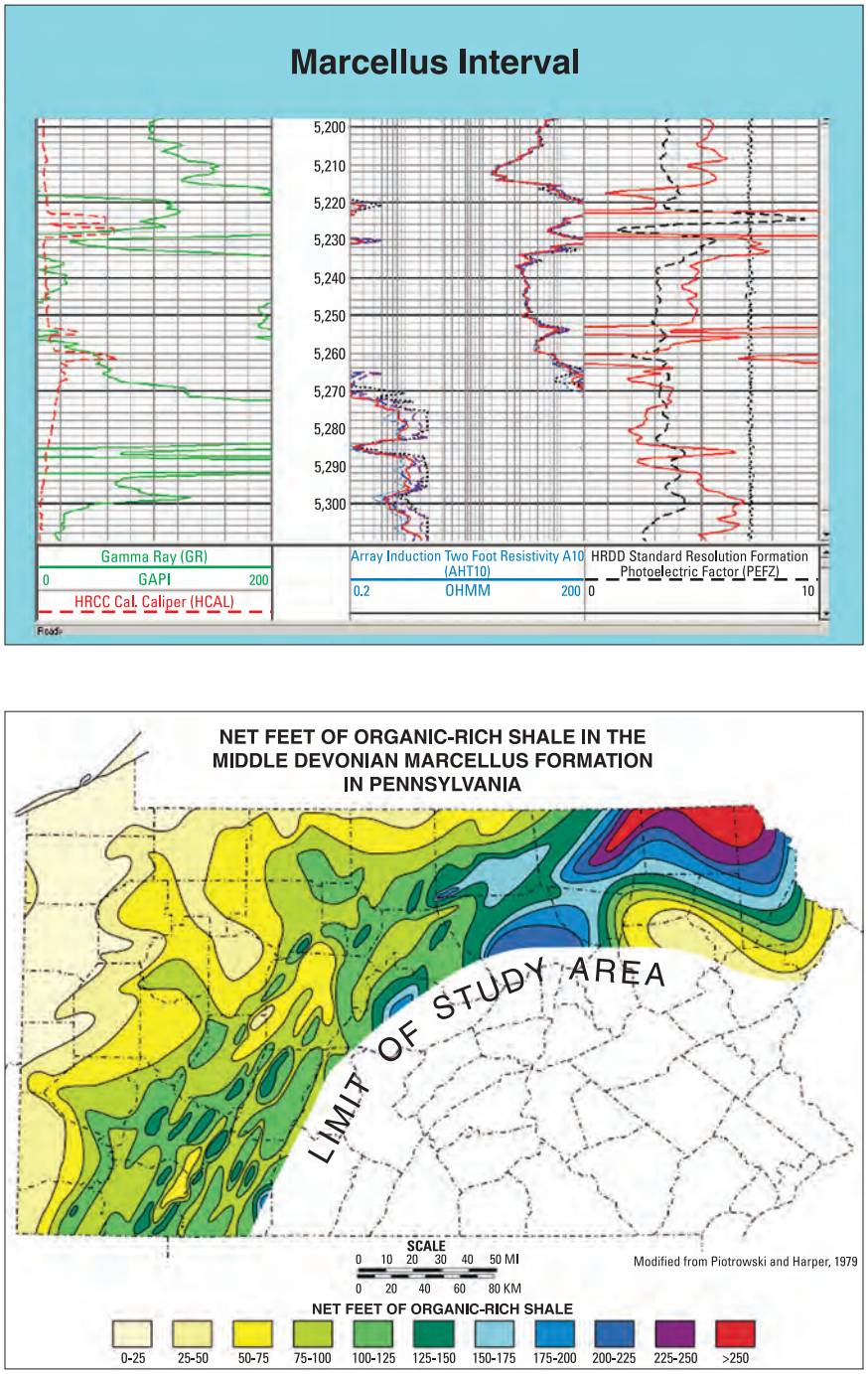

Figure 31. Top: organic-rich shale of upper and lower members of the Marcellus Shale identified by high values on the gamma-ray log; modified from Gottschling, 2007. Bottom: net feet of organic-rich shale in the Marcellus Shale of Pennsylvania; modified from Pennsylvania Department of Conservation and Natural Resources, no date.

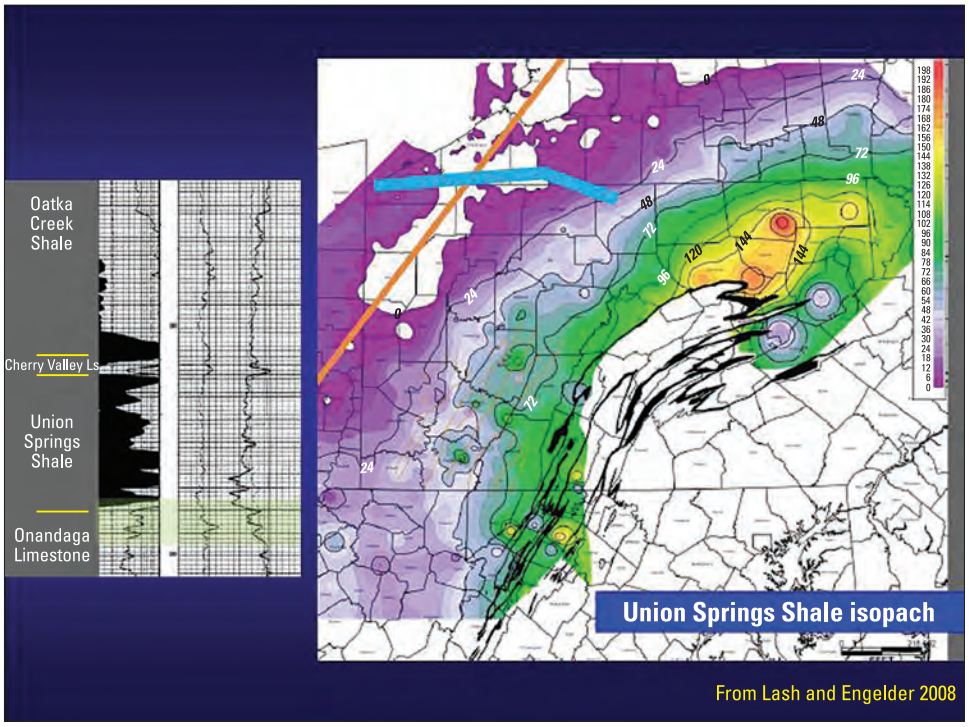

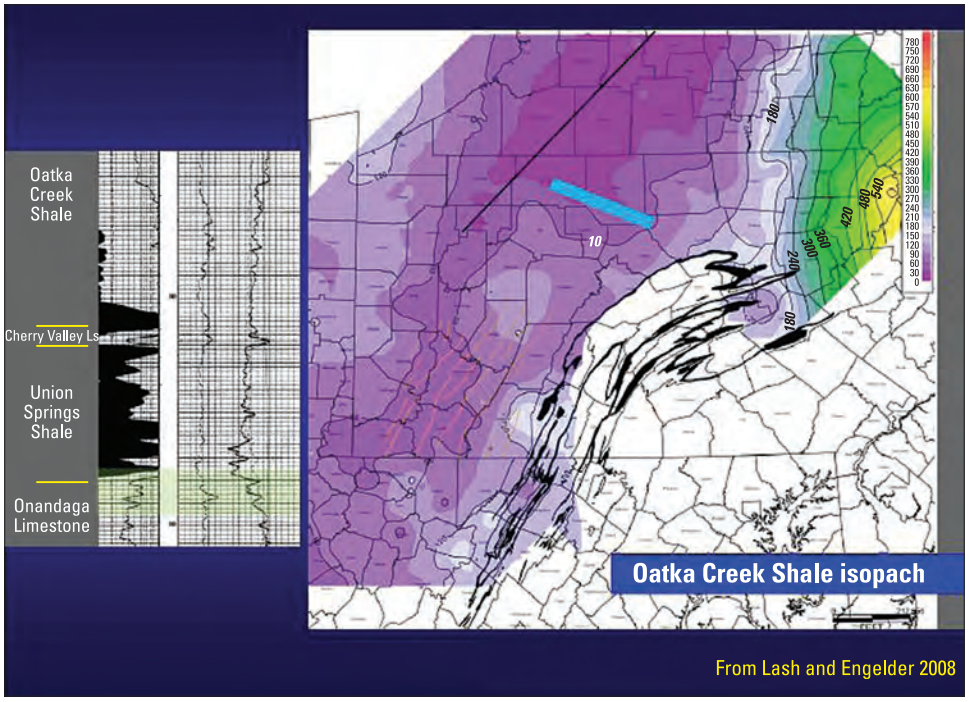

Figure 32. Isopach maps of Union Springs Member and Oatka Creek Member with well logs. Hotter colors represent higher values. Modified from Wrightstone, 2008.

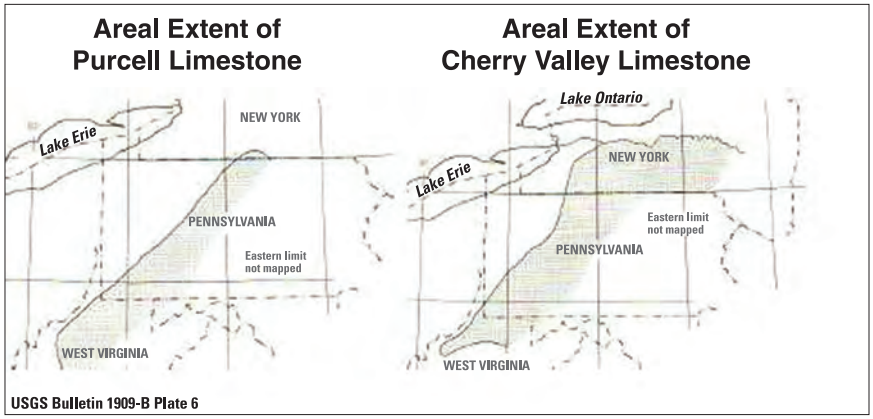

Figure 33. The distinct and different Purcell Limestone Member and Cherry Valley Limestone Member. Modified from Barrett, no date.

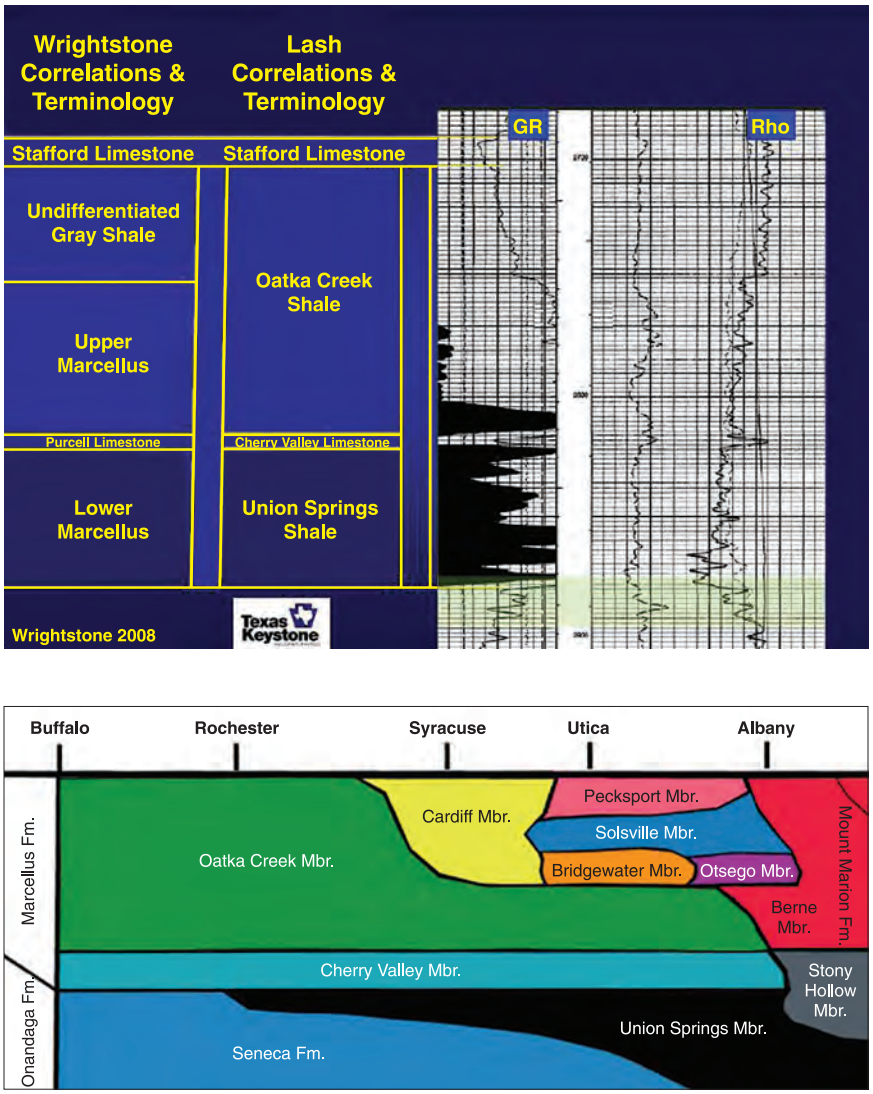

Figure 34. Top: members of the Marcellus Formation as recognized in the western subsurface with representative well log; modified from Wrightstone, 2008. Bottom: member nomenclature from west to east in New York; modified from Nyahay and others, 2007.

limestone and dark gray shale (Engelder, 2008a; Boyce, 2009). It generally occurs in the western and northern portions of the basin—Kentucky, Ohio, western West Virginia, western Pennsylvania, and southern New York (Milici and Swezey, 2006). The Huntersville Chert ranges from nearly pure chert to slightly calcitic or dolomitic chert to an intertonguing of chert and shale. It is present in the basin center of Pennsylvania and West Virginia. The Needmore Shale contains three members: the lower Beaver Dam of dark gray to gray-black fissile shale with chert nodules, a middle gray calcitic shale with limestone interbeds, and an upper calcareous shale and limestone (Dennison, 1961). It occurs in the eastern portion of the basin from Pennsylvania to Virginia, and correlates with the Esopus and Schoharie Formations of eastern New York (black shale, mudstone, silty and calcitic shale; Ver Straeten, 2007). The Needmore and Huntersville formations interfinger laterally in an east-west direction in Maryland and West Virginia (Dennison and Hasson, 1976), and the Huntersville and Onondaga formations also interfinger farther to the west-northwest. In the south-central Pennsylvania, a tongue of Onondaga Limestone extends eastward above the Needmore Shale and may be called the Selinsgrove Limestone (Engelder, 2008a). The upper contact of these formations with the Marcellus is usually sharp. Below the Onondaga/Huntersville/Needmore is the Oriskany Sandstone (Figure 36).

The Tioga ash fall, an interbedding of at least 8 tuffs and tuffaceous shales, occurs in the very uppermost Onondaga Limestone or Needmore Shale and the lowest Marcellus Shale, spanning a vertical interval of 2–8 ft at the stratigraphic contact. The ash fall cuts across the contact between uppermost Onesquethaw rocks and lowermost Marcellus, indicating a time equivalency between these strata. The rock consists of coarse angular quartz, sand-sized biotite flakes, and feldspar. These beds can be traced from Virginia to New York and westward into the Michigan and Illinois Basins, and they constitute a marker bed in subsurface correlations (Dennison and Hasson, 1976; Milici and Swezey, 2006; Engelder, 2008a). Dennison (1961) located the source volcano near Lexington, Virginia.

Above the Marcellus is the Mahantango Formation, the upper unit of the Hamilton Group. The Mahantango contains a variable mix of mudstone, limestone, sandstone, and conglomerate. In the eastern portion of the basin, shale and siltstone dominate the section, and a number of members have been designated (Gandes Run Shale, Chaneysville Siltstone, Frame Shale, Clearville Siltstone, and Pokejoy Limestone, from bottom to top; Dennison and Hasson, 1976). All of these members coarsen to the east, some even becoming sandstone with local quartz-pebble conglomerate. In eastern Pennsylvania, sandstone, siltstone, and claystone beds of the Mahantango are arranged into four members (Turkey Ridge Sandstone, Dalmatia, Montebello Sandstone, and Sherman Ridge from bottom to top; Harper, 1999). In the western part of the basin, shale and limestone dominate. Many members have been named (Stafford Limestone, Skaneateles Shale, Levanna Shale, Centerfield Limestone, Ledyard Shale, Ludlowville Shale, Tichenor Limestone, and Moscow Shale, from bottom to top), but the stratigraphic nomenclature has not been standardized (Hill and others, 2004; Lash, 2007; Wrightstone, 2008). The Skaneateles Member is shale that is locally black in western Pennsylvania and central New York (Roen, 1984). The thickness of the Mahantango Formation (upper Hamilton Group) reaches 1700 ft in northeastern Pennsylvania and adjacent New York, thinning to the west and southwest and pinching out near the Pennsylvania/Ohio border and in central West Virginia (clastic wedge shown in Figures 29 and 30) (Zielinski and McIver, 1982; Wrightstone, 2008; Boyce, 2009). Where the Mahantango is absent in the south and extreme west, the entire Hamilton Group is represented by black shale of the Marcellus (or the Millboro Shale of Dennison and Hasson, 1976, which also includes the overlying Harrell Shale).

The Tully Limestone, well bedded, fossiliferous, argillaceous, and pyritiferous micritic limestone and limey shale, lies above the Mahantango. It is more shaly below and a purer limestone above. Minor unconformities are recognized at the base and within the Tully (Milici and Swezey, 2006; Lash, 2008). Some workers classify the Tully as a formation, whereas others include it as the uppermost member of the Mahantango Formation. The Tully ranges in thickness from 0–200 ft and is distributed from central New York, to west-central Pennsylvania, and through central West Virginia (Figures 30 and 35) (Dennison and Hasson, 1976; Milici and Swezey, 2006; Wrightstone, 2008; Boyce, 2009).

Conformably above the Tully may be any of several Upper Devonian formations (Figures 26 and 27). To the far east is the Brallier Formation, dark gray, thickly laminated shale with thin interbeds of siltstone (Dennison and Hasson, 1976). The Harrell Shale of outcrops in Pennsylvania, Maryland, and West Virginia is medium- to dark-gray, generally organic-rich, fissile shale, and in particular the Burkett Member at the base of the Harrell is gray-black to black, carbonaceous, fissile clay shale containing abundant pyrite (Engelder, 2008a). In western outcrops of Pennsylvania, black fissile shale immediately below the Tully and above the Manhantango may also be called Burkett or Harrell (Dennison and Hasson, 1976). To the northwest in New York is the Geneseo Shale of the Genesee Group, another black, petroliferous shale; the Geneseo is apparently continuous with the Burkett through the subsurface of Pennsylvania (Hill and others, 2004; Lash, 2007).

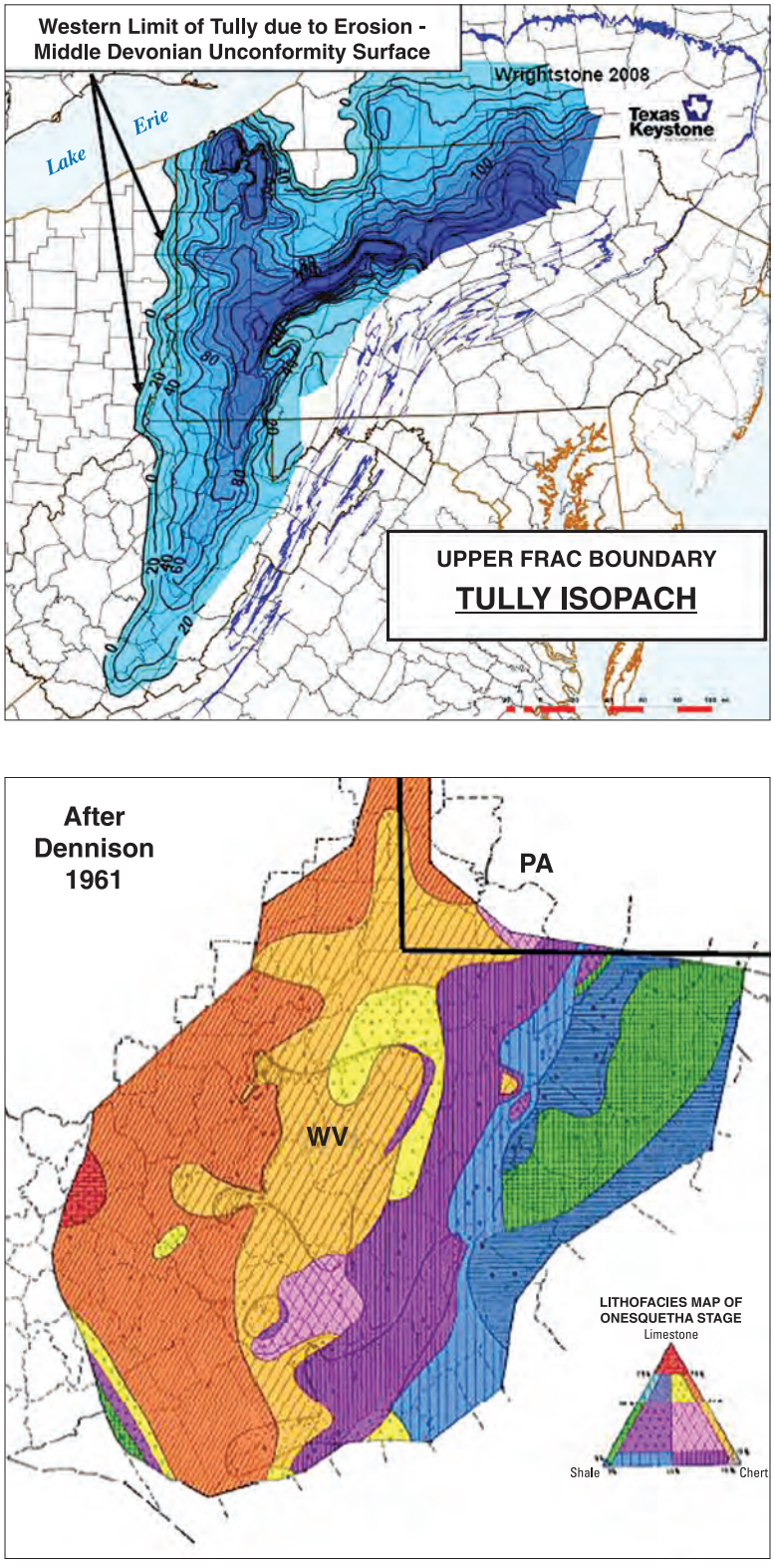

Figure 35. Top: isopach map of overlying Tully Limestone. Bottom: dominant rock type of underlying Onesquethaw units in West Virginia—Onondaga Limestone to the west, Huntersville Chert in the central region, and Needmore Shale to the east. Modified from Wrightstone, 2008.

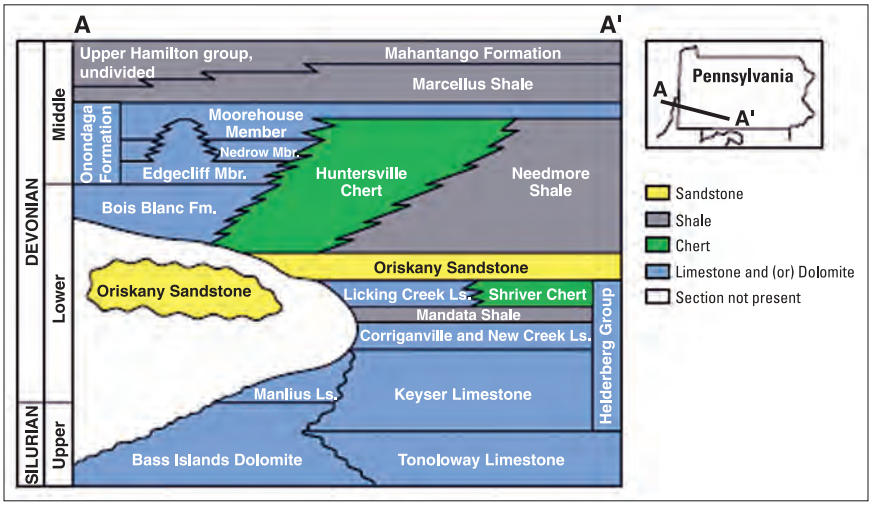

Figure 36. Generalized stratigraphy of Oriskany Sandstone (water bearing), Onondaga Limestone (fracture barrier), Needmore Shale and Huntersville Chert (not fracture barriers), and Marcellus Shale in Pennsylvania and Ohio. Modified from Milici and Swezey, 2006.

4.2.3 Tectonics and Structure

In the eastern thrust belt and the eastern section of the Allegheny Plateau Province, most major geologic structures are detached. These structures become less complex away from the orogen: deformed thrust blocks in a narrow duplex structure along the Allegheny Front, a zone of high-amplitude plateau folds, a zone of low-amplitude plateau folds, and finally undeformed strata in the far west (Shumaker, 1996). In the northern portion of the basin, the Marcellus is underlain by a regional decollement in salt beds of the Silurian Salina Group, whereas in the southern portion of the basin the thick package of Middle-Upper Devonian shales contains the major decollement fault (Shumaker, 1996; Milici and Swezey, 2006).

In addition, a number of large structural elements are basement-related (Shumaker, 1996), including the Cincinnati and Waverly Arches (peripheral bulges), the Cambridge Arch and the mid-foreland hinge (draping faults along the margin of basement blocks), and the eastern Pennsylvania depocenter (a rift graben). Other structures, too, may be basement-related: subsidence of small, semi-independent crustal blocks; drape folds above horst blocks; inversion anticlines above basement depressions (e.g. Warfield Anticline); and weak zones of the basement which localized the position of a forebulge (e.g.Clarendon-Linden fault system of New York; Lash, 2008). Much of the Marcellus play in Pennsylvania, New York, and West Virginia is in the Plateau area of low-amplitude folds (amplitude less than 700 ft, maximum dip of 2–3°) and associated fracturing. In eastern outcrops of West Virginia, a decollement usually develops at the base of the Marcellus, and the formation is nearly always drag-folded (Dennison, 1961).

The Rome Trough is a complex series of grabens which developed in association with Late Precambrian-Early Cambrian rifting of the passive continental margin and formation of the Iapetus Ocean (Figure 37) (Shumaker, 1996; Curtis, 2002). Offset of the Precambrian (Grenville) basement surface by Rome faulting can be traced from southern and eastern Kentucky, through western West Virginia, and into southern and central Pennsylvania (Shumaker, 1996). These basement faults demonstrate a complex history of slip direction and recurrent movement. Although almost all of their structural relief is due to Early-Middle Cambrian extension, reactivation of these faults occurred repeatedly through at least Middle Devonian time (demonstrated by detailed, regional lithofacies and isopach maps; Shumaker, 1996). Reactivation primarily took place in response to compressional stress of orogeny at the plate margin, forming depocenters within the epeiric seaway of the Appalachian Basin (Curtis, 2002). Topographic relief produced by reactivation affected the nature, distribution, and thickness of the sedimentary basin-fill (Donaldson and Shumaker, 1981).

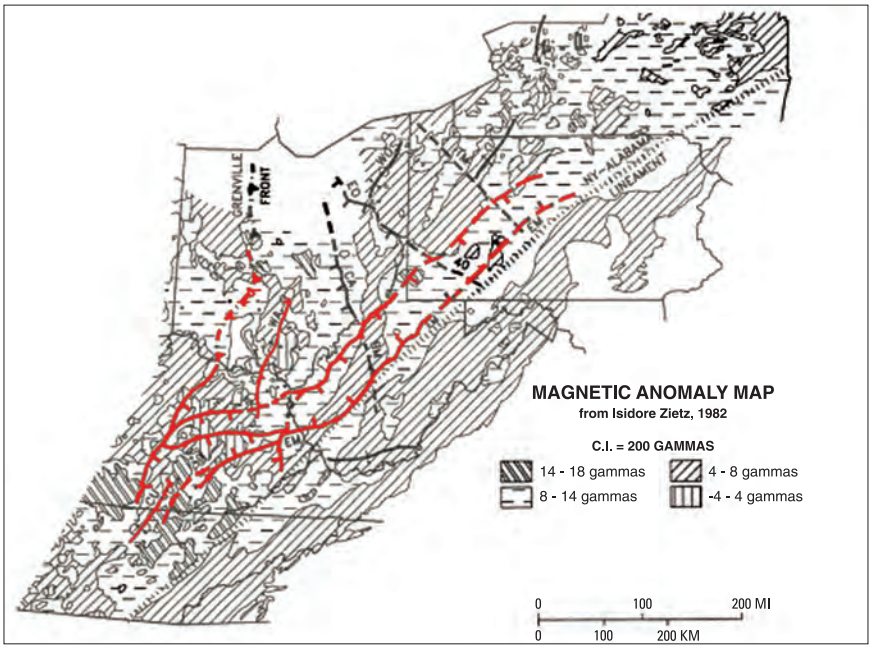

Figure 37. Trend of Rome Trough from Kentucky through Pennsylvania as indicated by basement faults (shown in red). Modified from Shumaker and Wilson, 1996.

In the central Appalachian Basin, the Devonian-Mississippian Acadian Orogeny is reflected by changes in subsidence rate, a large influx of siliciclastic sediment from the thrust-and-fold belt, and the assimilation of Cambrian grabens into a developing and deepening foreland basin (Shumaker, 1996). Ettensohn (1994) divided the Acadian Orogeny into four tectophases as interpreted from the stratigraphic record, marked by the Needmore, Marcellus, Geneseo-Burkett, and Sunbury black shales (Figures 38 and 39) (Lash, 2008). Each tectophase began with the emplacement of a new thrust load and consequent deepening of the foreland basin (Quinlan and Beaumont, 1984). The basin was initially starved of terrigenous sediment because insufficient time had elapsed for an efficient fluvial system to develop in the thrusted highland. Instead, deposition of autochthonous sediment—black shale—occurred (Curtis, 2002; Engelder, 2008a). As the basin subsided, a peripheral bulge rose (perhaps with erosion or nondeposition along the crest) and migrated away from the thrust load. Lash (2008) interpreted the several minor unconformities in New York (Marcellus through Tully Formations) to have resulted from intermittent uplift of the peripheral bulge. Eventually, sediment eroded from the eastern highland prograded across the basin as a thick clastic wedge, occasionally filling or overtopping the basin. At this point, weight of the static tectonic load caused the basin to deepen and narrow and the bulge to subside and migrate toward the orogen. With tectonic quiescence and erosional unloading, carbonate sediments accumulated and the tectophase was complete. The black-shale depocenters migrated westward throughout the Acadian Orogeny, reflecting the continual cratonward movement of the zone of deformation (Figure 26).

Several sets of planar systematic joints in the Marcellus were identified by Lash (2008), Engelder (2008a), Engelder and Lash (2008), and Engelder and others (2009) , chiefly in outcrops of New York and Pennsylvania but also in subsurface cores (Figure 40). Two joint sets (labeled J_1 and J_2) are pervasive throughout the basin and considered important to natural gas production, whereas two other sets (J_0 the earliest formed and J_3 attributed to glacial rebound) are of only minor or local distribution. J_1 joints exhibit a consistent strike of 60–75°, and J_2, a strike of 315–345°. J_1 joints are more closely spaced and are crosscut by J_2 joints. J_1 joints, which can be traced from Virginia to New York, predate Allegheny folding, whereas J_2 joints were synchronous with that folding (oriented perpendicular to fold axes). Both sets are thought to have been produced by natural hydraulic fracturing, having formed when increased fluid pressure in the shale near maximum burial depth (approximately 4 km) exceeded the compressive strength of the rock (Lash, 2008; Engelder and others, 2009). The buildup of fluid pressure is attributed to disequilibrium compaction because of the rock's low permeability and to volume changes in the shale as organic matter was converted to hydrocarbons

(Lash, 2008). However, Arthur and others (2008a) thought that the joints formed when rock pressure dropped due to overburden erosion and/or tectonic uplift. The fractures grew first as microfractures which then continued to open to full-scale joints (Engelder and Lash, 2008). J_0 joints (strike 352–007°) are only common locally. J_3 joints are vertical and oriented ENE; these are neotectonic in origin, probably related to glacial rebound since the Pleistocene. In eastern outcrops of Pennsylvania, Engelder (2008a) also noted the presence of pencil cleavage in the Marcellus (layer-parallel shortening from pressure solution), small-scale faulting (cleavage duplex), and complex folding.

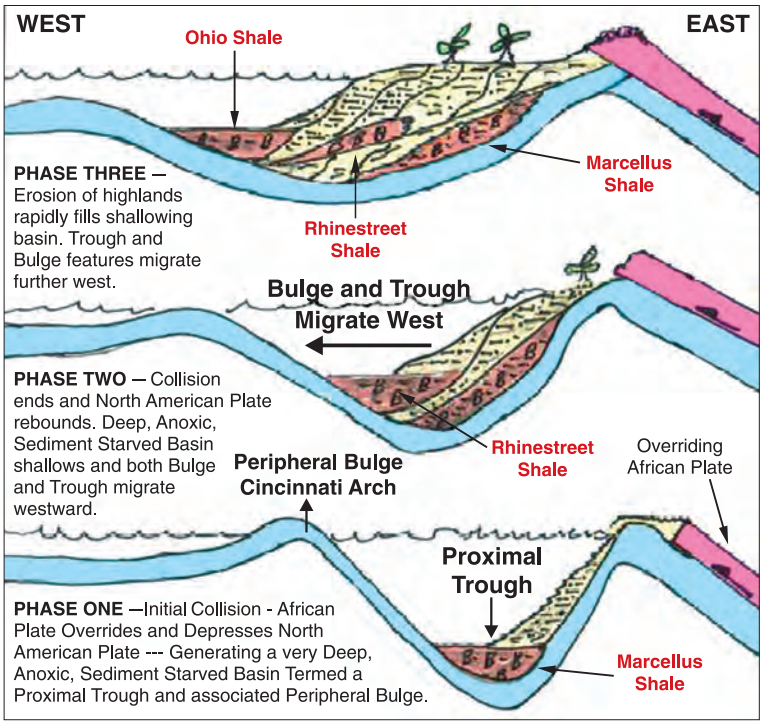

Figure 38. Sedimentary-structural model for black shales of the Appalachian basin. Modified from Barrett, no date.

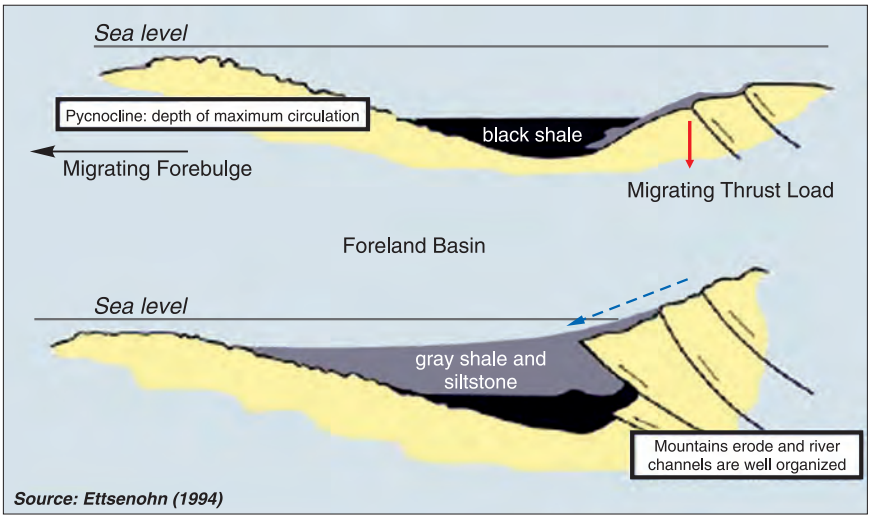

Figure 39. Sedimentary-structural model for black shales of the Appalachian basin. Modified from Engelder and Lash, 2008.

Figure 40. Outcrop photographs of J_1 joints (top), J_2 joints (middle), and gas-migration pathway from matrix to fracture (bottom). Modified from Engelder and Lash, 2008.

4.2.4 Lithology and Lithofacies

Little information about Marcellus lithofacies is published. Available lithological data are usually integrated with those of other black shales of the Middle and Upper Devonian.

Harper (1999) and Milici and Swezey (2006) described the well accepted, regional facies model for the Acadian clastic wedge (Figures 26 and 38). Five separate lithofacies are recognized, arranged into at least seven basinwide, coarsening-upward sequences that span Middle Devonian through Early Mississippian time (Filer, 1994; Engelder and Lash, 2008). These are:

1. Dark-gray to black (also brownish black and olive black), calcitic, pyritiferous, sparsely fossiliferous shale. Black-shale facies are present in the Needmore, Esopus, Marcellus, Geneseo, Burkett, Penn Yan, Renwick, Middlesex, Sonyea, Rhinestreet, Pipe Creek, Java, Huron, Dunkirk, Cleveland, and Sunbury stratigraphic units. Black shales mark the base of the vertically stacked sequences. They generally occur in the western part of the basin with numerous tongues extending eastward to varying distances (Hill and others, 2004; Ettensohn and others, 1988).

2. Sparsely fossiliferous, interbedded dark gray shale and light to medium-gray siltstone.

3. Light to dark green, brown, purple, and red, highly fossiliferous shale, siltstone, and fine-grained sandstone.

4. Silty, micaceous mudrock; fine- to coarse grained, fossiliferous siltstone, sandstone, and conglomerate; and interspersed limestone.

5. Gray and red beds of mudstone, siltstone, sandstone, and conglomerate.

Petrographic studies of the Middle-Upper Devonian shales usually rely on a combination of methods—light microscopy, SEM microscopy, X-radiography, and X-ray diffraction. Larese and Heald (1977) identified six lithofacies based on grain size and mineral composition: shale, silty shale, shaly siltstone, dolomitic shale, dolostone, and very fine-grained argillaceous sandstone. Nuhfer and others (1979) identified six lithofacies based on rock fabric: thinly laminated shale, lenticular laminated shale, sharply banded shale, nonbanded shale, siltstone, and concretions. Potter and others (1980) identified six major lithofacies based on the percent of clay: claystone, clayshale, mudshale, bituminous shale, siltstone, and siltshale. Minor facies include marlstone, sandstone, carbonate rock, and pyritic shale. And three types of lamination occur in these rocks: clay laminae (> 95% clay minerals oriented parallel to lamination), organic laminae (quartz + clay minerals + abundant organic matter, generally with sharp contacts), and quartz laminae (both ungraded and graded).

The black bituminous shale is laminated (fissile) and lacks bioturbation (Figure 28). The chief minerals are illite, chlorite, kaolinite, and mixed-layer clays (35%), fine angular quartz (10–25%), feldspar (< 10%), muscovite and chlorite (5–30%), calcite (25%), plus pyrite and organic matter (Roen, 1984). Wrightstone (2008) reported a much higher silica content (40–60%), and the quartz content is probably higher on the eastern side of the basin (Lyle, 2009). Zielinski and McIver (1982) presented additional mineral data: quartz 27–31%, sodium feldspar 0–4%, potassium feldspar 0%, calcite 3–48% and dolomite 0–10% (carbonate minerals much more abundant in the lower Marcellus member), siderite 0%, pyrite 5–13%, illite 9–34% (more abundant in upper member), mixed-layer clays 1–7%, chlorite 0–4%, montmorillonite 0%, kaolinite 0%, and gypsum 0–6%. Pyrite (which is more common toward the base of the formation; Engelder, 2008a) takes the form of framboids, microcrystals, and euhedral crystals. Calcitic zones occur higher in the formation. Siderite concretions also occur in the shales. Articulate and inarticulate brachiopods, ostracodes, cephalopods (goniatites), tentaculitids, conodonts, radiolaria, and crinoids have been reported in the black shale (Dennison, 1961; Schweitering, 1981; Avary and Lewis, 2008).

Zielinski and Nance (1979) related the bulk-density log to rock type in the shale. A density reading of 2.65–2.73 g/cm^3 units indicates calcitic shale, 2.50–2.65 g/cm^3 siliceous shale, and less than 2.4 g/cm^3 organic-rich shale.

4.2.5 Depositional Environment

The generalized sedimentary model for rocks of the Acadian clastic wedge entails a gently inclined ramp sloping from eastern highlands to western basin center (Harper; 1999; Castle, 2000; Milici and Swezey, 2006). The linear, mostly muddy shoreline extended from New York to Virginia but was interrupted by a number of

small, sandy, fluvial- and wave-dominated deltas. Time-transgressive lithofacies include (1) dark-gray to black shale of the deep basin center; (2) interbedded dark gray shale and siltstone produced by turbidity currents on the lower ramp; (3) green to brown shale, siltstone, and fine sandstone of a shallow, offshore-marine setting; (4) fossiliferous, fine- to coarse-grained sandstone, conglomerate, siltstone, mudstone, and occasional limestone deposited in nearshore, inshore, and paralic environments; and (5) red, nonmarine and marginal-marine mudstone, siltstone, sandstone, and conglomerate of meandering and braided streams. Dennison (1961), Van Tyne (1996), and Milici and Swezey (2006) envisioned a carbonate platform (Delaware, Dundee, and Seneca Limestones) bordering the Marcellus basin on its western side in central Ohio, western New York and adjacent Pennsylvania before being inundated by black shale; however, the major Middle-Upper Devonian Taghanic unconformity removed much of the stratigraphic section on the flank of the Cincinnati Arch (Figure 27) (Schweitering, 1981; Milici and Swezey, 2006).

Most geologists accept an anoxic, deep-water origin for the Marcellus Shale and other black shales of the Devonian-Mississippian (Boswell, 1996; Curtis, 2002; Ettensohn, 2008; Boyce, 2009). The beginning of the second Acadian tectophase was marked by increased tectonic loading in the eastern thrust belt and a rapid deepening of the epeiric sea. The newly raised Acadian mountains blocked the subtropical trade wind and created a rain shadow on the foreland side, which in turn led to reduced wave and current activity in the epeiric sea and to a greatly reduced influx of water-borne siliciclastic sediment (Ettensohn, 1985). Indeed, petrographic observations of quartz silt in the Marcellus show surface features indicative of an aeolian origin (Werne and others, 2002). Perhaps the basin was divided into fault-bound subbasins which further reduced circulation (Curtis, 2002; Harper, 2008). Marine circulation was poor, the water column stratified, the sea floor below the pycnocline, and the bottom water oxygen-poor, all favoring the preservation of organic matter.

The evolution of large vascular plants on land may have enhanced chemical weathering in the adjacent source area, thereby increasing riverine nutrient fluxes and promoting development of eutrophic conditions in the epeiric sea (Algeo and Scheckler, 1998; Rimmer and others, 2003). High biological productivity of organic carbon in the surface water because of periodic algal blooms—principally *Tasmanites* green algae—ultimately led to a high biological oxygen demand and anoxia in the bottom water. However, Zielinski and McIver (1982), in explaining the negative relationship between marine *Tasmanites* and river-borne woody material, speculated that these algae were adversely affected by large inputs of toxic mineral matter from terrestrial sources. Alternatively, a large input of fresh water from occasional floods on the eastern landmass may have proved detrimental to these marine algae, or more simply, a deluge of river-borne woody matter may have intermittently diluted algal remains in the sediment. In any case, the introduction of terrigenous sediment and chemical nutrients, particularly on the western side of the basin, would have been low most of the time because of the inferred arid climate, great distance to the source area, and disruption of the eastern river systems by thrust faulting.

Zielinski and McIver (1982) identified three palynological biofacies whose areal distribution changed over time (Figure 41). (1) The *Tasmanites* biofacies is characterized by very large numbers of these green algae, often to the exclusion of other marine forms. Any included herbaceous matter may have been wind-blown. (2) The marine biofacies includes normal-marine forms such as chitonozoans, acritarchs, scoleocodonts, leisospheres, and sphaeromorphs plus a few *Tasmanites* and some herbaceous material. (3) The terrestrial biofacies, although deposited in a marine environment, consists of mostly terrestrial plant material: fresh woody debris and oxidized and reworked woody material. In early Marcellus time much of the basin (western New York, western Pennsylvania, eastern Ohio, and northern West Virginia) was dominated by the *Tasmanites* biofacies with just minor occurrences of the terrestrial biofacies to the east. In late Marcellus time the western *Tasmanites* facies began to be replaced by the marine biofacies, while the terrigenous biofacies encroached from the east.

Water depth in the Marcellus sea may have been 80–310 m (Ettensohn, 2008). Subsequent infilling of the basin by prograding coarse-grained clastics led to shallower water and dysaerobic to aerobic conditions. The overlying limestone represents a time of shallow, well oxygenated water. Deposition was orderly, reflecting a regular change in water depth and chemistry—basal organic-rich shale of the Marcellus, overlying coarsening-upward clastic wedge of the Mahantango, capped by limestone of the Tully (Curtis, 2002). Superimposed on this large-scale sequence were a number of smaller facies changes (Purcell, Cherry Valley, and upper Oatka Creek Members) and disconformities (in the Marcellus and Tully), attributed to minor fluctuations of sea level and/or tectonic movements of the peripheral bulge or other basement features (Hill and others, 2004; Lash, 2008).

Lash (2008) interpreted the origin of carbonate concretions in black shale of the Upper Devonian Rhinestreet Shale to be very early diagenetic, and perhaps this model applies to carbonate concretions of the

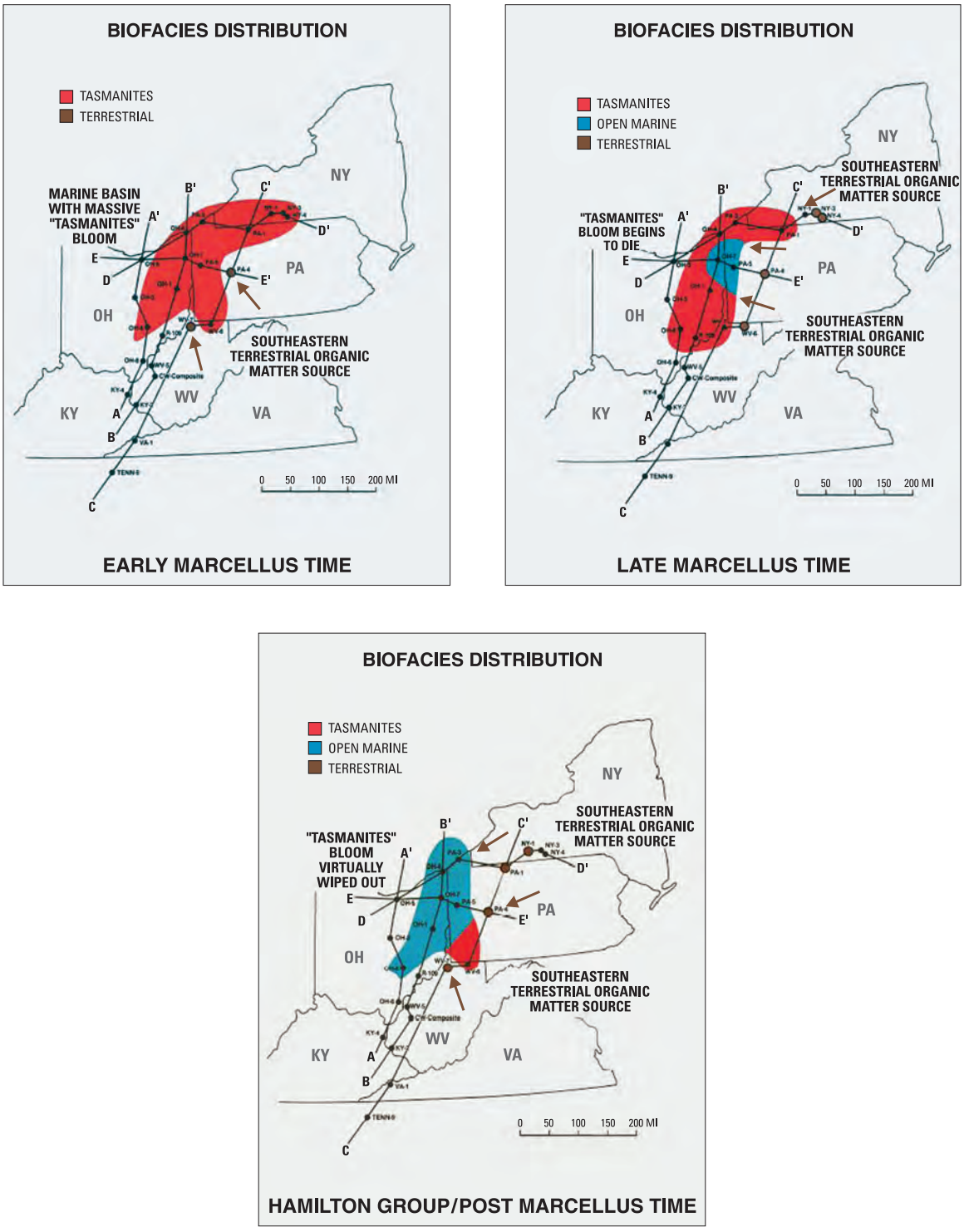

Figure 41. Palynological biofacies maps for the lower and upper members of the Marcellus Shale and the overlying Mahantango Formation. Red = Tasmanites, blue = normal-marine, and brown = terrestrial palynological forms. Modified from Zielinski and McIver, 1982.

Marcellus. They originated perhaps one meter below the sea floor, along a stratigraphic horizon, and before the onset of compaction. Passive precipitation of calcite within interparticle pores of the newly deposited mud (original porosity calculated to have been 74–93%) formed the concretions.

A few authors have proposed different interpretations for strata of the Acadian clastic wedge. For example, Schwietering (1978) favored a relatively shallow-water origin for the Devonian black shales. The black-shale facies may have accumulated on a western platform over the Cincinnati Arch, with water depth as shallow as 300 ft and salinity varying from normal-marine to brackish. Perkins and others (2008) postulated that the eastern trade wind initiated upwelling currents in the basin while the arid climate limited fresh-water input. Consequently the water column was unstratified, and the bottom water experienced a robust exchange with the open ocean. Bottom water was generally suboxic, but not continuously anoxic. And Dennison (1985) suggested that the limestones resulted from eustatic transgression.

4.3 Petroleum Geology

4.3.1 U.S. Department of Energy's Eastern Gas Shale Project

The Eastern Gas Shale Project of the late 1970s and early 1980s generated a vast amount of data concerning the stratigraphy, structure, petrology, geochemistry and petroleum potential of Middle and Upper Devonian black shales in the Appalachian Basin. Much of this information, particularly data relating to shale geochemistry, was assembled and published by Zielinski and McIver (1982), and this section summaries that report. Prophetically Zielinski and McIver (1982) realized that maximum recovery of shale gas could not take place without a better understanding and mapping of natural-fracture networks (which maximize drainage to the borehole) and without an improvement in stimulation techniques.

Organic Carbon Content. The total organic carbon (TOC) content of the Devonian shales changes rapidly from place to place and from layer to layer, even within a single formation like the Marcellus. Nevertheless, the overall organic richness of each formation can be determined. TOC in the lower Marcellus member is highest (6%) in northern West Virginia and southwestern Pennsylvania, decreasing somewhat (2–4%) elsewhere in the central Appalachian Basin. TOC in the upper Marcellus is excellent (4–6%) in central Ohio and somewhat less (2–4%) in eastern Ohio and southwestern Pennsylvania. TOC in the overlying Mahantango Formation is just 1–2% in western Ohio beyond the thick clastic wedge. TOC in the Geneseo (Burkett) is greatest (2–4%) in central Pennsylvania and northwestern West Virginia, but lower (1–2%) in Ohio, New York, and western Pennsylvania.

Biofacies. The nature and origin of the contained organic material is important in that algal matter generates a greater quantity of hydrocarbons than woody matter and at a lower temperature. Three palynological biofacies were identified. The *Tasmanites biofacies* contains a palynomorph assemblage dominated by this single genus of marine green algae. The extremely low diversity of the fossil assemblage suggests that water quality in the Devonian seaway was abnormal. The *marine biofacies* is a heterogeneous mix of algae and zooplankton and reflects normal sea-water chemistry. The *terrestrial biofacies* comprises mostly woody material derived from the adjacent landmass. Sea water there may have been influenced by a large riverine influx.

In early Marcellus time the *Tasmanites* biofacies covered most of the region while the terrestrial biofacies was confined to a small area in the southeast. By the late Marcellus the *Tasmanites* biofacies had retreated to the west, the marine biofacies occupied the center region, and the terrestrial biofacies occurred in the east. When the Mahantango clastic wedge formed, the western basin was dominated by normal-marine palynomorphs. *Tasmanites* blooms had been virtually eliminated presumably in response to changing water chemistry, and terrestrial organic matter from eastern lands encroached farther into the basin. In Geneseo time a biofacies pattern similar to that of the late Marcellus had become reestablished.

The δC^{13} value for natural gas in the Marcellus (ratio of carbon isotopes C^{13}/C^{12} compared to a chemical standard) varies between -22 and -28 ppt, indicating that it is a mix of thermogenic and biogenic gas.

Thermal maturity. The maturity of contained organic carbon in the shale was determined by the thermal alteration index (TAI, color variation of spores, pollen, and plant cuticle) and vitrinite reflectance (R_o). TAI analysis was generally preferred, proving to be more useful than R_o. TAI values more closely parallel areal geological trends and exhibit more detail in vertical section. For the Marcellus-Geneseo stratigraphic interval, TAI values are ≤ 2 in northeastern Ohio. Spores and pollen are orange in color, reflecting a maximum paleotemperature of 100–150°C. Expected hydrocarbons are oil and wet gas. Values increase progressively to the

east-southeast. TAI vales are 3 in southeastern Ohio, western Pennsylvania, and west-central New York where spores and pollen are brown. Maximum paleotemperatures were greater than 150°C, and the expected hydrocarbon is wet gas. TAI values are 4 in north-central Pennsylvania. The maximum paleotemperature was near 200°C, and the expected hydrocarbon is dry gas.

The content of heavier gaseous and liquid hydrocarbons in the shales (C_{2-5} and C_{15+}/TOC) and the quantity of gas (gas-in-place or GIP; relative weight of hydrocarbons to total organic carbon or HC/TOC) are both anomalously high for the degree of thermal maturity suggested by TAI and R_o. Rocks with a TAI indicative of beginning early-maturity in fact contain wet gas and oil of the peak- to late-maturity stage. This discrepancy was explained as the effect of time substituting for temperature during hydrocarbon generation in older Paleozoic rocks.

Source quality. An arbitrary rating system of source-rock quality was established by combining data for TOC, type of organic matter, and thermal maturity. The resulting source-rock potential was calculated per unit volume of rock. The source-rock potential of the lower Marcellus member is exceptional in southwestern Pennsylvania and northern West Virginia and excellent in western New York, western Pennsylvania, eastern Ohio, and western West Virginia. The source-rock potential of the upper Marcellus is exceptional in northwestern West Virginia and southeast Ohio and excellent in west-central Ohio and southwest Pennsylvania. The source-rock potential of the Mahantango is poor everywhere. And the source-rock potential of the Geneseo is exceptional in northwestern West Virginia and good in southwest through north-central Pennsylvania.

By taking into consideration stratigraphic thickness, the relative gas potential of the stratigraphic unit can be determined. The relative gas potential for the lower Marcellus member (only 20–50 ft thick) is rated low everywhere (that is, low for the Devonian section in the Appalachian Basin), although the best area is southwestern Pennsylvania. The relative gas potential for the upper Marcellus (20–150 ft thick) is also rated low everywhere, although the best area is northern West Virginia. The relative gas potential for the Mahantango (20–700 ft thick) is low everywhere. And the relative gas potential for the Geneseo (20–300 ft thick) is very large in south-central New York and north-central Pennsylvania.

Gas in place (GIP) was then calculated for the several stratigraphic units and expressed in terms of bcfg per square mile and total volume for the study area.

Lower Marcellus	2–5 MMcfg/ac = 1–3 bcfg/sq mi	total = 78 tcfg
Upper Marcellus	2–15 MMcfg/ac = 1–10 bcfg/sq mi	total = 100 tcfg
Mahantango	1–20 MMcfg/ac = 0.6–13 bcfg/sq mi	total = 213 tcfg
Geneseo	1–35 MMcfg/ac = 0.6–22 bcfg/sq mi	total = 242 tcfg

These values for Marcellus GIP (Zielinski and McIver, 1982) compare favorably with calculations of 0.3–2.5 bcfg/sq mi (Marcellus Shale in New York, 2009) but are substantially lower than the most recent estimates of 30–150 bcfg/sq mi (Wrightstone, 2008; Petzet, 2009). The total gas in place for the Marcellus Shale (178 tcfg) presented by Zielinski and McIver (1982) is also lower than recent calculations (generally 300–500 tcfg), in part because of the smaller study area (excludes south-central New York, northeast Pennsylvania, and southern West Virginia). Note, too, that gas in the Mahantango Formation (213 tcfg) was not sourced in that formation, but presumably migrated from the underlying Marcellus.

Natural fractures. Two sets of natural fractures were identified in the Marcellus: one striking NE and the other striking NW. The fracture density in Middle-Upper Devonian shales is higher in southwestern Pennsylvania, West Virginia, and eastern Ohio and lower in central-to-northeastern Ohio, northwestern Pennsylvania, and New York. Fracturing was attributed to local and regional tectonic stresses, uplift and erosion of the stratigraphic overburden, and mechanical compaction of the rocks.

4.3.2 Organic Carbon Content

The total organic carbon (TOC) content by weight for Marcellus black shales is reported to be 1.40–4.30% by Milici and Swezey (2006), 4.27% by Lash (2008), 4–6% Gottschling, 2007), 2–10% (Wrightstone, 2008), 3.87–11.05% by Hill and others (2004), and 10–12% (Engelder, 2008a). According to the classification scheme of Peters and Cassa (1994), the Marcellus is a very good to excellent source rock in terms of its organic richness. Stratigraphically, specific TOC values in Pennsylvania and New York include: 1–9% in the Union Springs Member, 1–10% in the Oatka Creek Member as a whole, 0.74–0.78% in gray shale of the Oatka Creek, 0.29% in the overlying Mahantango Formation, and 0.90–1.57% in the higher Burkett/Geneseo Shale (Nyahay and others, 2007; Engelder, 2008a).

In general, organic richness is greatest in the basal 50 ft of the formation in the Union Springs Member (Engelder, 2008a). Zielinski and Nance (1979) correspondingly cited mean and maximum values in the

basal section to be 5.19% and 8.81%, compared to 1.64% in the upper Marcellus in a well in West Virginia. Geographically, organic richness is highest in the central region (up to 9%) and decreases to the east (1–2%) and west (2–3%) across the basin in New York (Figure 42 and 43) (Hill and others, 2004; Nyahay and others, 2007; Sumi, 2008) and decreases from north to south along the basin axis (4.3% in New York, 3.61% in Pennsylvania, and less than 2% in West Virginia; Milici and Swezey, 2006). Somewhat similarly Zielinski and McIver (1982) showed the TOC in the lower Marcellus member to reach 4% in western New York and 6% in northern West Virginia and to decrease both eastward and westward from these maximum values. On the other hand, Zielinski and McIver (1982) showed the TOC in the upper Marcellus to reach 6% in central Ohio and to continuously decrease eastward (Lyle, 2009).

Zielinski and Nance (1979) reported that the uranium/thorium ratio of the shale (from API values on the gamma-ray log) is a good linear predictor of TOC (Figure 44). de Witt and others (1993) noted that in the western and central portions of the Appalachian Basin, black shale exhibits a gamma-ray reading of +20 API units above the base line for gray shale (and as high as 600 API units; Engelder, 2008a). However, Van Tyne and Peterson (1978) stated that black shale does not always display such a high API value. Lash (2008) claimed that the bulk-density is a better proxy for TOC (reflecting the low density of organic matter compared to framework minerals) because fixation of uranium to organic matter is influenced by sedimentation rate. Gottschling (2007) presented a nearly linear relationship between TOC and formation density (Figure 45). Density readings for the Marcellus are as low as 2.35 g/cm^3.

Regional variation in organic richness values does not necessarily parallel trends in Marcellus thickness (Sumi, 2008). For example, Lash (2007) presented a percentage map of black shale in the Oatka Creek Member, showing that this facies exceeds 90% of the stratigraphic thickness in central New York and Pennsylvania, decreasing both to the east (30%) and west (20%) (Figure 46). An isopach map of the basal black shale of the Oatka Creek Member illustrates the total thickness to exceed 45 ft to the east and to thin dramatically westward to less than 25 ft (Figure 46). In contrast, an isopach map of the entire Oatka Creek Member shows that it is thickest in eastern Pennsylvania and thick in Ohio, but thins through central New York (Figure 32). Furthermore, Van Tyne and Peterson (1978) cautioned that the thickness of a black-shale unit determined from well cuttings may be 10 times greater than the thickness based on API gamma-ray units because of facies misidentification on the well log.

Kerogen is mostly sapropelic (marine, algal) type II (Figure 47) (Lash, 2008). Certainly, though, the Marcellus contains an admixture of terrestrial humic Type III kerogen in the eastern portion of the basin (Zielinski and McIver, 1982). Hill and others (2004) and Nyahay and others (2007) showed that the kerogen type based on Rock-Eval analysis (hydrogen index HI as high as 250–400, oxygen index OI less than 50) is primarily type II with a mixture of type III (Figures 48 and 49).

4.3.3 Thermal Maturity and Burial History

Regional maps of vitrinite reflectance (R_o) have been published by Hill and others (2004), Repetski and others (2005), Milici and Swezey (2006), Nyahay and others (2007), and Wrightstone (2008) with values increasing from a minimum of 0.5–1.0 in eastern Ohio (that is, early to peak maturity) to a maximum of 3.0–3.5 in eastern Pennsylvania (post mature). Thermal maturity of the Marcellus increases more-or-less progressively eastward across the basin (Figure 50), and most workers relate maturity directly to maximum burial depth beneath the Acadian and Alleghenian clastic wedges (Repetski and others, 2005). Maximum burial depth was perhaps 5,000 ft in the west and 8,000 ft in the east (Milici and Swezey, 2006). Interestingly Zielinski and Nance (1979) calculated a maturity gradient with burial depth in a well in Monongalia County, West Virginia—R_o increases 0.3% per 1,000 ft, although a higher-than-normal heat flow associated with the Rome trough (in the middle Mesozoic) may have generated higher values of thermal maturity at shallower burial depths in the west (Repetski and others, 2005; Lash, 2008). Wrightstone's (2008) map also illustrates three salients of more-mature Marcellus extending northwesterly in Pennsylvania and West Virginia, hinting at the site of basement structures or lineaments that locally controlled migration of hot, basin-derived fluids or that locally controlled Upper Paleozoic overburden thicknesses (Repetski and others, 2005). Regional variation in Marcellus maturity explains the presence of wet gas in some areas and dry gas in others (Durham, 2008).

Thermal maturity is directly related to burial history. Lash (2008) published a burial-history curve for Devonian formations in a well in western New York. The Marcellus was subjected to a first stage of rapid burial in the Devonian-Mississippian (burial beneath Acadian clastic wedge), uplift in the Pennsylvanian (Alleghenian Orogeny), a second stage of rapid burial in the Permian-Triassic (burial beneath Alleghenian clastic wedge), followed by steady uplift to the present time (continuous erosion of 7,000–10,000 ft of

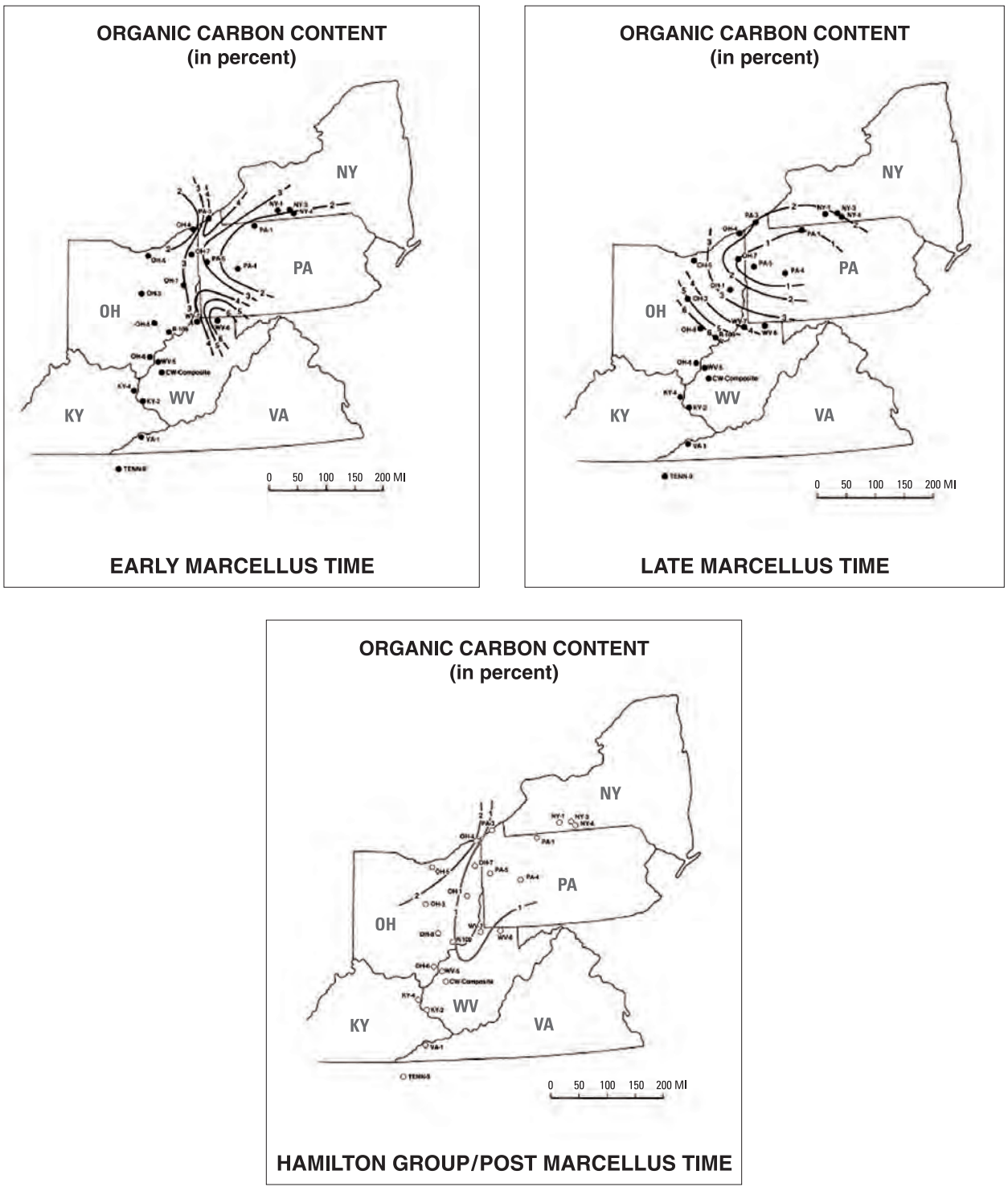

Figure 42. Total organic carbon for the lower and upper members of the Marcellus Shale and the overlying Mahantango Formation. Modified from Zielinski and McIver, 1982.

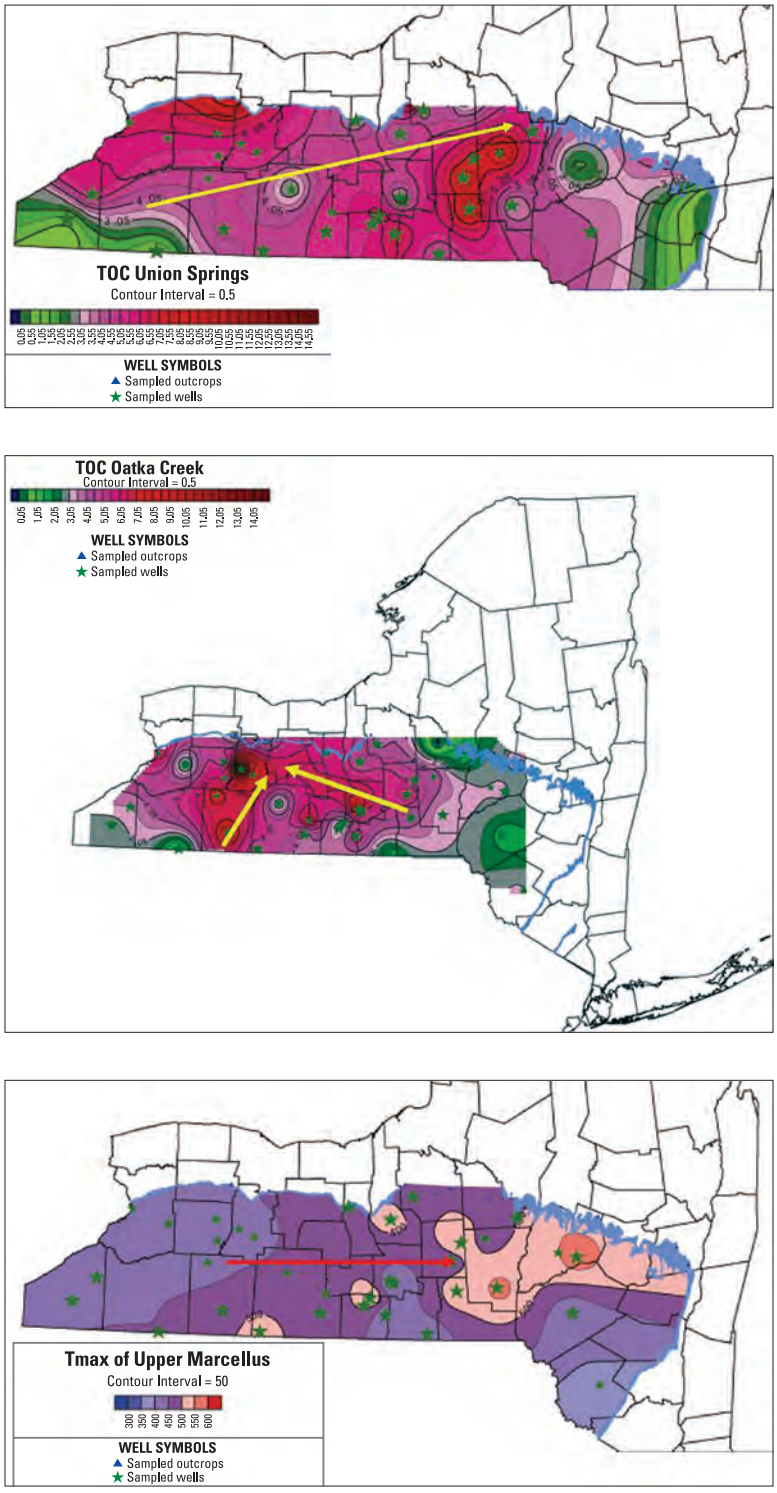

Figure 43. Top: total organic carbon (TOC) in the Union Springs Member across New York. Middle: TOC in the Oatka Creek Member. Bottom: Tmax of the Oatka Creek member. Hotter colors represent higher values. Arrows indicate direction of increasing values. Modified from Nyahay and others, 2007.

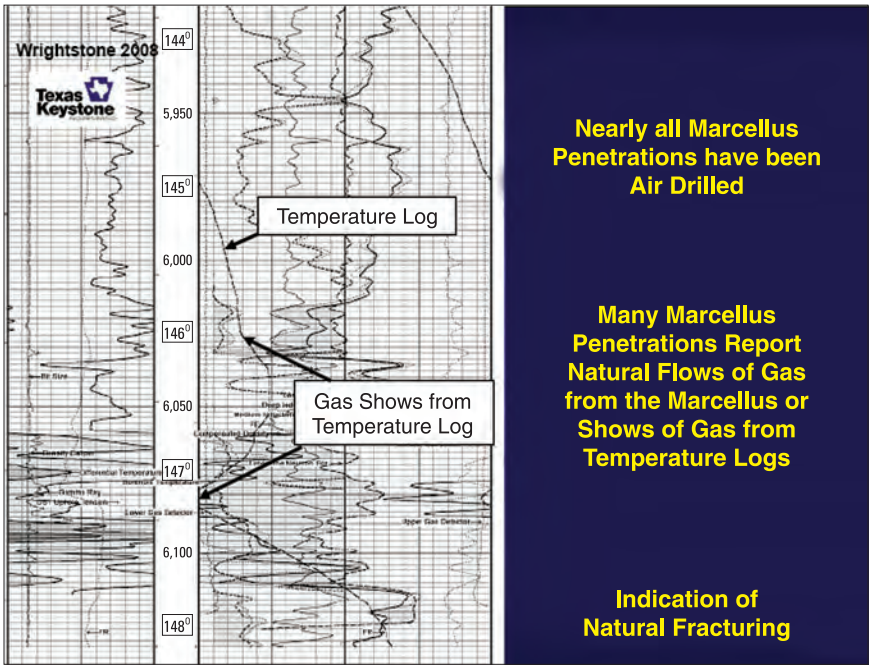

Figure 44. Well log of Marcellus showing gamma-ray values (left) and gas shows from temperature log (right). Modified from Wrightstone, 2008.

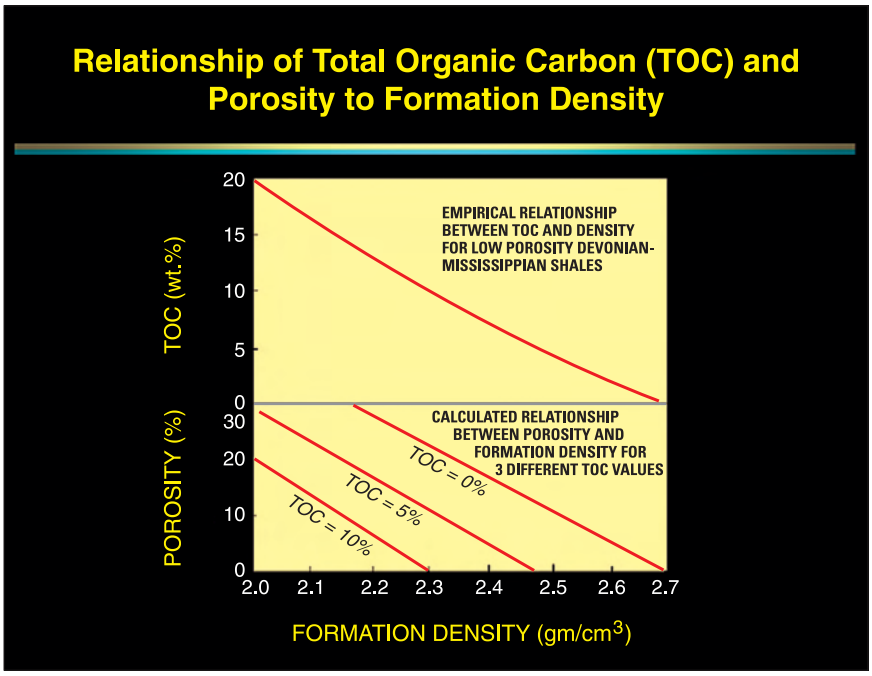

Figure 45. Relationship between TOC and formation density (top) and shale porosity and formation density (bottom). Modified from Gottschling, 2007.

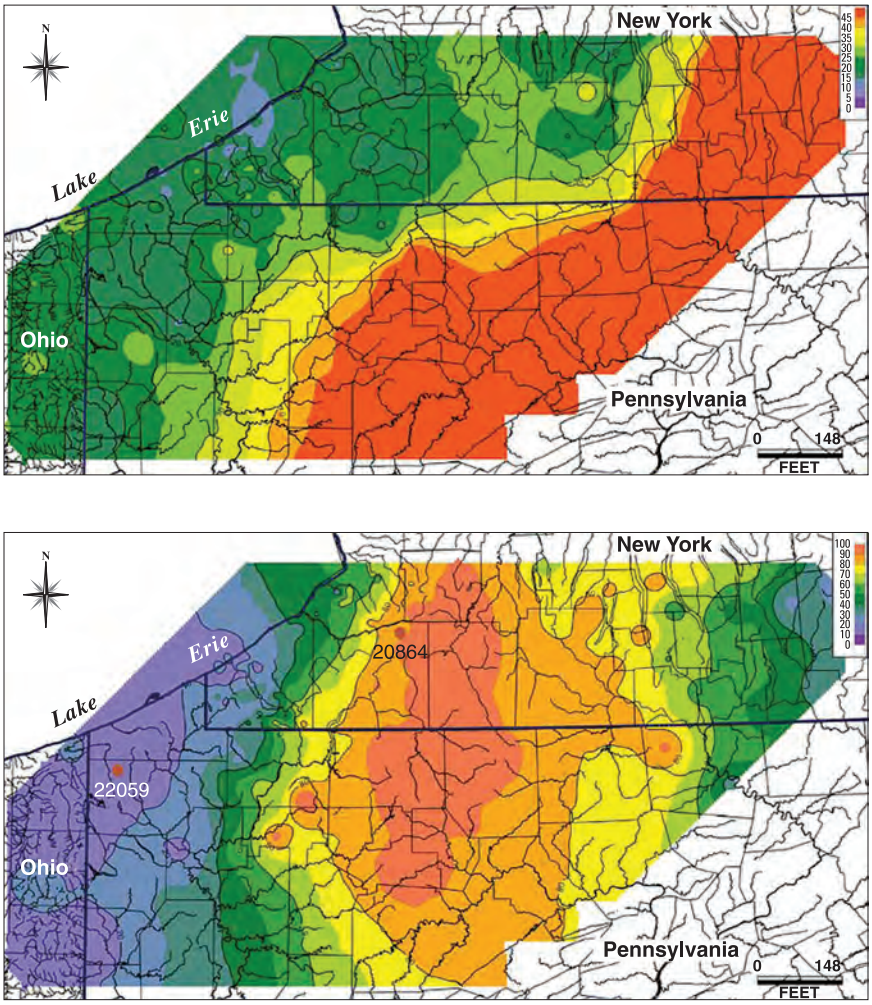

Figure 46. Top: map showing the percentage of black shale facies of the Oatka Creek Shale (contours in 10% increments). Bottom: isopach map (thickness in feet) of the basal organic-rich black shale facies of the Oatka Creek Shale. Modified from Lash, 2007.

overburden). At that location the Marcellus entered the early mature oil zone (R_o = 0.5–0.7, temperature = 75–110°C, depth = 8,000–11,000 ft) near the end of the Pennsylvanian period about 280 million years ago (MA) and entered the mid mature oil zone (R_o = 0.7–1.0, temperature 110–140°C, depth = 11,000–14,000 ft) near the end of the Permian about 250 MA (Lash, 2008). To the east where burial depths were significantly greater, the Marcellus undoubtedly matured earlier in the Paleozoic.

An increasing value of R_o influences the expected hydrocarbons generated, although the exact limits are not universally accepted (Table 4). Much of the Marcellus Shale lies outside of the oil window (Sumi, 2008). Using R_o = 1.60 as a cutoff value (Repetski and others, 2005; Milici and Swezey, 2006), the formation should contain oil and/or wet gas in western New York, northwestern Pennsylvania, eastern Ohio, and far western West Virginia. The formation should contain dry gas in eastern New York, most of Pennsylvania, Maryland, and central-to-eastern West Virginia.

In the Appalachian Basin the Conodont Alteration Index (CAI) has also been used successfully to measure thermal maturity (Figure 51). CAI is a scale of color alteration in conodonts as a result of increasing temperature and burial depth. The table above provides approximate equivalents with R_o. Hill and others (2004) presented a map of CAI isograds across New York, reporting that Middle Devonian shales display values of 1.5 (early-peak oil) in the west to 2.5–3.0 (wet gas) in the central area. Repetski and others (2005) prepared a map of CAI isograds across West Virginia, showing values of 1.5 (early-peak oil) in the west along the Ohio River to 4.0 (dry gas) in and near the Valley and Ridge province in the east. This map also points out

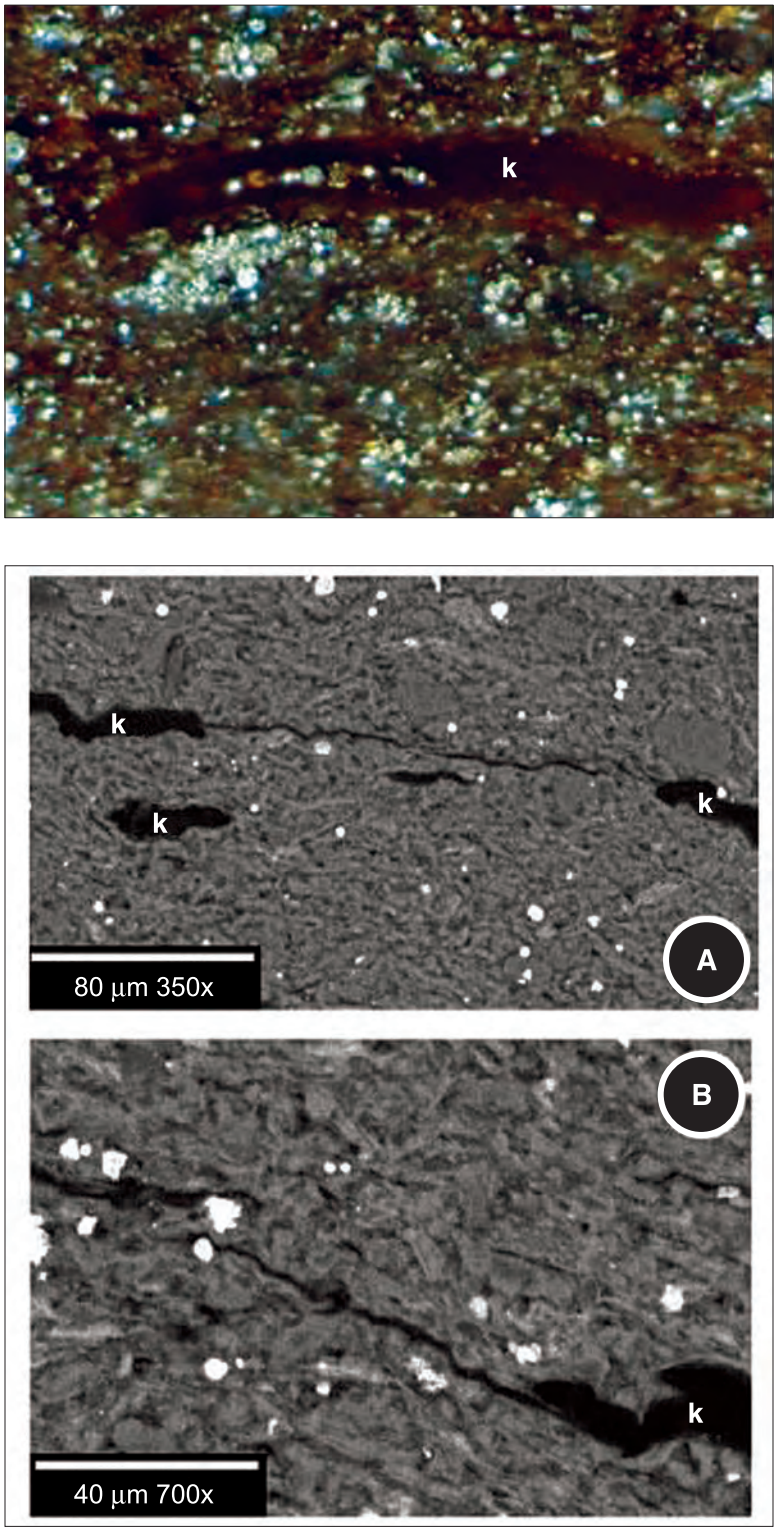

Figure 47. Top: photomicrograph of kerogen particle in Marcellus Shale; modified from Geology.com. Bottom A and B: microfractures propagating between kerogen particles; modified from Engelder and Lash, 2008.

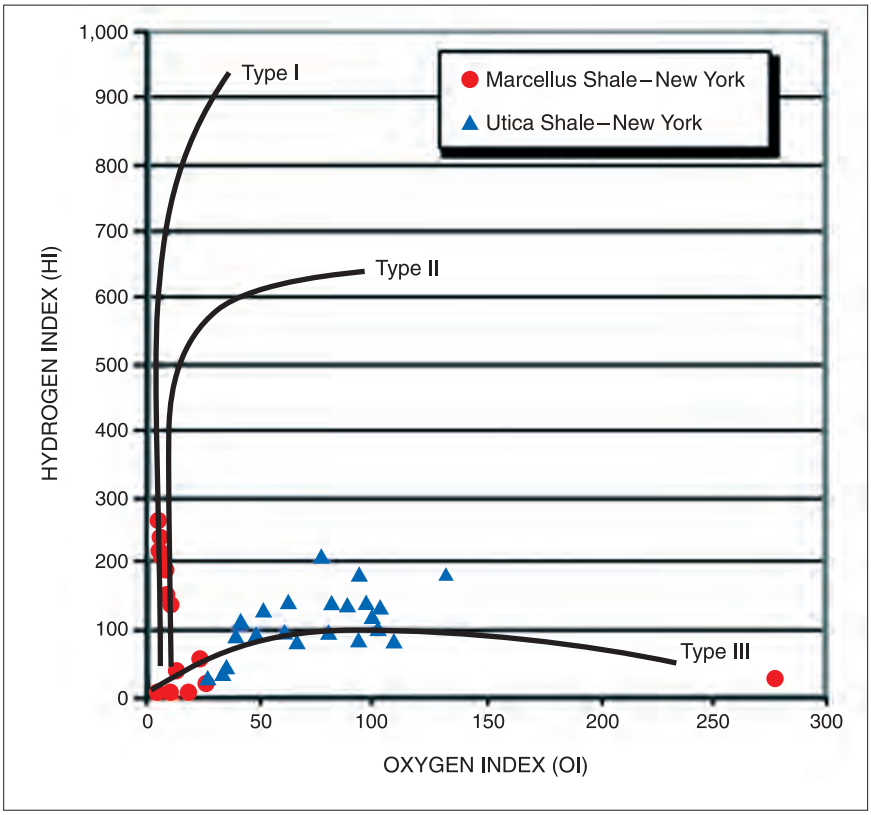

Figure 48. Rock-Eval data for Marcellus and Utica Shales in New York plotted on a modified Van Krevlen diagram. Modified from Hill and others, 2004.

local maturity highs and salients associated with basement structures, such as the Rome Trough and central West Virginia Arch. Repetski and others (2005) noted that the correlation between CAI and R_o isograds is only mediocre.

From Rock-Eval analysis, the level of thermal maturity of the shale can be determined from Tmax, the temperature at which the peak release of hydrocarbons occurs by pyrolytic cracking of kerogen (Figure 43). The top of the oil window (early mature) occurs at Tmax = 435–445°C and the bottom of the oil window (late mature), at 470°C. Hill and others (2004) presented Tmax values in the Marcellus from central and western New York. Values range from 430°C (immature) to 515°C (post mature).

Lastly, a few geologists have examined the thermal alteration of index (TAI) of spores, pollen, and plant cuticle, a progressive color change in these fossil materials as an indication of increasing thermal maturity (Hill and others, 2004; Gottschling, 2007). Zielinski and McIver (1982) published a map of TAI values across the western portion of the basin (Figure 51). In northeast Ohio TAI = 2 where the rocks are immature. Values increase progressively (as they do for R_o, CAI, and Tmax) into north-central Pennsylvania where TAI = 4 (wet gas).

Lash (2008) noted that vitrinite reflectance values measured for Appalachian black shales can be suppressed, that is, they may underestimate the degree of thermal maturity and maximum burial depth. Vitrinite suppression occurs in the lower to middle oil window and is related to kerogen type and amount. Shales with a high TOC (hydrogen index > 125 mg/g) and especially those rich in liptinite and exinite (hydrogen-rich, sapropelic type II kerogen, like that of the Marcellus) experience a marked suppression. In western New York and northwestern Pennsylvania, organic-rich shales (HI > 100 mg/g) exhibit suppressed values of R_o in the range of 0.5–1.0% compared to interbedded organic-lean shales (HI < 50 mg/g) with unsuppressed R_o values of 1.0–2.5%. Perhaps early diagenesis of the sapropelic kerogens formed stable components, and little change took place in their reflectance characteristics as burial temperature increased significantly. Similarly, Zielinski and McIver (1982) noted that Devonian shales of the central Appalachian Basin have suppressed TAI values in the oil window. If suppression of R_o and TAI values extends into the post-mature stage, then the mapped core area of the Marcellus (dry gas where $R_o \geq 1.6$ and TAI ≥ 4) would shift to the west some considerable distance. Many workers, though, do not evaluate the effects of suppression on thermal-maturity indices.

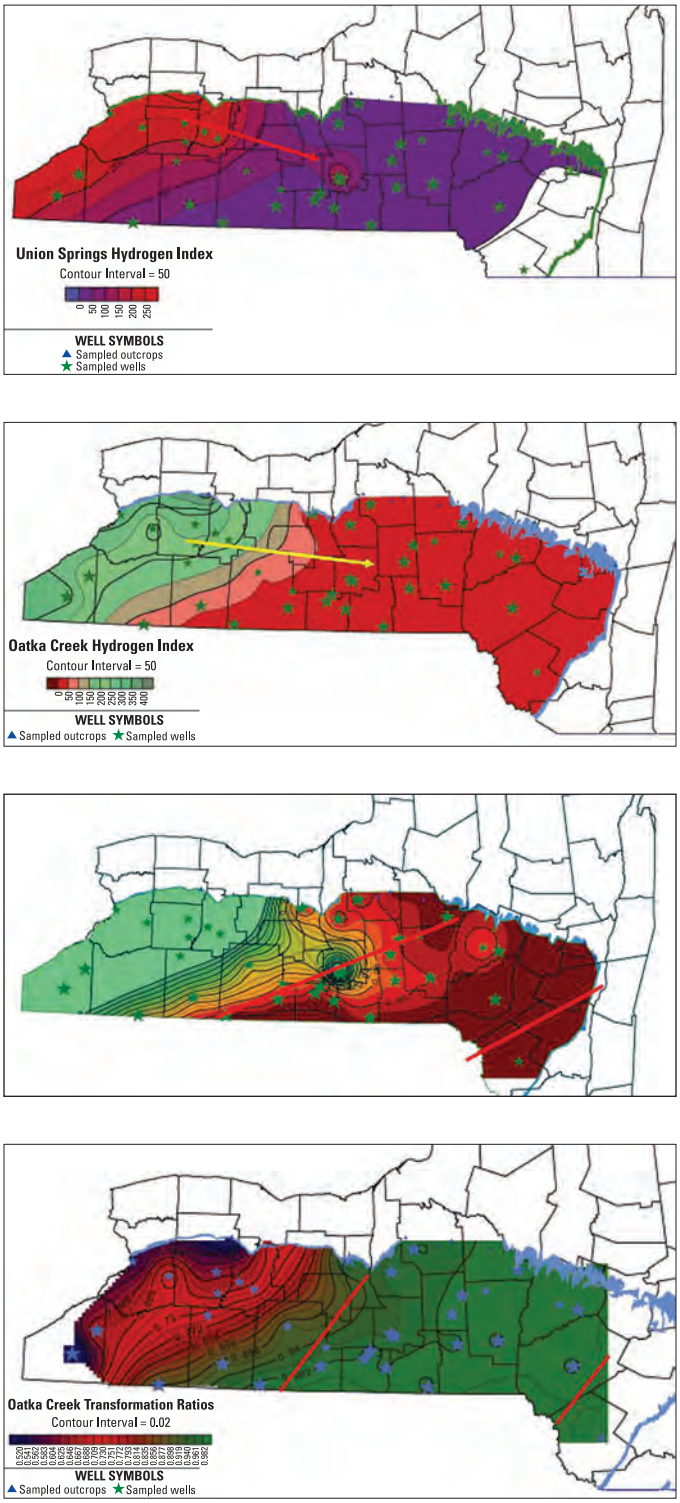

Figure 49. Top to bottom: Hydrogen index for Union Springs Member across New York and for Oatka Creek Member of the Marcellus, and production ratio for Union Springs Member and for Oatka Creek Member. Hotter colors represent higher values. Modified from Nyahay and others, 2007.

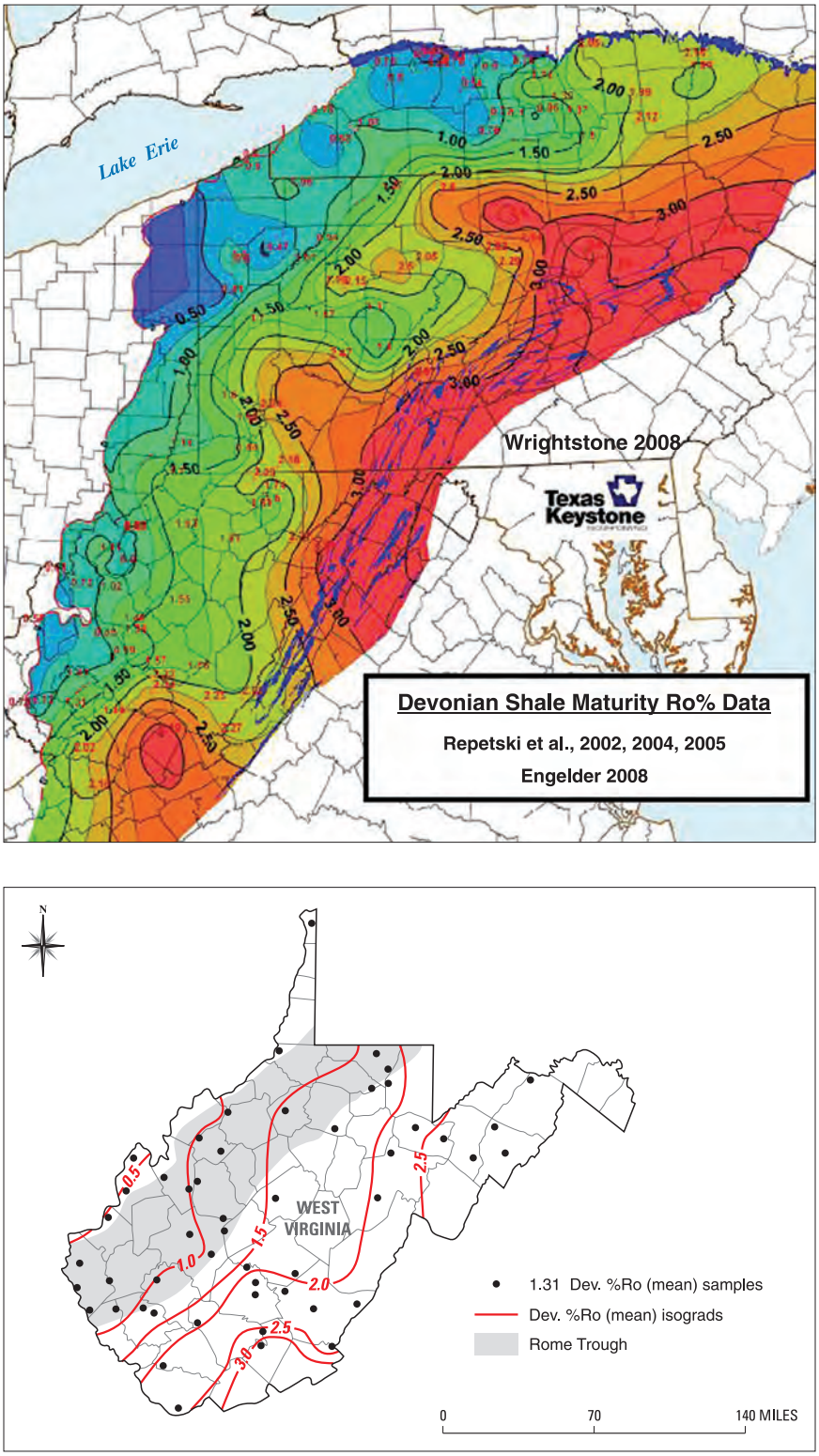

Figure 50. Vitrinite reflectance (R_o) isogradient map across the central Appalachian Basin (modified from Wrightstone, 2008) and in West Virginia (modified from Repetski and others, 2005).

Table 4. Relationship between vitrinite-reflectance value (% R_o), Conodont Alteration Index (CAI), stage of thermal maturity, and generated hydrocarbons in the Marcellus Shale.

[<, less than]

R_o (percent)	Conodont Alteration Index (CAI)	Maturity	Thermogenic hydrocarbons
<0.55	1-1.5	Immature	none
0.55-0.70		Early Mature	top of oil window
0.70-1.10	1.5-2.0	Peak Mature	peak oil
1.00-1.10			top of gas window
1.10-1.60	2.0-3.0	Late Mature	oil and gas
1.20-1.50			peak wet gas
1.60-3.50	3-4	Post Mature	peak dry gas

4.3.4 Reservoir Characteristics

The Marcellus Shale is in effect a single, very large (continuous) gas resource that underlies thousands of square miles. It is a stratigraphic trap within the structurally-bound Appalachian Basin, occupying a structural low and straddling the basin axis. Drilling depth to the base of the shale (top of Onondaga Limestone) increases to the southeast, varying from 2,000 ft along Lake Erie to 8,000 ft in northern West Virginia and Maryland to 8,000–10,000 ft in central Pennsylvania (Figure 25) (Geology.com, 2008; Wrightstone, 2008).

Porosity has two components—interparticle (or matrix porosity located between silt and clay particles and organic matter) and open fractures. Average porosity is in the neighborhood of 6% (Wrightstone, 2008) to 10% (Soeder, 1988; Arthur and others, 2008b). Interparticle porosity contains both free and adsorbed gas (Durham, 2008), and much of this porosity may have resulted from thermal decomposition of organic matter to petroleum. At a high thermal maturity (R_o > 2.0), matrix porosity can be 2% higher (Barrett, no date). Gottschling (2007) offered a linear relationship between formation density (g/cm^3) and porosity for three different TOC values (0%, 5%, and 10%; Figure 45). Lash (2008) calculated that original interparticle porosity in black shale of the Rhinestreet (perhaps similar to that of the Marcellus) was 74–93%. Porosity had been greatly reduced by a combination of physical compaction, pressure solution (chemical compaction), cementation, neoformation of clay minerals such as chlorite and kaolinite, and volume change accompanying the conversion of organic matter to bitumen.

Zielinski and Nance (1979) reported permeability values of 0.13–0.77 millidarcies with an average of 0.363 millidarcies. Hill and others (2004) cited values of 4–216 microdarcies, and Engelder (2008a) reported values of 200–400 nanodarcies. The very low permeability may have resulted from ductile squeezing of the contained organic matter (Lash, 2008). Soeder (1988) maintained that Marcellus permeability is strongly influenced by geostress exerted on the rock: a doubling of the net confining stress lowers the rock's permeability by nearly 70%. The presence of liquid hydrocarbons will also lower the permeability with respect to natural gas (Soeder, 1988).

Reservoir pressures range from 400 to 4,000 psi (Wrightstone, 2008; Lyle, 2009). The Marcellus Shale can be slightly overpressured, especially in the northern section of the basin (Sumi, 2008). Deacon (2009) claimed that the overpressured areas are located in northeastern and southwestern Pennsylvania and northeastern West Virginia. In the core area of the Marcellus, the pressure gradient ranges from 0.46–0.51 psi/ft (Hill and others, 2004). Lash and Blood (2007) attributed overpressuring of the Rhinestreet Shale to have resulted from a marked increase in sedimentation rate during Late Devonian progradation of the Catskill deltaic complex. In contrast, the Marcellus in southwestern West Virginia is thought to be underpressured (Marcellus Playbook, 2009). Wrightstone (2008) cited pressure gradients of 0.10–0.20 psi/ft in southwestern West Virginia and 0.20–0.35 psi/ft in central West Virginia.

Gas saturation ranges from 55–80% and water saturation, from 20–45% (Zielinski, 1977; Kuuskraa and Wicks, 1984). The production of formation water is nil (Arthur and others, 2008b), suggesting that the shale has no free water or that the relative permeability for water is zero.

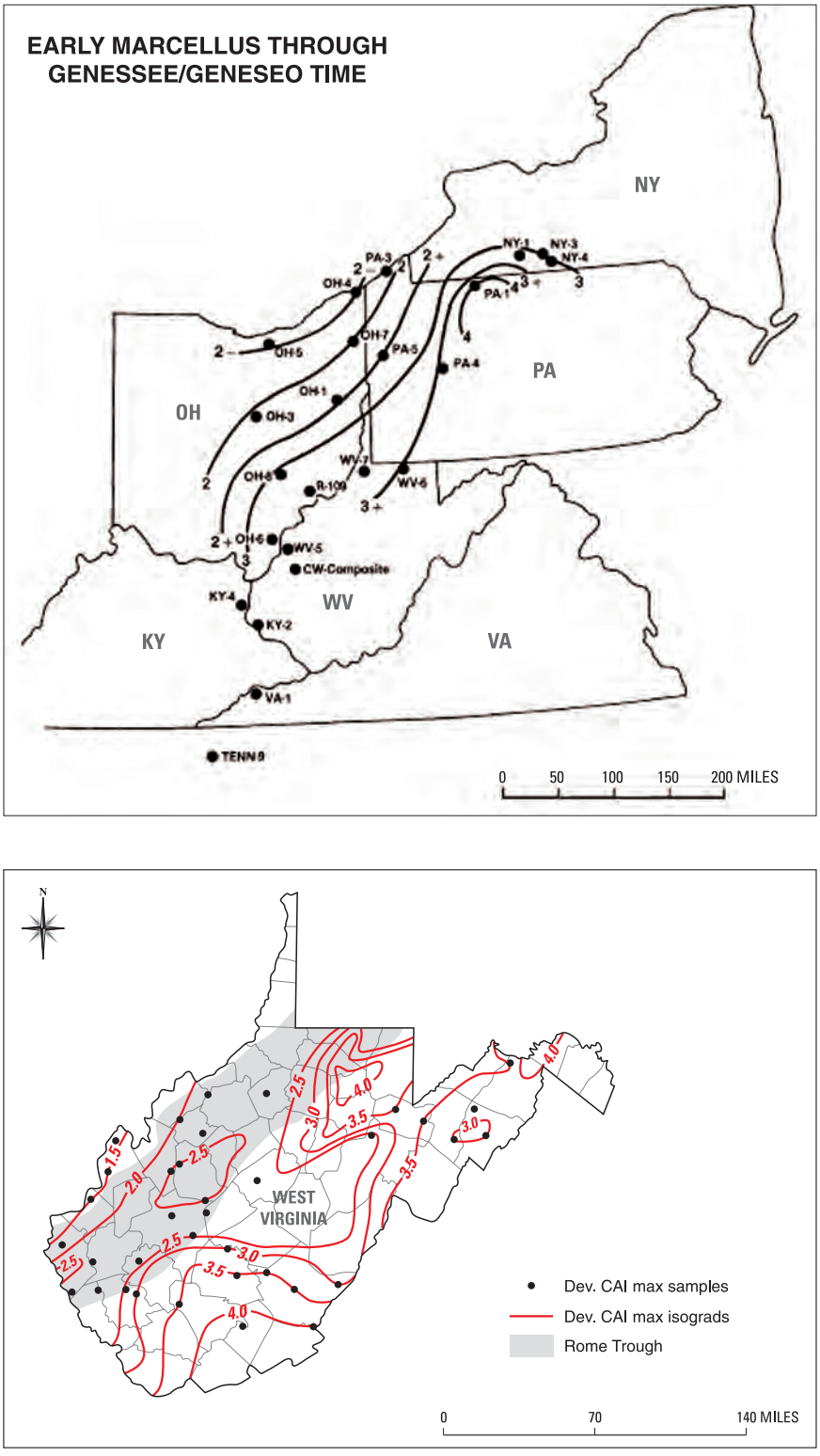

Figure 51. Top: values of Thermal Alteration Index (TAI) for the Marcellus-Geneseo stratigraphic interval in the central Appalachian Basin; modified from Zielinski and McIver, 1982. Bottom: values of Conodont Alteration Index (CAI) for the Marcellus Shale in West Virginia; modified from Repetski and others, 2005.

Zielinski (1977) cited fracture porosity in the Devonian shales as high as 3.5–4.5%, but Hill and others (2004) found that fracture porosity is less than 1% even in shale with the highest joint density. Fracture width ranges up to 1 cm (Geology.com, 2008), and minerals that partly fill the fractures keep them open and maintain the pore network (Figures 47 and 52). The density of fractures is directly proportional to the shale's TOC; J_1 joints are better developed in the organic-rich shale and J_2 are better developed in siltstone. Both sets are rarely mineralized, presumably because methane remained in the openings since they formed 250 MA (Engelder, 2008a). Less than 0.01% of the fractures observed in outcrop have been mineralized (calcite veins). If unmineralized, J_1 joints prove to be more permeable than J_2 joints.

Vertical growth of a natural fracture is dictated by thickness of the mechanical unit containing the joint set. Homogeneous thick shales act as a single mechanical unit, and joints there tend to have great height and close spacing (Engelder, 2008a). In New York outcrops Lash (2008) noted that although the shale is heavily jointed, joints do not penetrate carbonate concretions within the Marcellus (Figure 40) nor do they extend into the overlying Stafford Limestone. In contrast, joints in outcrop extend upward from black shale into overlying gray shale for at least 50 m (Engelder, 2008a). Thus it appears that limestones in the stratigraphic section (Onondaga, Purcell, Cherry Valley, Mahantango limestones, and Tully) have a higher fracture threshold than the shales.

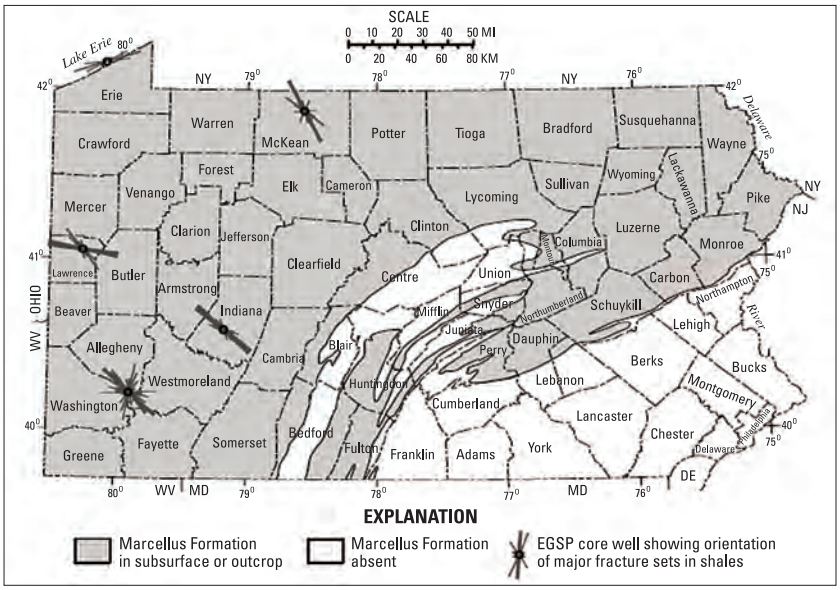

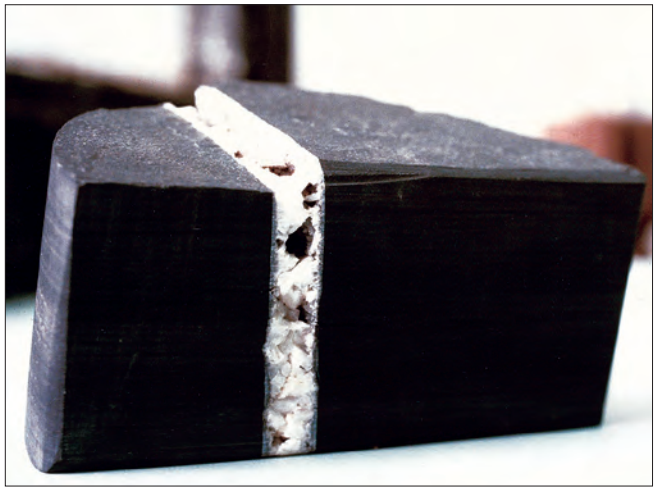

Figure 52. Top: general distribution of Marcellus Shale in Pennsylvania and the location of five EGSP cores with orientations of measured fractures; modified from Harper, 2008. Bottom: photograph of partly mineralized fracture; from Soeder and Kappel, 2009.

4.3.5 Generation of Hydrocarbons

Hydrocarbons in the Marcellus Shale are thermogenic in origin. The natural gas is adsorbed onto solid organic matter and kerogen (20–40% of the total according to Jarvie and others, 2004; 18–85% according to Kuuskraa and others, 1983) and stored in interstitial pores and microfractures. The quartz content in the shale increases eastward across the basin, suggesting that there is less adsorbed gas and more free gas in that direction (Lyle, 2009). Recent experiments by Busch and others (2009) also suggested that clay minerals may play a role in increasing the adsorption of gas. Gas distribution and movement in the black shale is thought to be: molecular diffusion through the shale matrix, adsorption onto fracture faces, and free gas in the open fractures (Soeder, 1988; Gottschling, 2007). Gas in place (GIP) is currently estimated to range from 20–150 bcfg per sq mi (Wrightstone, 2008; Lyle, 2009; Petzet, 2009) or 60–100 scfg/ton rock (Arthur and others, 2008b; Deacon, 2009). Total GIP for the Marcellus Shale Assessment Unit may be 295 tcfg (Milici and Swezey, 2006), 168–516 tcfg (Sumi, 2008), as much as 1,500 tcfg (Arthur and others, 2008b), or a high of 2,455 tcfg (Petroleum Technology Transfer Council, 2009). Engelder and Lash (2008) proposed that the GIP exceeds 500 tcfg over a four-state area (New York, Pennsylvania, West Virginia, and Ohio) with technically recoverable reserves of 50 tcfg. Engelder's (2009) more recent calculation yields a 50 percent probability that the Marcellus will ultimately produce 489 tcfg (assuming a power-law decline rate, 80-acre spacing, and 50-year well life). Similarly, Arthur and others (2008b) cited reserves of 363–500 tcfg.

Zielinski and McIver (1982) implied a 54% loss of gas to migration by comparing their GIP calculation for the Marcellus in the central region of the play (178 tcfg) to that of the overlying Mahantango (213 tcfg and sourced by the Marcellus). The calculated loss would be even greater if gas in other conventional reservoirs sourced by the Marcellus were included (e.g., Billman and others, 2000).

Rock-Eval pyrolysis provides several geochemical parameters to assess the petroleum potential of a source rock based on the amount of hydrocarbons present (Table 5). S_1 measures hydrocarbons already generated in the rock and distilled from the sample by heating to a temperature of 350°C. Free hydrocarbons generally increase with depth. The minimum value for a good source rock is S_1 = 1.0 mg HC/g rock. S_2 measures the amount of hydrocarbons generated through thermal cracking of kerogen as the pyrolysis temperature is increased to 550°C. S_2 is an indication of the quantity of hydrocarbons that the rock may potentially produce should burial and maturation continue. The minimum value for a good source rock is S_2 = 5.0 mg HC/g rock.

S_1 values for early-mature Marcellus samples (calculated R_o = 0.58–0.90%) in western New York range from 0.66–5.61 mg HC/g rock (Engelder, 2008a). These rocks have a fair to excellent (mostly very good) petroleum potential. S_1 values decrease to 0.02–0.40 mg HC/g rock in east-central Pennsylvania (R_o = 1.28–3.51, late to post mature) and to 0.02–0.05 mg HC/g rock in far eastern Pennsylvania (R_o = 3.00–3.50%, post mature), reflecting an eastward change in gas expulsion and the experimental loss of volatiles.

S_2 values for early-mature Marcellus samples in western New York range from 1.66–40.67 mg HC/g rock (Engelder, 2008a). Based on these values, the shale there has a poor to excellent petroleum potential. S_2 values decrease to 0.03–0.79 mg HC/g rock in east-central Pennsylvania and to 0.00–0.04 mg HC/g rock in far eastern Pennsylvania, illustrating an increasingly greater thermal maturity.

The production index, defined as the ratio of already generated hydrocarbons to total potential hydrocarbon yield and quantified by $S_1/(S_1 + S_2)$, averages 26% in western New York where the Marcellus is immature

Table 5. Petroleum potential of an immature source rock based on analyses of the contained organic matter, bitumen, and hydrocarbons[1].

[TOC, total organic carbon; wt. %, weight percent (1.0 wt. % carbon means that in 100 grams of rock sample there is 1 gram of organic carbon); ppm, parts per million; >, greater than]

Petroleum potential	Organic matter			Bitumen		Hydrocarbons
	TOC	Rock-eval pyrolysis				
	wt. %	S_1	S_2	wt. %	ppm	ppm
Poor	0-0.5	0-0.5	0-2.5	0-0.05	0-500	0-300
Fair	0.5-1	0.5-1	2.5-5	0.05-0.10	500-1,000	300-600
Good	1-4	1-2	5-10	0.10-0.20	1,000-2,000	600-1,200
Very good	2-4	2-4	10-20	0.20-0.40	2,000-4,000	1,200-2,400
Excellent	>4	>4	>20	>0.40	>4,000	>2,400

[1] From Peters and Cassa, 1994.

to early mature, 30% in east-central Pennsylvania where the shale is late to post mature, and 78% in far eastern Pennsylvania where the formation is post mature (Engelder, 2008a). These values indicate that between 26 and 78 percent of the potential hydrocarbons have already been generated. Furthermore, Nyahay and others (2007) showed that the transformation ratio, that is, the extent of kerogen conversion to hydrocarbons, exceeds 90 percent in both the Union Springs and Oatka Creek Members of south-central New York (Figure 49).

Marcellus shales become more brittle to the east across the basin (containing more quartz) and thus exhibit greater fracture porosity and permeability. However, the hydrocarbon potential in that direction may be low because of the formation's lower TOC (Sumi, 2008), or conversely it may be high because of the formation's high thermal maturity (Barrett, no date).

4.3.6 Delineation of the Marcellus Play

Wrightstone (2008) mapped the geographic distribution of permitted well sites (N = 2,215) and drilled/completed wells (N = 1,182) to the Marcellus Shale as of September 2008 (Figure 22). The map delineates a prospecting fairway that extends from south-central New York, through northeastern-southwestern Pennsylvania, and into western West Virginia (see also Gottschling, 2007; Sumi, 2008; Marcellus Playbook, 2009). This fairway measures 500 miles long and 100–130 miles wide, but most geologists consider Pennsylvania and New York to be most favorable (Sumi, 2008; Lyle, 2009).

Geological characteristics that are generally used to assess the Marcellus and to locate the sweet spots for exploration and development include:

- Thickness of organic-rich shale, more-or-less arbitrarily chosen at 50 ft or more. All else being equal, greater thickness means more gas in place and higher production.
- Total organic carbon, TOC ≥ 4%. Greater organic content means more gas in place. Organic content also influences joint development: joint density is higher in black shale than in gray shale (Hill and others, 2004).
- Thermal maturity $R_o \geq 1.6\%$, post mature. The hydrocarbon generated is dry gas. At lower maturity, the presence of liquid hydrocarbon lowers the shale's permeability with respect to natural gas.
- Spacing, aperture, and direction of natural fractures (joints). Open fractures significantly increase permeability and thus strongly influence production. Permeability is higher in unmineralized fractures and in fractures aligned ENE with the contemporary stress field. Fractures in black shale are closely spaced relative to their height. Well stimulation should thus be designed to intersect this set of natural fractures.
- Fracture barriers below and above. The underlying barrier is the Onondaga Limestone. Within-Marcellus barriers are the Purcell and Cherry Valley Limestone Members. Overlying barriers are the Tully Limestone and perhaps any thick Mahantango siltstone or limestone.
- Stratigraphic relationship between black and gray shales. Thickness of a mechanical unit (thick black shale vs. interbedded black and gray shales) controls the vertical growth of fractures (Engelder, 2008a).

The prospecting fairway is seemingly identified by four essential properties: (1) greatest thickness of black, organic-rich, radioactive shale, (2) thermally post-mature source rock, (3) position over or close to the Rome trough, and (4) underlying fracture barrier of Onondaga Limestone. Note that these properties are not necessarily independent. Reactivation of basement faults within the Rome trough may have divided the foreland basin into locally deep subbasins which accumulated thick successions of black shale. Marine circulation in these subbasins was poor, the water column stratified, and the bottom water oxygen-poor, all favoring the preservation of organic matter (TOC ≥ 4%). A higher-than-normal heat flow associated with the Rome trough conceivably generated higher values of thermal maturity at a shallower burial depth. Basement structures, too, could have influenced the migration of hot, basin-derived fluids into the Marcellus or controlled the thickness of its stratigraphic overburden. Natural fractures in the shale, which greatly increase gas permeability, were perhaps created by tectonic movement along Rome faults. Fractures also formed by disequilibrium compaction of the Marcellus and a buildup of fluid pressure during the late-mature and post-mature stages of burial (when $R_o > 1.3\%$). In particular, J_1 joints (unmineralized, permeable) are better developed in organic-rich shale, and the density of these joints is directly proportional to the shale's TOC. The Onondaga Limestone has a higher stress gradient than organic-rich shale, and thus it serves as a fracture barrier.

5.0 DRILLING AND STIMULATION TECHNIQUES

5.1 Fracture Stimulation

5.1.1 Natural Fractures and Faults

Barnett wells that intersect natural fractures are usually thought to produce the most gas. However, Steward (2007) stated that natural fractures are of limited size, frequently healed, and contribute little to gas production (unless opened by fracture stimulation). Open fractures in the middle Forestburg Limestone may favorably connect the upper and lower shale members during stimulation (Gale and others, 2007). Electric-image logs, when calibrated with resistivity data and evaluated along with accurate mud-resistivity measurement, can indicate the presence of open fractures, their dip angle, and aperture width (minimum cut-off 0.06 mm). Wells that do not encounter open fractures in general do not produce as much gas—having a flow rate at least one order of magnitude less and total gas production of one third (Johnston, 2004a). Open natural fractures, though, may inhibit the growth of hydraulically induced fractures. The role of mineralized or healed fractures remains questionable. Jarvie and others (2007) stated that healed fractures, usually located near major fault planes, are less responsive to stimulation than open fractures, and they cannot connect sufficient shale surface area to the wellbore. Bowker (2007a), on the other hand, claimed that healed fractures enhance the effectiveness of fracture treatment in that they serve as zones of weakness in the shale. The tensile strength of the contact between shale wall rock and calcite fracture fill is low, and mineralized fractures open during stimulation.

Existing faults tend to divert the flow of fracture fluids (thereby reducing the volume of reservoir rock being fractured), or they allow water into the Barnett from adjacent aquifers. For example, hydraulic fractures in wells drilled as close as 500 ft to a major fault reportedly did not propagate into the water-bearing Ellenburger Group, but those located within the fault zone did (Bowker, 2007a). For the same reason, wells located near karst (fault chimneys) and structural flexures (anticlines and synclines) are apt to be poor producers (Steward, 2007). A karst chimney is a circular system of faults developed over the karst surface below the Barnett. Chimneys range up to 200 acres in size and can extend from the basal unconformity upward to the overlying Bend Formation (Steward, 2007; Givens and Zhao, 2009). In addition, wells drilled on a fault or structural high have a higher fracture gradient, and they tend to fracture toward or down the fault plane (Givens and Zhao, 2009). This would lower the efficiency of fracture treatment. Hayden and Pursell (2005) believed the geographic area of the Barnett play that is drillable and not affected adversely by faults and karst may be 50–85% of the total extent.

Many geologists similarly consider natural fractures in the Marcellus Shale critical to commercial rates of gas production (Sumi, 2008). The borehole and/or induced fractures must intersect natural fractures—serving as permeability pathways—in order to economically drain the shale reservoir (Hill and others, 2004; Gottschling, 2007; Lash, 2008; Durham, 2008; Lyle, 2009; Engelder and others, 2009). Two sets of natural vertical fractures or joints are pervasive in Devonian shales of the Appalachian Basin—J_1 fractures with a strike of 60–75° and J_2 fractures with a strike of 315–345° (Figure 52) (Gottschling, 2007; Lash, 2008; Engelder, 2008a; Engelder and others, 2009). Approximately 6% of the vertical Ohio Shale wells in the giant Big Sandy field produce with no stimulation as do 20% of the recent horizontal wells, demonstrating that many wells to the Upper Devonian intersect open natural fractures (Curtis, 2002; Engelder, 2008a). Marcellus J_1 and J_2 fractures have been identified in the subsurface throughout the basin (Hill and others, 2004; Lash, 2008; Engelder, 2008a; Harper, 2008; Durham, 2008; Engelder and others, 2009), but of course they cannot be open in areas of abnormally high pore pressure (Hill and others, 2004; Sumi, 2008; Deacon, 2009). Indeed, fractures observed in core are often mineralized (Gottschling, 2007). Because they are vertical, such fractures are difficult for image logs to detect (Durham, 2008).

J_1 fractures are more densely spaced in the thinly bedded, organic-rich shales than the J_2, and if unmineralized, J_1 fractures have the greater permeability (Hill and others, 2004; Lash, 2008). In a vertical Marcellus well, artificially induced fractures develop ENE and intersect J_2 fractures. Gas drains from the J_2 natural fractures (less permeable) to the induced fractures and to the borehole (Figure 53). On the other hand, in a horizontal Marcellus well drilled NNW or SSE, hydraulic fracture treatment reopens J_1 fractures. Gas drains from the reopened J_1 natural fractures (more permeable) to the borehole (Lash, 2008), and the horizontal well

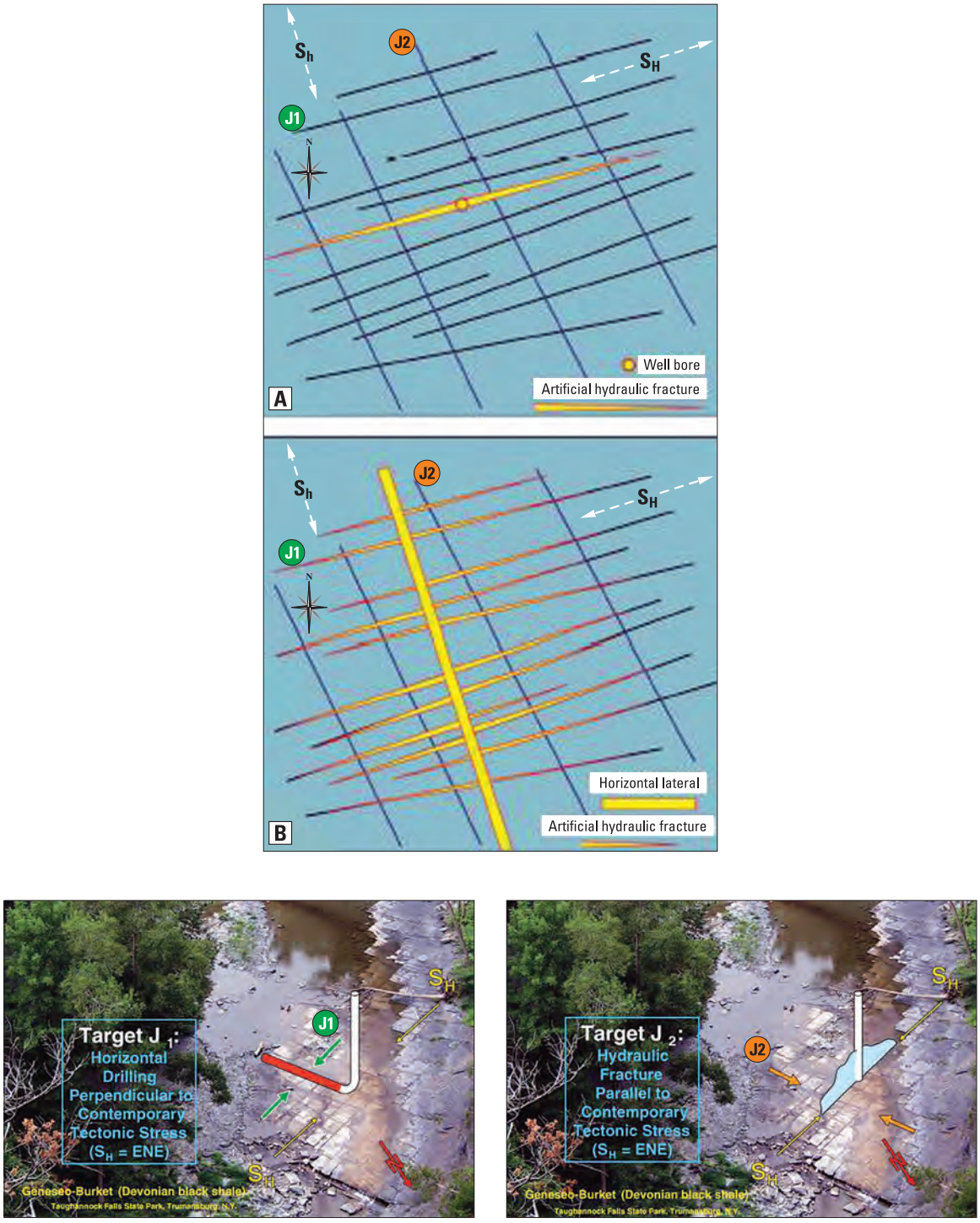

Figure 53. Relationship between natural fractures J_1 and J_2, artificial hydraulic fractures, and well bore. See text for discussion. Modified from Lash, 2008.

should be the better producer (Figure 53). Other geologists, though, argue that drilling a horizontal well in a NNW or SSE direction is preferable because the lateral itself intersects the maximum number of open J_1 natural fractures (Lyle, 2009; Wells and Gognat, 2009). Engelder and others (2009) claimed that in a horizontal well drilled to the NNW or SSE, the lateral drains J_1 fractures while artificially induced fractures drain the J_2.

5.1.2. Slickwater-Fracturing Treatment

The Marcellus has had a long history of fracture stimulation in vertical wells, and lessons learned from the Eastern Gas Shale Project of the late 1970s were subsequently applied to the Barnett. Conversely, horizontal drilling and slickwater-fracture treatment have been used in the Barnett since the mid 1990s and are now being successfully adapted to the Marcellus.

Because of the Barnett's extremely low permeability (typically less than 0.001 millidarcies), wells almost always require some form of hydraulic fracturing to make them economic. Initially, stimulations were small, conventional 500,000-lb sand-gel fracture treatments that soon gave way to large, conventional 1,500,000-lb sand-gel fracture treatments (Johnston 2004b). Difficulties were often encountered in that gel residue damaged the fracture conductivity. By the mid 1990s more economical slickwater (or low-sand) fracture treatments were applied, pumping large volumes of lightly treated fresh water (about 1 million gallons) with a low sand concentration (100,000 lb). Fisher and others (2002) reported a typical treatment of 750,000 gal water with 80,000 lb of proppant (proppant concentration averaging 0.1–0.5 lb/gal), pumped at 60 bbl/min. Martineau (2007) stated that since 1998 vertical wells have treated the lower and upper Barnett members separately, usually with 900,000 and 500,000 gal of fresh water, respectively, a total of 200,000 lb sand, and a pumping rate of 50–70 bbl/min. Slickwater fracs use a friction-reducing chemical additive which allows the water to be pumped into the formation at a high rate. Illite, the primary clay mineral in the Barnett, does not react adversely to the water. Although not dramatically increasing well performance, slickwater fracs achieve an effective extension length of the hydraulic fractures at one half to one third the cost of conventional stimulation. Additionally, a routine completion practice is to re-stimulate Barnett wells after several years of production (Pollastro, 2007). Wells previously stimulated by conventional techniques can be re-stimulated by slickwater treatment, connecting additional reservoir rock to the borehole and sometimes exceeding the original initial production (Bowker, 2003; Jarvie and others, 2007).

Good conductivity near the borehole is required to allow of flow back the fracture fluid (from as little as 20-30% to as much as 60–70% of the injected volume returned over 2–3 days or more; Johnston 2004b; Givens and Zhao, 2009) because water that remains trapped in the Barnett will impede hydrocarbon production. Also, water remaining in induced fractures from a nearby well can limit the extent of the fracture fairway in wells closely drilled in space (40 acres or less) and time (few weeks) (Givens and Zhao, 2009). The produced gas should lift the load of the fracture fluid to the surface; otherwise, the well may need swabbing or pumping (at additional cost) to eliminate standing water. Standing water chokes the gas flow from perforations, and the problem of water production regularly occurs throughout the life of a well. Barnett wells can produce a lot of water—median volume of 1.6 gal per Mcfg and as much as 400–500 bbl per day for the life of the well (Sumi, 2008). On the other hand, Kuuskraa and others (1998) reported that many wells have little or no water production, indicating an improvement in completion techniques.

Prior to 1983 wells in the Marcellus Shale were commonly treated with 50,000–80,000 lb sand foam fracs, and stimulation in general produced a marginal increase in production. Beginning in the mid 1980s operators developed a stimulation design of normal to moderately large, single-stage, straight nitrogen or nitrogen-foam fracs (5–10 MMscf nitrogen) with a moderate amount of sand (2,000–5,000 sacks sand) (Gottschling, 2007). Nitrogen-foam fracs are commonly applied in shallower shale and shale with low reservoir pressure (Sumi, 2008). A more recent design comprises large to massive slickwater fracs with 2,500–20,000 bbl water and a moderate volume of sand (2,000–5,000 sacks of silica or quartz sand) at a pumping rate of 30 to 100 bbl per minute and a low pressure (Gottschling, 2007). Horizontal wells may involve as much as 95,000 bbl water (Arthur and others, 2009). Additives include friction reducer (KCl or petroleum distillate), biocide (glutaraldehyde), oxygen scavenger (ammonium bisulfide) or stabilizer (N,n-dimethyl formamide) to prevent corrosion of metal pipes, surfactant, scale inhibitor (ethylene glycol), HCl acid to remove drilling-mud damage near the borehole, breaker (sodium chloride), gel (guar gum or hydroxyethyl cellulose), and iron controller (2-hydroxy 1, 2, 3-propanetricaboxylic acid) (Arthur and others, 2008a; Sumi, 2008). The exact makeup of the fracture fluid varies to meet specific conditions of the well. Slickwater-fracture treatment is more commonly applied in deeper, high-pressure shale. A typical slickwater frac in a vertical Marcellus well uses 800,000 gal water and 250,000 lb sand (Sumi, 2008). The water is pumped out after fracturing (flow back) by a large electrical submersible pump, and about half of the frac fluid remains in the reservoir after initial cleanup (Lyle, 2009). Sumi (2008) reported that refrac treatment can use up to 25% more fracture fluid than the original fracture stimulation.

5.1.3 Fracture Barriers

Hydraulic fractures should stay in the gas-shale reservoir and not grow into, or connect with fluids from, the formations above and below. Invading water from the bounding formations will impede production unless stimulation treatment avoids such connection. Fracture barriers are also necessary to control the height of the induced fractures so that stimulation energy is not conducted away from the shale.

The underlying Viola-Simpson Formations, consisting of 30 ft or more of dense, coarsely crystalline to micritic limestone and dolomitic limestone, provide a reliable floor for hydraulic fractures in the Barnett. These rocks are not prone to fracture at the gradients required to fracture the shale (Johnston, 2004a); instead, they confine individual fractures to the Barnett and maximize their effectiveness during well completion. The Viola-Simpson Formations are present only in the northeastern part of the Fort Worth Basin, disappearing along an erosional pinch out that trends northwest-southeast through Wise, Tarrant, and Johnson Counties (Figures 9 and 11). Beyond this line the Barnett is underlain by the Ellenburger Group. The Ellenburger, however, is composed of porous dolomite and limestone with karstic features and is often water-bearing. It presents a significant problem of water encroachment although the problem can be solved by horizontal drilling and smaller, multiple fracture treatments (Jarvie and others, 2007). Limestone and shale of the overlying Marble Falls Formation serve as a good containment ceiling for hydraulic fractures. The limestone in particular has a higher fracture threshold than the Barnett and serves as a barrier to stimulation (Jarvie and others, 2007). But the Marble Falls pinches out east of Johnson County where it is replaced by the Bend Formation (Figures 9 and 11). Porous sandstone and conglomerate of the Bend (itself a gas reservoir in areas of the Fort Worth Basin) also pose difficulties related to water encroachment. A high value of total dissolved salts in any produced water would indicate the presence of water encroachment from below or above the Barnett.

The only water-bearing units stratigraphically close to the Marcellus are the porous Oriskany Sandstone and possibly the fractured Huntersville Chert. Where present, the intervening Onondaga Limestone (up to 200 ft thick) and the Selinsgrove Limestone tongue can adequately isolate Oriskany formation water from the Marcellus (Figures 35 and 36). The Onondaga occurs across much of the play—in the western half of West Virginia, southwestern to northeastern Pennsylvania, and southern New York (Dennison, 1961; Van Tyne, 1996). The Selinsgrove occurs directly beneath the Marcellus in central Pennsylvania. The Onondaga and Selinsgrove Limestones, however, are absent in eastern West Virginia (no barrier). Gottschling (2007) maintained that the Huntersville Chert was also a good fracture barrier to isolate formation water, but his conclusion is debatable. The Huntersville Chert is quite porous due to an extensive fracture network (Flaherty, 1996) and may itself contribute water to the Marcellus. It extends north-south through western Pennsylvania and central West Virginia with a maximum thickness of 250 ft. In the northern part of this area, the Huntersville is frequently separated from the Marcellus by a thin tongue of Onondaga Limestone (a fracture barrier); however, to the south in West Virginia the Huntersville frequently lies directly beneath the Marcellus (no barrier) (Dennison, 1961; Flaherty, 1996). Lastly, the Oriskany was removed by erosion at the Taghanic unconformity through wide areas of western Pennsylvania and New York (Harper and Patchen, 1996), and where absent there should be no problem of water encroachment from below.

Limestones in the Middle Devonian section appear to have a higher fracture threshold than the Marcellus Shale (Lash, 2008), and with proper stimulation design they should serve as a fracture barrier during well treatment. These rocks are not prone to fracture at the gradients required to fracture the shale; instead, they may confine individual fractures to the Marcellus and maximize their effectiveness during well completion. Thus, fracture-containment units exist immediately below the Marcellus (Onondaga Limestone and Selinsgrove Limestone), between lower and upper members of the Marcellus (Cherry Valley and Purcell Members), and above the Marcellus (Tully Limestone and limestones of the Mahantango Formation) (Figure 35). Isopach maps of these several units are provided by Dennison (1961), Van Tyne (1996), Wrightstone (2008), and Boyce (2009). The Tully, though, lies from 100 to 1,700 ft above the Marcellus (the thickness of the intervening Mahantango Formation; Wrightstone, 2008), and as such, its value as a fracture barrier may be very limited. Engelder (2008a) noted that fracture height in black shale is restricted by thick interbeds of siltstone, and perhaps siltstone members of the Mahantango Formation can instead serve as an overlying fracture barrier. In contrast, fractures can extend upward from black shale into overlying gray shale for a considerable distance (Engelder, 2008a).

The presence or absence of lithological barriers that facilitate a large fracture treatment plays a major role in assessing both gas-shale plays. The standard suite of well logs (Table 6) will identify the rock type above and below (sandstone, shale, or carbonate), and the dipole sonic log can be used to calculate rock properties, including fracture gradients in the surrounding formations, from which the engineer can model the reaction

Table 6. Types of well logs and the geological characteristics measured by each[1].

Log type	Characteristic measured
Resistivity	Bound water volume, both clay and pores
Density	Minerals and fluids content measurements
Neutron	Clay and gas content measurements
Sonic	Clay and gas content measurements
Gamma ray	Clay and organic material volume
Electrical images	Identify/quantify natural and drilling-induced fractures, pyrite, calcite nodules, and other geologic features
Spectroscopy	Organic carbon content, clay and carbonate minerals

[1] From Johnson (2004a).

of stimulated fractures when they hit the floor and ceiling rocks (Johnston, 2004a). Underlying and overlying formations may contain anisotropies (such as natural fractures, faults, vugs, and karst elements) that conduct stimulation energy away from the shale (Jarvie and others, 2007). Standard well logs cannot always discover these features; however, electrical images can aid in locating troublesome water-bearing features . 3D-seismic analysis can also locate faults that may serve as a water conduit, and the operator may be able to cement the production casing and not perforate near a fault (Givens and Zhao, 2009).

5.1.4 Fracture Geometry and Fracture Mapping

A very large total surface area of the hydraulic fractures must be created by stimulation, and an understanding of the exact fracture geometry provides insight into reservoir depletion dynamics and can help optimize reservoir management. Because modeling has shown that fractures drain only a small surrounding area (Fisher and others, 2002; Johnston, 2004b), large and wide fairways must be established between the hydraulically created fractures and natural fractures. Natural fractures in the Appalachian black shales have a typical spacing of 1.5 to 6 ft (Avary and Lewis, 2008; Engelder, 2008a), suggesting that gas flows just a few feet through the shale matrix to a natural fracture (Figure 40). Fracture mapping in the Barnett indicates that a very complex fairway is generated during stimulation (rather than a single bi-wing planar crack) with many fractures in multiple orientations (Figure 54) (Fisher and others, 2002). Johnston (2004a) suggested that a fairway's shape varies from square to rectangular, and stimulated wells within 1,500–2,000 ft interfere with one another (Givens and Zhao, 2009). Natural fractures in the Barnett Shale (strike 330–350°) are oriented roughly perpendicular to the hydraulic fractures (strike 45–80°) and may be opened by fracture stimulation. Gale and others (2007) noted that reactivation of natural fractures during fracture stimulation improves the efficiency of treatment. The density of fractures within the fairway is also important: additional wells can be drilled in less densely fractured areas, and refracture stimulation may either create more densely populated fractures within the fairway or extend the fairway itself (Fisher and others, 2002).

Fisher and others (2002) discussed the techniques of fracture mapping in the Barnett Shale. Surface tilt meters detect change in the gradient of displacement of the ground surface caused by hydraulic fracturing at depth (Figure 55). Surface deformation also indicates the volume percent of treatment fluid placed in each orientation when fractures grow in several planes (Figure 56). Down-hole tilt meters placed in an offsetting wellbore determine the fracture dimensions (Figure 55). For example, the tilt-meter map in Figure 56 shows a 900-ft-wide fracture fairway (typical range = 400–1,000 ft and of course a wider fairway means better productivity), trending 39° and containing 45% of the fracture-fluid volume (each crosstie in Figure 56 represents 5% of the fluid). Microseismic mapping, also based on instruments placed in offsetting wellbores, depicts the location and orientation of microseisms in the reservoir resulting from hydraulic fracture (Figure 57). As treatment proceeds, a map of microseisms develops which provides fracture azimuth and dimensions. Analysis of microseismic data (Figure 58) provides the azimuth of hydraulic and natural fractures, the order in which they are created, and an estimate of total fracture-segment length of all mapped fractures (more than 25,000 ft in many treatments). Several nearby wells were affected (killed) by the stimulation, giving physical evidence of the geometry of the fracture fairway. Fisher and others (2002) showed a fracture fairway in the lower Barnett

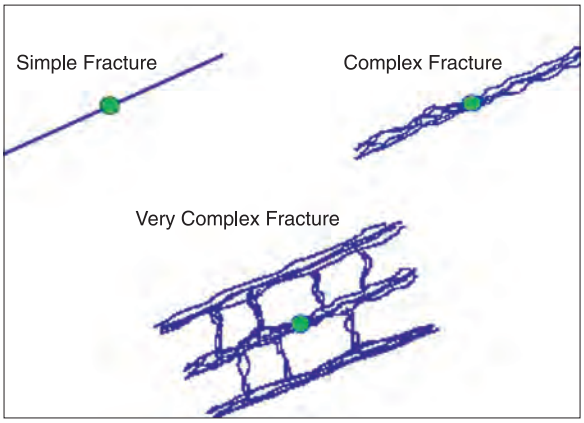

Figure 54. Complexity of hydraulic-fracture fairways. Modified from Fisher and others, 2002.

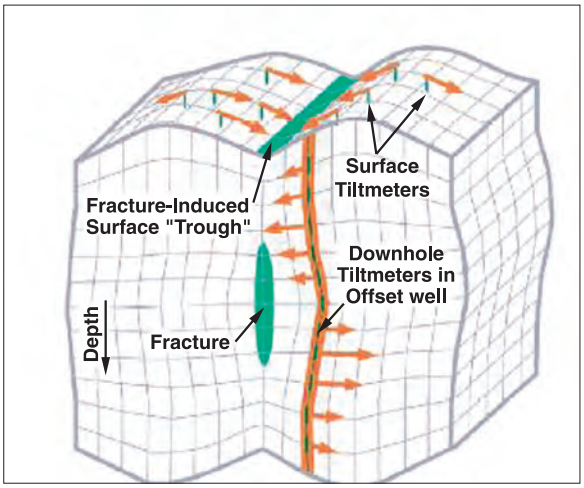

Figure 55. Deformation patterns from hydraulic fractures detected by tiltmeters. Modified from Fisher and others, 2002.

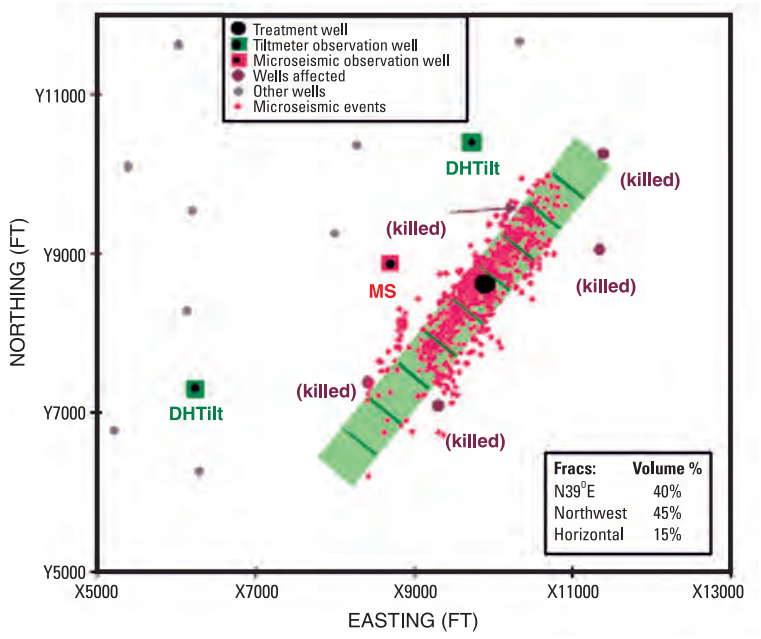

Figure 56. Plan view of study area showing orientation of Barnett fracture fairway and fracture volume in the various fracture planes. Modified from Fisher and others, 2002.

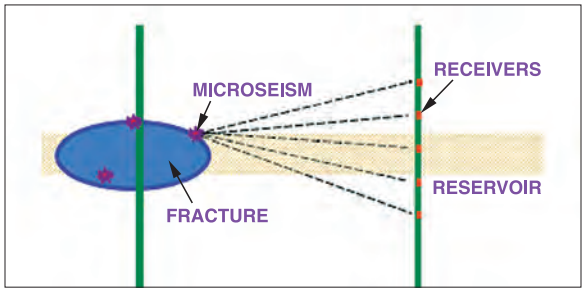

Figure 57. Microseism event location. Modified from Fisher and others, 2002.

member with a fairway half-length of 2,500 ft (typical range = 1,500–3,000 ft); the integrated fracture geometry extends from the underlying Viola Formation up to the top of the middle Forestburg Member. Hydraulic fracturing in the Marcellus is thought to create a comparable fairway of induced fractures (Engelder, 2008a), and computer simulation suggests that induced fractures there may have a width of 0.1 in and reach a length of 2,500 ft (Figure 59) (Arthur and others 2008a). The map in Figure 60 shows results from microseismic analysis of seven fracture treatments in the Barnett. Holes in the fracture fairway represent either a lack of fractures or the presence of rock types that are microseismically aseismic. Other conclusions include the following. Fracture fairway length is longer for an individual stage treatment (lower or upper Barnett) than for combined fracture stimulation. Well productivity is not greatly influenced by conventional fracture half-length; in fact, Fisher and others (2002) discovered that the fracture half-length stops growing before the end of the treatment. In contrast, well productivity and drainage patterns correlate better with the width and the total length (that is, geometry complexity) of the fracture fairway. A larger fracture treatment creates a wider fracture fairway and greater surface area, and these have a favorable effect on gas production (greater flow).

Rock strength affects how easily a stratigraphic zone will fracture (Johnston, 2004a and 2004b). For example, a zone with an average stress gradient 0.1 psi/ft greater than other zones may not fracture when treated with the rest of the formation. The dipole sonic log can determine such variation in stress gradient, and analysis of production logs (spinner, gradiometer, and bubble counter) can identify an unfractured zone that does not contribute significant production (Schlumberger, 2007). Silica-rich shale behaves in a more brittle fashion and fractures easier than clay-rich shale, and these two rocks types can be differentiated on lithologic logs (Johnston, 2004b; Jarvie and others, 2007). The highly brittle character of siliceous shale results in a rapid transition from zero propagation to almost rupture-crack velocity as load increases by a small amount (Gale and others, 2007). Thus, siliceous shale stimulated at the same time as clay-rich shale usually develops a more effective fracture fairway. On a larger scale, various sections of a shale reservoir can exhibit a different fracturing gradient and must be stimulated separately (Martineau, 2007). Multi-stage stimulations (as many as 3- to 4-stage fracs) are thus common, including the isolated stimulation of any zone with higher stress gradient. Conversely the stimulation treatment can be focused toward more brittle zones to improve well deliverability.

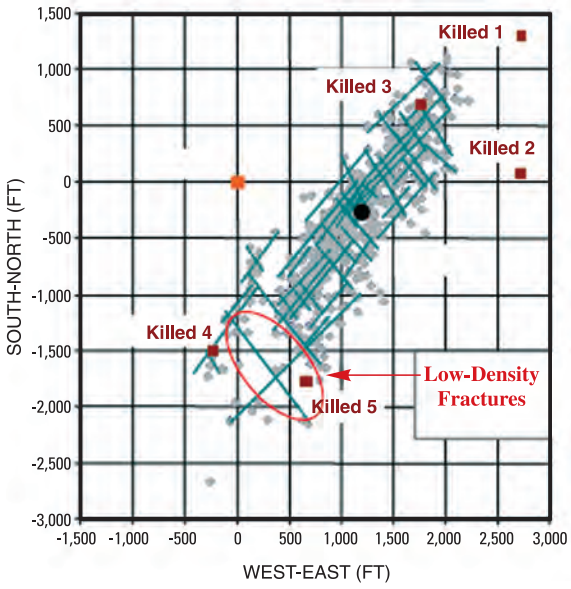

Figure 58. Plan view of fracture-structure plot from one treatment showing size and complexity of fracture segments. Hydraulic fractures trend NE-SW and natural fractures, NW-SE. Modified from Fisher and others, 2002.

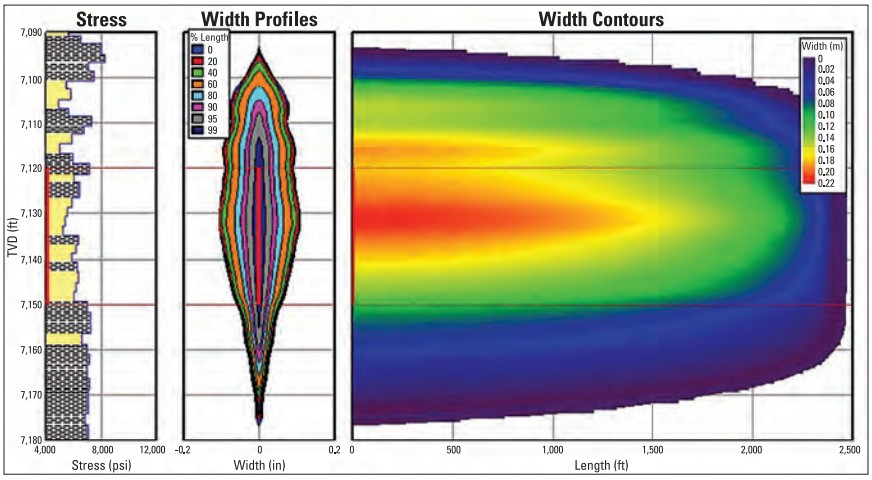

Figure 59. Output of a hydraulic fracture stimulation model, illustrating width profile of the fracture (middle) and length (right). Modified from Arthur and others, 2008a.

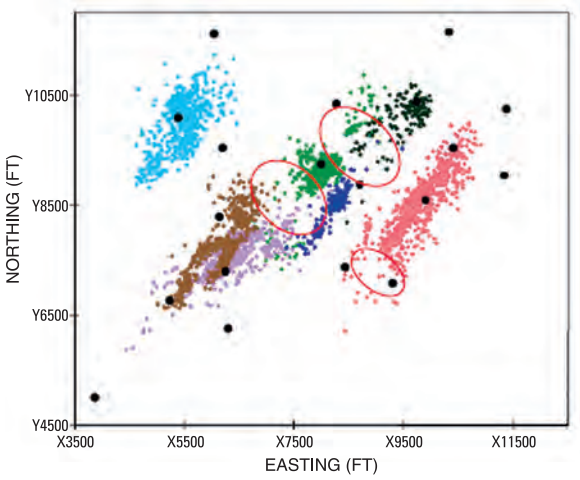

Figure 60. Plan view of seven fracture treatments in one study area illustrates holes in several fracture fairways. Modified from Fisher and others, 2002.

5.2 Horizontal Drilling

Horizontal drilling in the Barnett Shale play is in its infancy, having become commonplace only since 2003. As a consequence, published data concerning drilling/completion techniques and production results are generally sparse.

Horizontal drilling began when drilling expanded into areas with greater risk and to reduce the chance of fractures breaking into the water-bearing Ellenburger Group. Horizontal wells can also be drilled beneath the Fort Worth metropolitan area and DFW airport. The wells are able to drain several parallel sections of reservoir, thus expanding the overall drainage area (Montgomery and others, 2005). By its nature, horizontal drilling increases reservoir exposure to the wellbore, and compared to conventional vertical wells, the EUR can be three times as great for a two-fold increase in cost. In addition, where fracture barriers are thin or absent, stimulations in horizontal wells tend to remain in the target interval much better than those in vertical wells (Montgomery and others, 2005). The drilling/completion technique combines horizontal laterals with multistage fracturing, slickwater treatment, and sand as proppant. While drilling horizontally, a computer guides the motorized drill bit using GPS information. Gamma-ray readings are sent continuously to the surface, and gases in the cuttings are measured by gas chromatography. The gamma-ray readings and gas analysis allow the driller to keep the bit within the pay zone.

By 2008, 85% of the Barnett wells were being drilled horizontally, turning the well 90° over an interval of 500 ft or less (Powell, 2008). The horizontal lateral can reach 5,000 ft although the optimum length is about 2,500–3,500 ft. Companies have experimented with 4,500-ft laterals (equivalent to 100-acre spacing), 2,500-ft laterals (60 acre) and even 30-acre spacing. However, the overlap of fracture treatments on the denser patterns (30 acres) could cause a fall of 25% in per-well reserves (Hayden and Pursell, 2005).

Horizontal wells are stimulated with a low-proppant, water-based hydraulic-fracture treatment pumped at a high flow rate. Martineau (2007) reported horizontal wells in the lower Barnett member with laterals ranging from 1,000–3,500 ft and treatments with 2,000,000–6,000,000 gal fresh water and 400,000–1,000,000 lb sand. The pumping rate ranges from 50 to more than 100 bbl/min. To maximize the rock volume stimulated, wells are commonly drilled normal to the expected propagation direction of the hydraulically induced fractures (that is, normal to the maximum horizontal stress) (Gale and others, 2007). Hayden and Pursell (2005) compared initial potentials of vertical and horizontal wells. Vertical wells drilled between 1999 and 2003 had production rates of 700–1,000 Mcfg/d. Horizontal wells drilled between 2002 and 2003 had production rates of 1,600–2,500 Mcfg/d (Figure 61). The best production results reported by various operators in 2004 were: 789–974 Mcfg/d for vertical wells and 1,786–2,004 Mcfg/d for horizontal wells.

Ketter and others (2008) discussed the techniques of fracture stimulation in horizontal wells. Wells with shorter laterals require single stimulation, and the casing is uncemented. Fractures, though, are prone to grow in such a way that unstimulated gaps remain in the reservoir, meaning a smaller overall fracture area and reduced productivity. Wells with greater lateral length require multiple-stage stimulation, and the casing is cemented. Problems, though, develop with fracture initiation. The fluid-injection rate is then unable to pump the designed proppant concentration, the generated fracture fairway is ineffective, overall fracture-surface area smaller, and the well's productivity reduced.

Ketter and others (2008) noted that the rock is not homogeneous, and stress anisotropy common to layered shale causes problems in initiating artificial fractures (Gottschling, 2007). For example, the state of stress along the lateral in one well with a 4-stage stimulation varied from 0.63 to 0.75 psi/ft (Figure 62). Areas with low horizontal-stress anisotropy exhibit both longitudinal and transverse hydraulically induced fractures on image logs. The fracture system has a shorter fracture length and wider fairway, and the fracture-initiation pressure is low. Areas with high horizontal-stress anisotropy exhibit only transverse fractures. The fracture fairway is longer and narrower, and fracture-initiation pressure is moderate. Areas of high stress have no fractures. It is difficult to initiate fractures because the fracture-initiation pressure is high. Analysis of the image logs allows an operator to select the optimum locations for perforations, avoiding areas of high stress (also avoiding faults that extend into water zones).

Ketter and others (2008) also considered the spacing of perforation clusters in the lateral because an optimal spacing can lead to fewer required fracture stages. If the spacing is too close, a stress shadow can restrict fracture growth in the middle cluster; fracture growth will then be disproportionately higher in the heel and toe. If the spacing of perforation clusters is ideal, fracture growth will be enhanced in the orthogonal direction. The optimal cluster spacing to reduce fracture interference is 1.5 times the fracture height (which is typically 300–400 ft). To reduce the probability of creating multiple, competing fractures, the cluster length should be less than 4 times the wellbore diameter (that is, less than 4 ft). If the cluster length is less than 4 times the

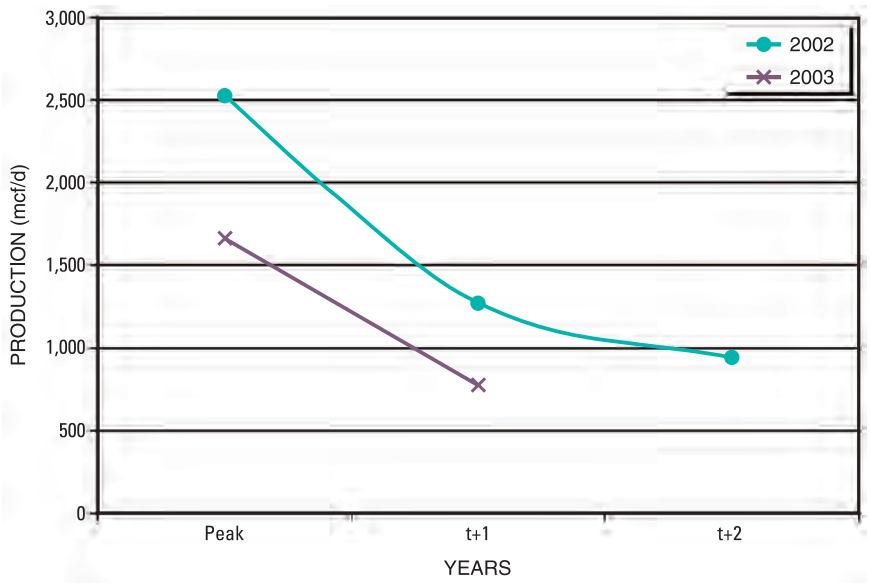

Figure 61. Decline curve for horizontal wells from both core and non-core areas. Modified from Hayden and Pursell, 2005.

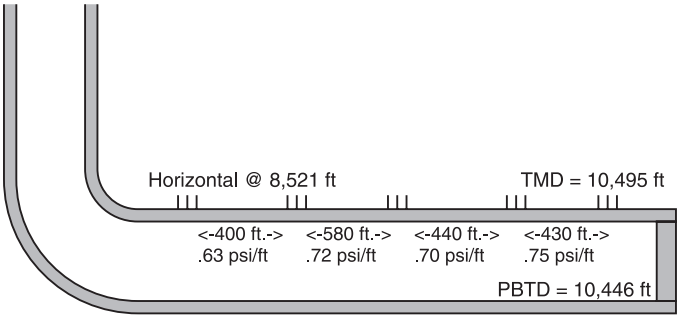

Figure 62. Horizontal lateral showing measured depths, perforation clusters along the top, and variable stress gradients. Modified from Ketter and others, 2008.

wellbore diameter, a single dominant fracture is more likely to form. If the cluster length is greater, multiple fractures form. The treating rate and treating pressure thus needs to be high to adequately stimulate the formation. The optimum rate is 2 bbl/min per perforation, and the optimum total-perforation differential pressure is 500 psi.

Cementing is designed to isolate the annulus between perforation clusters when they are placed at desired distances. Cementing enables the creation of independent hydraulic fractures at each perforation cluster. Ketter and others (2008) recommended the use of an acid-soluble cement system (acid volume of 1,000–2,000 gal per cluster stimulated) in which the cement dissolves within the perforation cluster. Utilizing a cross-linked gel and 100-mesh sand in the pad stage of treatment produces fewer and wider dominant fractures, which improves the ability to disperse later proppants in the region around the borehole.

Currently in the Appalachian Basin there are more vertical wells than horizontal, but the future trend is toward reversing this ratio. At the end of 2007, 135 vertical wells and 20 horizontals had been drilled, and 430 vertical wells and 138 horizontals, planned (Lyle, 2009). Horizontal wells result in a reduced level of disturbance at the surface, greater exposure of the wellbore to reservoir rock, and higher initial potential and estimated ultimate recovery (Figure 63).

The well is usually drilled vertically with air to the kick-off point where the operator switches to an inhibited, water-based mud to drill to total depth (TD) (Ghiselin, 2009). Some operators have tried mineral-oil-based mud for its compatibility with the shale; this mud can also enhance the penetration rate. Others too have

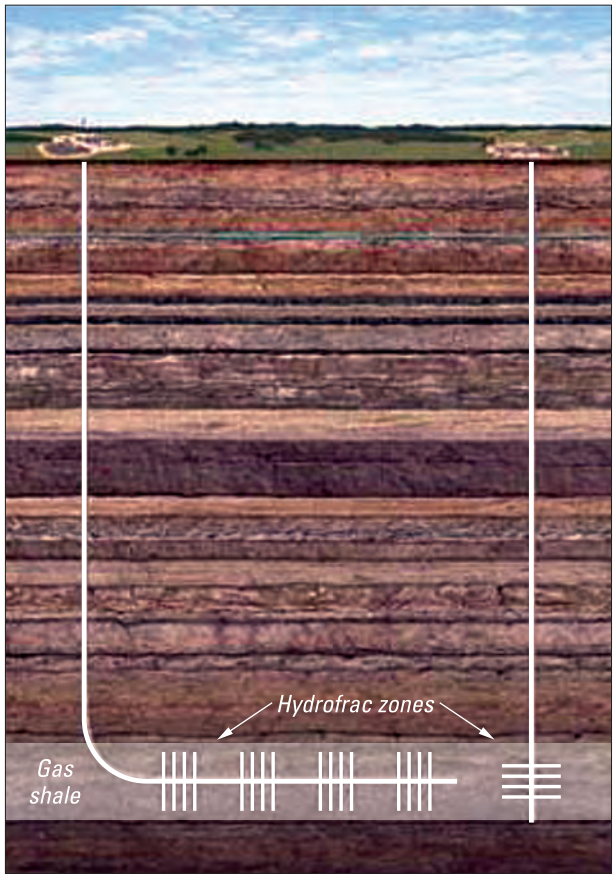

Figure 63. Drilling and stimulation of horizontal (left) and vertical (right) Marcellus wells. Modified from Arthur and others, 2008a.

experienced a shorter overall drilling time with oil-based mud. Laterals extend for 2,000 to 6,000 ft (Atlas, 2008; Arthur and others, 2009). Cemented production casing is most commonly used whereby each zone is isolated, perforated, and fractured in stages (Ghiselin, 2009). One variation involves an open hole with isolation by mechanical packer in conjunction with fracture-stimulation-initiation sleeve.

Horizontal wells are generally stimulated in four to eight stages (Figure 64). Arthur and others (2008a) presented an example of one stage of a sequenced hydraulic fracture treatment for either a vertical or horizontal well (Table 7). Horizontals, however, require multiple stages to fracture-perforate the Marcellus interval because sufficient pressure cannot be maintained to induce fractures over the complete lateral thousands of feet in length. Stimulation begins with an acid treatment to clean drilling mud from around the borehole. Acid treatment can also initiate the fracturing process. Next is the slickwater pad, a volume of fluid large enough to effectively fill the borehole and open the formation with slickwater for friction-reduction purposes. The slickwater pad helps to facilitate the flow and placement of the proppant sequences farther into the fracture network. Next is the fine-proppant sequence which combines a large volume of water with fine-mesh sand at a low concentration. In the ensuing sequences the concentration of fine proppant increases incrementally by decreasing the volume of water used. Fine sand is preferred because it is carried deeper into the induced fractures. Next is the coarse-proppant sequences, and finally the well is flushed with fresh water to remove excess proppants from the wellbore (Arthur and others, 2008a).

A simultaneous frac involves two wells that are fractured together. Gottschling (2007) described a simultaneous frac in which the wells were 30 ft apart on the well pad and 1000 ft apart at the toe. One was fractured in 4 stages and the other in 5 so as to prevent communication between the fracture fairways. These wells yielded a significantly higher initial potential than individually fractured offset wells.

A zipper fracture treatment involves adjacent wells that are fractured alternatively in a back-and-forth pattern, stage by stage (Ghiselin, 2009). This procedure helps to prevent fractures from intersecting one another and maximizes borehole contact with the reservoir.

Lastly, Sumi (2008) stated that problems are encountered drilling through the Hamilton in West Virginia and Ohio. Circulation can be lost because of incompetent, fluid-sensitive shale, and the Hamilton may be underpressured in these areas.

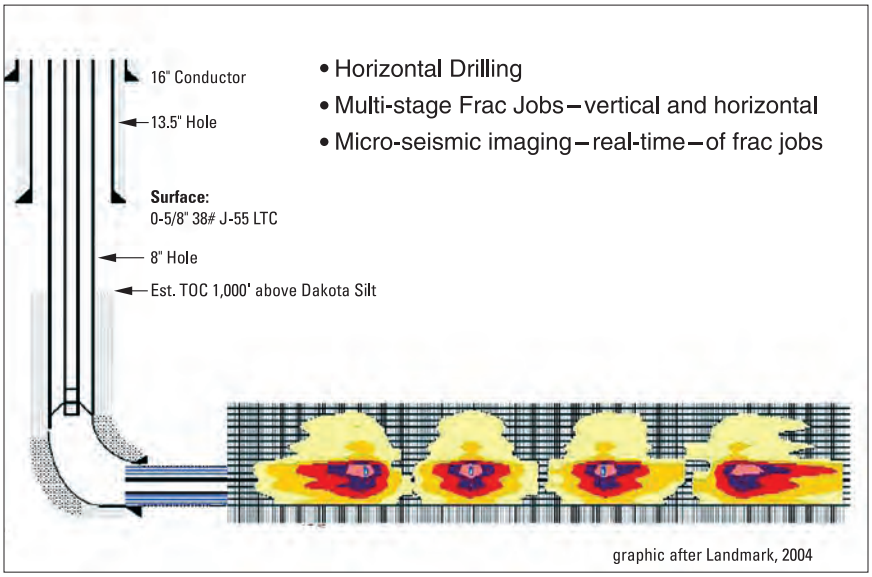

Figure 64. Technological innovations in drilling applied to the Marcellus Shale. Modified from Wickstrom and Carter, 2008.

Table 7. Example of a single stage of a sequenced hydraulic fracture treatment in the Marcellus Shale[1].

[%, percent; HCl acid, hydrochloric acid]

Stage	Volume[2] (gallons)	Rate[3] (gallons per minute)	Fluid type	Proppant size
Acid	5,000	500	15% HCl acid	none
Pad	100,000	3,000	slickwater	none
Prop 0.1	50,000	3,000	slickwater	100 mesh
Prop 0.3	50,000	3,000	slickwater	100 mesh
Prop 0.5	40,000	3,000	slickwater	100 mesh
Prop 0.75	40,000	3,000	slickwater	100 mesh
Prop 1	40,000	3,000	slickwater	100 mesh
Prop 2	30,000	3,000	slickwater	100 mesh
Prop 3	30,000	3,000	slickwater	100 mesh
Prop 0.25	20,000	3,000	slickwater	40/70
Prop 0.5	20,000	3,000	slickwater	40/70
Prop 0.75	20,000	3,000	slickwater	40/70
Prop 1	20,000	3,000	slickwater	40/70
Prop 2	20,000	3,000	slickwater	40/70
Prop 3	20,000	3,000	slickwater	40/70
Prop 4	10,000	3,000	slickwater	40/70
Prop 5	10,000	3,000	slickwater	40/70
Flush[4]	13,000	3,000	slickwater	none

[1] From Arthur and others, 2008a.

[2] Volumes are presented in gallons (42 gallons = 1 barrel; 5,000 gallons = ~120 barrels).

[3] Rates are expressed in gallons per minute (42 gallons per minute = 1 barrel per minute; 500 gallons per minute = ~12 barrels per minute).

[4] Flush volumes are based on the total volume of open borehole; therefore as each stage is completed, the volume of flush decreases as the volume of borehole is decreased.

5.3 Well Performance

On well logs the organic-rich Barnett Shale displays a high resistivity (matrix and hydrocarbons are nonconductive), gamma-ray readings of 150–400 API units, and a mean density of 2.50 g/cc (Kuuskraa and others, 1998). Basic data necessary to evaluate its production potential include reservoir thickness, average matrix porosity and permeability, fracture footage, and hydrocarbon type. The sonic-neutron log-overlay can type the hydrocarbons: crossover of 0–2 porosity units indicates 40° or higher gravity oil, 2–5 porosity units indicates condensate and wet gas, 5–10 porosity units indicates wet gas, and 10–15 porosity units indicates dry gas with no condensate (Johnston, 2004a).

Initial gas production comes from matrix and fracture porosity. Later, when the formation pressure drops below 1,000 psi, long-lived production comes from gas desorption from solid organic matter and kerogen (Lancaster and others, 1993; Johnston, 2004a). Initial potential rate generally relates to thermal maturity of the organic content and drilling technique: 1 MMcfg/day where R_o = 1.65 in the core area, 100–500 Mcfg/day where R_o = 0.8–0.9 outside the core, and 1 MMcfg/day in a horizontal well where R_o = 1.0 outside the core (Jarvie and others, 2007). Within the core area, some areas produce better than others, perhaps involving some better (though unknown) gas-transmission mechanism or more gas in place (Bowker 2007b). In areas of low maturity (the oil window), the gas-flow rate tends to be lower because of lower volumes of generated gas and the presence of residual hydrocarbon fluids that occlude pore throats (Jarvie and others, 2007). The transformation ratio is low (30%), and the only gas generated is oil-associated. Also, where the rock is immature (R_o < 1.0), the presence of liquid hydrocarbons leads to a steeper gas-production decline curve and ultimately less recoverable gas. These negative characteristics are a function of discontinuous pore throats in immature shale or pore-throat constriction by adsorbed hydrocarbon (requiring an elevated energy for gas to break through). The presence of C_{20+} paraffins likewise leads to a much lower gas-flow rate and a lower gas-to-oil ratio (GOR; Jarvie and others 2007). The ratio of liquids/gas is 1.5 bbl NGL/MMcfg (Kuuskraa and others, 1998), but this too depends on the level of thermal maturity and hence varies across the basin. Hayden and Purcell (2005) cautioned that some of the Barnett liquids in the oil-gas transition area are retrograde condensates. These liquids would drop out of the gas while still in the reservoir, not at the surface, and adversely affect gas production.

The lower Barnett member contributes 75–80% of total production and the upper member, 20–25%. All pay zones must be treated for maximum economic return, and perforations typically span 200–300 ft (Kuuskraa and others, 1998). If the reservoir sections are not stacked directly on top of one another, the completion must be designed with more than one stimulation stage. Perforations should be placed in zones that are easiest to break, that is, silica-rich shale with low clay/carbonate content and shale with naturally occurring fractures. The resulting induced fractures will have the maximum areal extent and provide more migration pathways for the hydrocarbon (Johnston, 2004b).

The first refracture treatment of the lower Barnett occurred in 1998, completing the B.S. Carter Jr. No. 4 well a second time (Figure 65). Production curves demonstrate that slickwater refrac of a well initially stimulated by slickwater frac may perform substantially better than the original completion. But the increase in performance can be even better in the slickwater refrac of a well initially stimulated by massive hydraulic-gel frac (Givens and Zhao, 2009.

Most wells are drilled on 55-acre spacing, and the drainage area is estimated to be 10–30 acres/well (Kuuskraa and others, 1998). Operators have noted that some Barnett wells show interference when drilled on 27-acre spacing. Givens and Zhao (2009) have recommended that, because of unfavorable interference, infill wells with a spacing of 40 acres or less should be drilled only after frac water of nearby wells has been produced and some depletion has occurred in the fracture fairway. Horizontal wells are estimated to drain two 55-acre spacing units, and a range of 10–110 acres/well is used in the USGS assessments of the Barnett Shale play (section 3.3.5) (Pollastro, 2007).

Barnett wells typically have modest gas-flow rates, but they have modest drilling costs so that the rate of return is commonly 100% within one year and 65% in non-core areas (Jarvie and others, 2007). At a gas price of $6/Mcfg, Hayden and Pursell (2005) estimated that a vertical well would break even economically with a minimum peak monthly production of 400–450 Mcfg/d, and a horizontal well with a peak monthly production of 650–750 Mcfg/d. EUR (estimated ultimate recovery) ranges from 1.0–3.5 bcfg/well depending on whether the well was drilled vertically or horizontally, and a reasonable average is 1.75 bcfg per well. The minimum EUR to be considered a successful well is 0.2 bcfg (Pollastro, 2007). Recovery estimates vary from 7–12% (Jarvie and others, 2007). The recovery factor may be increased to 12–20% by spacing wells more closely and drilling shorter laterals (Hayden and Pursell, 2005). The production decline for a vertical well is 60–65% in

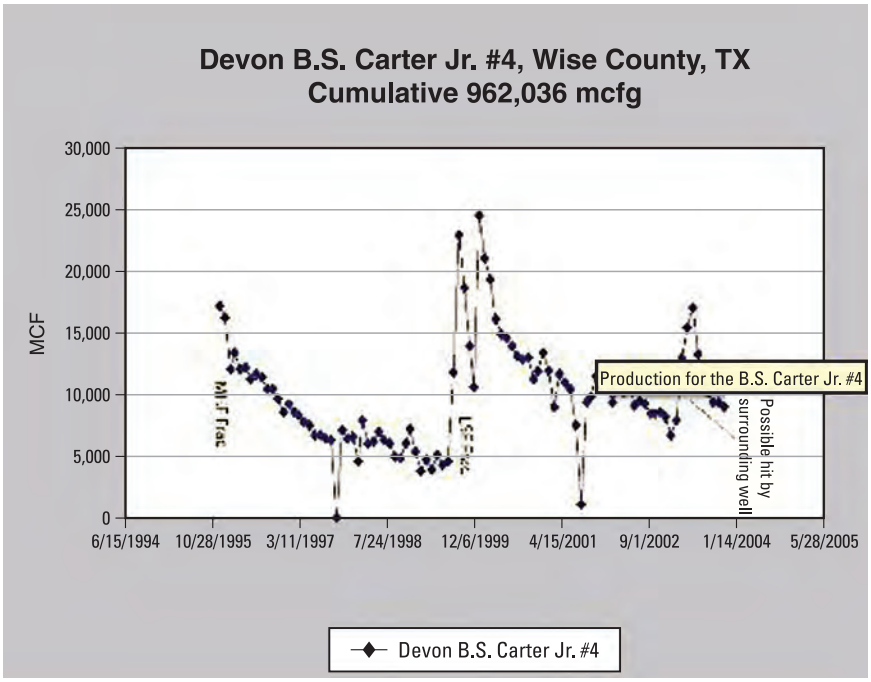

Figure 65. Production from a Barnett well drilled in 1995, refractured in 1998, and perhaps hit in 2003 by stimulation of a nearby well. Modified from Givens and Zhao, 2009.

the first year, production leveling to 10% in 4–5 yrs. In contrast, the production decline for a horizontal well is less steep, 50–55% in the first year (although data are sparse; Hayden and Pursell, 2005).

Kuuskraa and others (1998) characterized the historical drilling results through 1996 as follows. (1) Initial wells drilled in the 1980s were completed in 180 ft of shale with small fracture treatments. Matrix permeability ranged between 0.002-0.003 millidarcies. Wells drained about 10 acres, and EUR was 0.4–0.5 bcfg per well. (2) The Stella Young No. 4 well, drilled in 1986, better defined the production potential of the Barnett. Permeability was 0.003 millidarcies, the drainage area 30 acres, and the hydraulic half-length 190 ft. EUR was estimated to be 1.16 bcfg. (3) Wells reflecting the improved completion practices of 1991–1996 were completed in 230–290 ft of shale with moderate high-conductivity hydraulic fractures. Permeability was 0.002 millidarcies. Wells drained 11–21 acres, and EUR was 0.8–0.9 bcfg per well. Production performance (median initial peak production) from both vertical and horizontal wells decreased notably from a maximum in 2000. Possible explanations include the Newark East field continuing to mature with reduced well spacing and expansion of drilling outside of the core area (Hayden and Pursell, 2005).

Table 8 illustrates comparative Barnett economics for the core area and Tier 1 and Tier 2 counties (see section 3.1) (Hayden and Pursell, 2005).

Reporting requirements in Pennsylvania and New York allow operators extended time periods of confidentiality, making it a challenge to monitor activity in the Marcellus play (Wells and Gognat, 2009). Furthermore, because of the newness of the play, production records rarely exceed 500 days.

Drilling a vertical well is less costly on a per-well basis, but production is less economical than for horizontals. Furthermore, overall development may require four or more vertical wells compared to one horizontal, or 16 vertical wells compared to one multiwell pad for horizontals (Arthur and others, 2008a). A horizontal Marcellus well costs approximately 2–3 times that of a vertical well, but the initial potential can be 3–4 times as much (Engelder and Lash, 2008; Sumi, 2008; Arthur and others, 2008b; Durham, 2008; Wells and Gognut, 2009; Deacon, 2009). Typical costs for a vertical well are $800,000 to $1,300,000 at depths of 3,000-9,000 ft; and for a horizontal well, $3,000,000 to $4,000,000. Reported initial potential (IP) for a vertical well is 1 MMcfg/d or less; and for a horizontal well, 1.4–9 MMcfg/d. One horizontal well reported an IP of 9 MMcfg/d and was producing 8.8 MMcfg/d after 5 days; another with a reported IP of 6.4 MMcfg/d was producing 4.3 MMcfg/d after 105 days (Wells and Gognut, 2009). Engelder (2009) cited a median IP of 4.2 MMcfge/d for

Table 8. Comparison of gas volumes and costs for Barnett wells in the core area, Tier 1 and Tier 2[1].

[Mcfg/d, thousand cubic feet of gas per day; Mcfge, million cubic feet of gas equivalent; MMcfg, million cubic feet of gas; %, percent; EUR, estimate ultimate reserves; M, thousand]

	Core area vertical	Tier 1 horizontal	Tier 2 horizontal
Peak monthly production (Mcfg/d)	650	1,520	900
Year one decline	61%	53%	53%
EUR (MMcfg)	733	2,356	1,395
Well cost ($M)	1,000	2,000	1,500
F&D cost ($/Mcfge)	$1.71	$1.06	$1.34

[1] From Hayden and Pursell (2005).

50 horizontal wells in Pennsylvania. The record IP for a horizontal well may be 24.5 MMcfg/d (Wells and Gognut, 2009). Estimated ultimate recoveries (EUR) for a vertical well range from 175–350 MMcfg; and for a horizontal well, from 0.6 to 3.0 bcfg (Gottschling, 2007; Petzet, 2009; Lyle, 2009).

The anticipated decline curve for horizontal wells drilled by Chesapeake Energy Corp was depicted by Engelder (2009). The initial decline is very steep, following a power-law rate. For example, production should decline by 51% over the first 105 days. Analogous to the Barnett Shale, the EUR for a Marcellus well may be estimated as 1000 times greater than the 30-day production test (Engelder, 2009).

Recently Atlas (2008) reported using a two-stage fracture design in a vertical well in southwestern Pennsylvania. The IP was twice that of a typical one-stage vertical well at an extra cost of $125,000, and the decline rate was shallower.

Operators characteristically drill on a spacing of 40–160 acres, 40 acres for vertical wells and 160 acres for horizontals (Arthur and others, 2008b). The recovery rate for Marcellus shale-gas is approximately 10%, and refracture treatment can add an additional 8–10% (Sumi, 2008; Engelder and Lash, 2008). Zielinski and McIver (1982) also determined a 10% rate of recoverable gas from shot wells with 160-acre spacing, noting that decreasing the well spacing to 80 acres should double the estimated ultimate recovery. Lyle (2009) claimed that the finding-and-development cost for the Marcellus Shale is $1.34/Mcfg. The rate of return for a horizontal well is calculated to be 86% at a gas price of $9.30/MMBTU and 70% at $5.00/MMBTU (Lyle, 2009).

5.4 History of the Barnett Shale Play

Barnett exploration and development remain a low-risk, high-reward venture because of steady, long-term production. There are few truly dry holes, but recovery efficiency is not always good. The challenge in producing Barnett Shale gas has always been to obtain sufficient well deliverability from a tight, though naturally fractured reservoir (Johnston, 2004a). To learn more about the shale's petrophysical properties, Mitchell Energy Corp, the principal operator, carried out more and more detailed reservoir-characterization analyses. To improve recovery efficiency as drilling expanded across the play, completion techniques were increasingly selected to fit specific local conditions. This section of our report summaries the history of the Barnett Shale play as undertaken by Mitchell Energy and detailed by Steward (2007).

The discovery well was the C.W. Slay No. 1 in Wise County, drilled in 1981 by Mitchell Energy Corp to the Viola Limestone (total depth 7,950 ft). The Viola proved unproductive after acidizing, and the well was plugged back. The well was then perforated in the lower Barnett member and acidized with a slight show of gas. Mud logging in the Slay No. 1 indicated the presence of gas. In addition, the well logs looked encouraging when compared to the Devonian Shale play of the Appalachian Basin. Stimulation was planned to connect with any open fractures. The stimulation used nitrogen, creating a short fracture network (250-ft theoretical half-length, TFHL) contained by the Viola below and Forestburg Limestone Member above. The initial potential was 246 Mcfg/d, and the well began to produce in 1982.

A regional study of the Barnett was hampered by limited deep-well control, the high proportion of older wells without modern log suites, little information about thermal maturity and shale permeability, and a lack of seismic data. Mitchell Energy Corporation began to deepen development wells in the Bend Conglomerate

to gain additional information concerning the Barnett. The geological hypothesis was that Barnett success would be tied to finding open natural fractures, especially in areas of faulting and flexures and associated with structural highs. Core data was used to evaluate fluid sensitivity for the completion design, compare rock mineralogy and porosity to open-hole log response, and measure permeability. As more wells were drilled, transient-test analysis of pressure buildup and drawdown were performed. The Newark East field was named as a new field discovery in 1982.

Production rate of the Slay No. 1, after cleanup, was 120 Mcfg/d in June 1982. The next year the well was re-perforated and refractured with CO_2 foam, having a TFHL of 500 ft. Production jumped to 274 Mcfg/d, but completion costs were judged to be prohibitive. Two other wells were drilled and cored, but there the Barnett was underlain by the Ellenburger Group. Cores showed a permeability of 0.0009–0.008 millidarcies. The wells were fractured with CO_2 foam, but the produced gas was contaminated with CO_2. Engineers then experimented with nitrogen foam and nitrogen-assisted gelled water fracture. The W.D. Johnson No. B-1 well had a strong show of gas that required a mud weight of 12.5 lb/gal (the Barnett was frequently drilled with 9.7 lb/gal mud), and a safe drilling rate of 1–2 min/ft was established.

The W.C. Young No. 2 well was cored continuously from the base of the Forestburg Limestone Member through the lower Barnett, Viola, and into the Ellenburger. Core analysis showed the following: TOC 1.0–8.0% with an average of 4.5; thermal maturity R_o 1.4; and porosity approximately 3.7% (coring allowed the density-log response to be correlated with true rock porosity). High-porosity intervals also had the highest TOC with only minor volumes of carbonate cement. The shale was highly indurated, with a clay content of 20–54% (illite, chlorite, mixed-layer varieties) and quartz content of 28–47% (detrital silt, siliceous cement, diagenetically altered radiolarian ooze). The Barnett contained some lenses of limestone and dolomite, and pyrite, apatite, and feldspar occurred in trace amounts. Surprisingly the natural fractures were completely healed (open fractures were judged to be drilling induced). One fracture system had an azimuth of north and another, northwest.

Next, wells were drilled with nitrogen-assisted gelled fracture stimulation and 500-ft, 750-ft, and 1,500-ft TFHLs. Initial potentials were reported to be 730–1,100 Mcfg/d. Larger stimulation design did not always result in a consistent, stepwise increase in production, and the completion costs prevented TFHL designs of greater than 1,500 ft.

The I.M. Peek No. 2 well (drilled in 1983) encountered a relatively thin section of Barnett (243 ft) with low porosity, poor to no gas shows, and directly overlying the Ellenburger. This failure emphasized the need for new regional seismic data. When acquired, these data showed that the Peek No. 2 had been drilled on the upthrown side of the Rhome/Newark fault (down-to-the-north normal). The H.A. Smith No. 1 well (1985) expanded the play into Denton County where the Barnett was thicker and deeper. The rock contained healed fractures and was quite calcareous. Although gas shows were poor and the log and core porosities low, the well was perforated and fractured and began to produce with an acceptable 700 Mcfg/d. Based on seismic data, the J.R. Witt No. A-4 in Wise County was drilled directly over a large fault, expecting open natural fractures. Fracturing, in fact, was substantial with apertures almost 0.25 in, but they were all mineralized. The completion encountered high fracture gradients and fracture pressures, and the fracture job was terminated (and the Barnett produces essentially nothing without stimulation). The best producers were in structurally uncomplicated areas with low dip, and Mitchell Energy generally chose to stay 2,000 ft away from known major faults. Successful Barnett wells, in the depth range of 6,500 ft or more, were measuring formation pressure gradients of 0.44–0.50 psi/ft, resulting in reservoir pressures in excess of 3,000 psi.

Seismic data from 1983–1986 showed the existence of pronounced regional fault systems, such as Mineral Wells and Rhome-Newark, generally *en echelon*, vertical, and down to the north. At this time, too, Mitchell Energy realized that the presence of the underlying Viola Limestone played a role in Barnett success, and regional mapping identified the Viola pinch-out line. The company defined the technical parameters for the better producers:

- thickness of the lower Barnett Shale greater than 230 ft,
- greater than 100 ft of 3% porosity and porosity-thickness greater than 4.0 ft,
- formation pressure gradient from 10-day test greater than 0.43 psi/ft,
- current sub-sea depth below 6,000 ft, and
- wells located 5,000 ft from known major faults.

Every one of these requirements eventually proved to be mistaken.

Barnett wells appeared to follow a hyperbolic decline curve for two or three years, then change to an exponential decline. Data suggested that a well with initial potential of 900–1,200 Mcfg/d would be expected to produce approximately 1.0 bcfg in a 25-year life. The only way to improve these economics was to improve initial rates for the hyperbolic or exponential flow periods or to decrease costs. Mitchell's economics in the early 1990s were: with a gas price of $3.50 MMBTU and completed well cost of $700,000, the payout volume would be 350 MMcfg. By 1997 a core area of production was established in Wise and Denton Counties. The area south of the Rhome-Newark fault zone was thought to have potential, especially with future technological advances or drastic reductions in well costs. The area north of the Mineral Wells fault zone and west of the Viola pinchout showed little promise of becoming commercial.

In 1990 Mitchell Energy teamed with the Gas Research Institute to address the following projects: reservoir and production modeling, reservoir characterization, induced-fracture analysis and design, rock properties, gas-in-place analysis, natural- and induced-fracture orientation, application of horizontal drilling to the shale, and refracturing of Barnett producers. Average rock porosity was estimated to be 4.5%, and water saturation, 30–40%. The Barnett was shown to contain free gas, indicating that the adsorbed gas was at its sorptive capacity for any given TOC content and reservoir pressure. Gas-in-place was 82 MMcfg/ac (53.2 bcfg/sq mi) for the lower Barnett member at 3,800 psi bottom-hole pressure and 175°F bottom-hole temperature. Twenty-one percent of the gas was adsorbed. A single set of natural fractures existed (determined from cores and imagery logs) striking 114°. Drilling induced and open-hole stress-test fractures had a strike of 54–60°. The natural fractures encountered were of very limited size, and the drainage volumes depended almost entirely on the size of the induced fracture. Most areas had very few natural-fracture networks contributing to well production.

It was thought that the drainage pattern for each well was elliptical with a major axis of 3,000 ft. If drilling on an 80-acre unit, 8 wells with a EUR of 1 bcfg would produce 8.0 bcfg/sq mi at a recovery efficiency of 16%. Lower Barnett wells with 1,500-ft TFHL gel fracs and a total depth of 7,000–8,000 ft cost from $750,000–$950,000, and the stimulation cost initially accounted for approximately $350,000–$450,000.

2-D and 3-D seismic analyses in the early 1990s identified fault/karst compartments in the area, with fewer karst features where the Viola (as opposed to the Ellenburger) is present at the underlying unconformity. Seismic data also identified small, localized faults and karst chimneys (about one per sq mi and 20–200 ac in size) that extend up through the stratigraphic section from the unconformity to the Atoka (Bend). Wells drilled within 300–500 ft of a fault had significantly lower frac-stimulation success. The Forestburg Limestone Member acted as the upper barrier.

Dual completions provided a significantly higher initial rate from a wellbore by having production from two different formations, and the Barnett's extremely long life almost required a dual completion (rather than delaying uphole completion). To reduce the cost of completion, engineers experimented with different fracture treatments. Eventually they settled on slickwater fracs (or light sand frac), suited for low-permeability rock where fracture aperture is less important than size of the induced-fracture network. Sand in very low concentrations was used not so much as a proppant, but to scour the fault surface, and the frac fluid was water with surfactants (the shale is not sensitive to water). Initial results were positive (70–146 MMcfg per well in the first year of production). A well's cost was reduced by $200,000. Reduced costs allowed a follow-up well to be completed in the lower and upper members in combination (perforate both zones and pump one slickwater stimulation). In areas with a lower Viola barrier, slickwater fracs performed comparably to hydraulic-gel fracs at a fraction of the completion cost. Furthermore, slickwater fracs were interfering with older wells, not just in the direction of the induced fractures (45–55°), but in every direction. More importantly, such interference improved production in the hit well by 200–800 Mcfg/d at essentially no cost.

An upper barrier for fracture stimulation of 100 ft of Forestburg Limestone yielded good producers, and 30–50 ft of limestone was needed for lower fracture containment. Tight, dense, unfractured limestone had the highest fracture integrity, whereas shaly, porous or fractured limestone tended to fail. In 1999 the upper Barnett member became a target, and wells were routinely fracture-stimulated in both lower and upper members where the Forestburg Limestone member was a questionable barrier. Where the Forestburg is a known excellent barrier, a two-stage completion technique was used. The drilling program at this time averaged 1.021 MMcfg/d per well. At about the same time Mitchell Energy began to refracture wells producing in both members. Refracs seemed to work best with understimulated wells and high cumulative production, generally with greater than 0.4 bcfg. Refracs were done using a single stage with lower and upper members combined. Results varied considerably, but it was not unusual for a reworked well to perform substantially better than after the original completion.

In 1998 an effort was made to reevaluate gas-in-place and recovery efficiency (by way of test wells, conventional cores, pressure cores, and gas recovery). Average porosity was closer to 4.5% (previously thought

3.7%) and water saturation, 25% (down from 50–60%), and a direct correlation was found between adsorbed gas to TOC. Gas-in-place was now calculated to be 145± bcfg/sq mi, and the recovery efficiency was 6%.

Changes were next made in infill drilling. Wells were drilled on 100-acre spacing and as close as 30 acres (more closely packed wells tended to be poorer producers) and within 3 months of each other on a 1,000-acre lease. Production averaged 1.050 MMcfg/d. Tiltmeter mapping and microseismic analysis demonstrated a dendritic induced-fracture fairway with elliptical or rectangular geometry oriented 40–60°. Water fracs were seen to break down existing healed fractures (with a northwest orientation), and the Viola, Forestburg, and Marble Falls Limestones were shown to be effective fracture barriers. Fracture monitoring proved quite successful, and 55-acre spacing seemed best. Wells that are fractured close together in time and space appear to share induced-fracture fairways unless a stress shadow exists with the pre-existing fracs. Also, in areas of multiple, closely spaced, large fracture stimulations, artificial lift can significantly improve the elimination of frac fluids from the fracture fairway (by assisting flow back and cleanup of the fracture), thereby improving long-term performance.

In the Wesley Ballman No. 3 well (drilled in 1985), the Barnett had a thermal maturity of R_o = 1.3, seemingly transitional between oil and gas and nonprospective. In several other wells, R_o measured in core proved to be 0.15 greater than in cuttings. Mapping of BTU content of gas in shallow reservoirs was found to be a useful tool to estimate the thermal maturity of the deeper Barnett (source of the shallow gas). Simultaneously it was realized that many early Barnett failures were due to a lack of fracture containment, rather than insufficient thermal maturity. The Anna Woody No. 5 well (drilled in 2000), where R_o = 1.4–1.5, produced 206 MMcfg and 10,600 barrels of condensate in its first year. The Hanna Khraish No. 1 well was drilled in the deepest part of the basin, and the expected R_o was 2.0; however analysis of cuttings showed that R_o = 1.2–1.3. Another Barnett test showed the presence of native copper. The thermal maturity and burial history of the Barnett were now re-evaluated, concluding that hydrothermal brines emanating from the Ouachita Thrust front significantly raised the temperature of the Barnett. Other faults in Wise County acted to reduce hydrothermal flow and produce lower paleotemperatures. Additional drilling indicated that in some areas the lower Barnett is in the rich gas window and the upper Barnett, in the oil window. Where the intervening Forestburg Limestone Member is thick, the thermal maturity of the upper shale can be significantly reduced.

In 2000–2001 engineers experimented with new techniques to improve drilling success in areas where the Viola had poor integrity as a fracture barrier: drill to just above the Viola, fracture the Barnett in uncemented casing, prefrac the Viola to create a stress shadow, break down the Viola and inject cement to increase the frac gradient near the well-bore, utilize natural cavitation in uncemented casing in an attempt to reduce the Barnett fracture gradient, reduce pumping rates, and use silica flour or 100 mesh sand slugs as fracture diverters. The technique produced better success than conventional slickwater fracs, though only 60% success. The Waggoner No. C-12 was re-entered in 2001, a cement plug spotted from TD up through the Viola (isolating a wet porous interval) and across the bottom half of the lower Barnett Shale. The top half of the lower Barnett was thus cased but uncemented. The lower Barnett was then fracture-stimulated using 100–mesh sand as a diverter, and the upper Barnett was completed conventionally. The well produced at a rate of 660 MMcfg and 35 bbls condensate per day.

Initial interest in horizontal drilling was for use in areas beyond the Viola pinch out where a bottom fracture barrier was absent. In 1997 the L.B. Wilson GU No. 1 was drilled horizontally to the southeast, perpendicular to the induced-fracture direction, and the nearby L.B. Wilson GU No. 2 to the southwest. The wells were designed to have 1,700-ft and 2,700-ft laterals respectively, with targets in the upper third of the lower Barnett. A heel frac was also planned for the Wilson GU No. 1. The measured depth in the No. 1 well was 8,628 ft, and it was completed with 4.5-inch cemented production casing (cemented because of shale plugging problems in other wells). The first stage of stimulation was pumped with minimal problems, but the second and third stages encountered high treating pressures and very little fluid was pumped. A 1,500-ft interval was perforated, but only the toe perforations were effectively stimulated. Initial rate of production was 700 Mcfg/d, and after frac-fluid cleanup it was a nearly water-free completion. All indications were that the stimulation stayed in zone. The production decline showed a much lower rate than in conventional, vertical wells. The offset well L.B. Wilson GU No. 2, drilled parallel to the direction of induced fractures (southwest), seemed not to perform as well (initial potential rate 463 Mcfg/d). Costs were approximately three times that of a vertical Barnett completion. Mitchell Energy then experimented unsuccessfully with slim-hole (4.5 to 5 in casing), short-radius (drilling the curve over an interval of 150 ft) techniques.

Republic Energy Inc. drilled a west-to-east horizontal well in Parker County (not directed perpendicular to the assumed induced-fracture direction because seismic analysis detected a fault and karst chimney). The well was drilled with a 2,200-ft lateral and stimulated with Halliburton SurgiFrac using high-velocity water

injection to fracture the area adjacent to the perforations. This technique allowed the operator to perform a large number of fracs along the lateral, one at a time, giving better control over placement and fracture-height growth. The well was treated with 10 separate stages of 75,000 gal water per stage, one third to one fourth of what most operators were using at the time. Initial potential rate was 1.3+ MMcfg/d.

For the years 2001–2002, new Barnett wells (total of 384) had an average initial potential rate of 1 MMcfg/d, including exploration and infill wells. The average rework production rate was 700 Mcfg/d (an increase of 500 Mcfg/d). Although drilling and completion costs were rising, they were more than offset by higher gas prices and better well performance, thereby resulting in excellent profitability. Mitchell Energy merged with Devon Corporation in January 2002. Devon immediately drilled five horizontal wells that outperformed anything previously seen in the Barnett play: initial rates of 2.5–3.5 MMcfg/d (even in areas with a weak or no Viola lower frac barrier). Devon experimented with a number of completion techniques and frac sizes from 2.5–4.5 million gal water, and laterals from 2,000–2,500 ft in length. Devon learned that faults or karst near a well bore could act as a thief zone for frac fluids or a conduit to the Viola or Ellenburger. 3-D seismic data were needed to assess structural problems. Frac mapping by use of microseismic analysis proved critical in gaining insight into fracture breakout. Devon began drilling horizontal wells in areas with developed vertical completions, giving a net density of 20 acres, and other operators spaced horizontals at 500 ft, a resultant density of 40 acres.

From 2003, when there was a major increase in horizontal drilling, through 2006, vertical wells had an average annual production of 195 MMcfg and horizontals, 390 MMcfg. By June 2006 operators completed 6,200 wells in the Barnett Shale, 1,800 of which were horizontals. Barnett completions covered more than 8,000 square miles in 17 counties of northern Texas.

6.0 COMPARISON OF BARNETT AND MARCELLUS SHALES

Our conclusions compare significant geological characteristics of the Barnett and Marcellus Shales as well as successful engineering techniques used in the drilling and stimulation of shale wells (Table 9).

Table 9. Comparison of Barnett and Marcellus Shales.

	Barnett	Marcellus
Location	15 counties of north-central Texas.	Extends from New York through Pennsylvania to West Virginia and westward from Maryland to Ohio.
Play size and reserves	9,000 sq mi, core area 1,800 sq mi. Estimated 39 tcfg of undiscovered, technically recoverable gas.	75,000 sq mi, core area 53,000 sq mi. Estimated 50 tcfg of undiscovered, technically recoverable gas.
Formation thickness and age	50–1,000 ft, typically 150–600 ft. Upper Mississippian.	50–660 ft, typically 50–260 ft. Middle Devonian.
Stratigraphy	Bend Formation Marble Falls Formation Barnett Shale—upper shale member Forestburg Limestone Member lower shale member Chappel Limestone Viola-Simpson Formations Ellenburger Group	Tully Limestone Mahantango Formation Marcellus Shale—Oatka Creek Shale Member Purcell Limestone Member Cherry Valley Limestone Member Union Springs Member Tioga Ash Onondaga Limestone/Huntersville Chert/ Needmore Shale Oriskany Sandstone
Lithology	Dense, organic-rich, siliceous, thin-bedded, petroliferous, fossiliferous shale and hard, black, finely crystalline, petroliferous, fossiliferous limestone. Silica-rich shale behaves in a more brittle fashion and fractures easier than clay-rich shales, responding well to stimulation.	Splintery, soft to moderately soft, gray to brownish black to black, carbonaceous, highly radioactive shale with beds of limestone and carbonate concretions. Silica-rich and organic-rich shales behave in a more brittle fashion and fracture easier than clay-rich shales, responding well to stimulation.

Table 9. Comparison of Barnett and Marcellus Shales.—Continued

	Barnett	Marcellus
Mineral composition	35–50% quartz, 27% illite with minor smectite, 8–19% calcite and dolomite, 7% feldspars, 5% organic matter, 5% pyrite, 3% siderite, and traces of native copper and phosphate material.	27–31% quartz, 9–34% illite, 1–7% mixed-layer clays, 0–4% chlorite, 3–48% calcite, 0–10% dolomite, 0–4% sodium feldspar, 5–13% pyrite, and 0–6% gypsum.
Basin	Asymmetrical foreland basin bounded by prominent thrust belt, structural arches, and Precambrian uplift.	Asymmetrical foreland basin bounded by prominent thrust belt, structural arches, and Precambrian uplift.
Influential geological structures	Ouachita Thrust front, Mineral Wells and Newark East faults, local faults overlying Ellenburger karst surface, and natural fractures.	Rome Trough, two sets of planar systematic joints (J_1 and J_2), weak zones of basement rock which localized the position of the forebulge, and low-amplitude folds with associated fractures.
Depositional environment	Deep-water basin with poor circulation, stratified water column, and anoxic bottom water; marine upwelling contributed to algal blooms; water depth perhaps 500–650 ft.	Deep-water basin with poor circulation, stratified water column, and anoxic bottom water; marine upwelling contributed to algal blooms; water depth perhaps 300–1,000 ft.
Drilling depth	4,000–8,500 ft.	2,000–10,000 ft.
Organic carbon content	TOC = 2–6%, type II kerogen with minor admixture of type III.	TOC = 1–10%, primarily type II kerogen with a mixture of type III.
Thermal maturity	$R_o \geq 1.2$ (maximum 1.9) or Tmax ≥ 465°C in the core area of dry gas; maturity related to burial depth and to hydrothermal heating around deep-seated faults; thermal-maturity boundary (and hence potential gas production) based on chemical assessment may extend farther westward in the basin compared to assessment made by vitrinite reflectance.	$R_o \geq 1.60$ (maximum 3.5) or CAI ≥ 3 or TAI ≥ 5 or Tmax ≥ 470°C in the core area of dry gas; maturity related to burial depth and to high heat flow over deep-seated faults; R_o and TAI values may be suppressed meaning that the mapped area of dry gas would shift to the west some considerable distance.
Reservoir characteristics	φ = 3–6%, k = microdarcies to nanodarcies, S_w = 25% but no free water, S_g = 75%. Gas is stored within interstitial pores and microfractures, and also it is adsorbed onto solid organic matter and kerogen (20–60%). The generation of hydrocarbons produced microfractures in the shale as well as a slight overpressuring (0.52 psi/ft); however microfractures have subsequently been healed by residual oil and pyrobitumen. At a subsurface pressure of 4,000 psi, 80% of the Barnett gas is free and stored in open pores, but below 1,000 psi desorption of methane can play an important role in gas production.	φ = 6%, k = microdarcies to nanodarcies, S_w = 30% but no free water, S_g = 70%. Reservoir pressure = 3,000–4,000 psi, overpressured (0.51 psi/ft) in some areas but underpressured (0.10–0.35 psi/ft) in others. Gas is stored within interstitial pores and microfractures, and also it adsorbed onto solid organic matter and kerogen (20–85%). The generation of hydrocarbons produced the pervasive joints.
Generation of hydrocarbon	Gas in place (GIP) is a function of organic richness, thermal maturity, volume of oil cracked to gas, and formation thickness. Estimated to be 140–200 bcfg/sq mi or 170–350 scfg/t. Transformation ratio (conversion of kerogen) ranges from 36 to 93% depending on the rock's maturity (immature to post mature). 20–60% of the generated hydrocarbons were lost by migration.	Gas in place (GIP) is a function of organic richness, thermal maturity, and formation thickness. Estimated to be 30–150 bcfg/sq mi or 60–100 scfg/t. The volume of adsorbed gas decreases eastward with an increasing quartz content. Transformation ratio ranges to over 90% (post mature). Perhaps 54% or more of the generated hydrocarbons were lost by migration.
Delineation of play	*Core area* defined by $R_o \geq 1.1$ and presence of underlying and overlying frac barriers (Viola-Simpson and Marble Falls Formations). *Play* defined by limit of shale to the east and north and a minimum thickness of 100 ft to the west.	*Core area* defined by $R_o \geq 1.6$, presence of underlying frac barrier (Onondaga Limestone), and minimum thickness of 50 ft. *Play* defined by limit of the shale.

Table 9. Comparison of Barnett and Marcellus Shales.—Continued

	Barnett	Marcellus
Fracture stimulation	A typical slickwater frac consists of 500,000–6,000,000 gal fresh water (higher volumes in horizontal wells), 80,000–1,000,000 lb sand proppant (greater weights in horizontal wells), and pumping rate of 50–100 bbl/min. Lower and upper shale members of the Barnett are treated either in combination or individually. Refracture stimulation is accomplished after several years. Geometrically complex fairways are generated by stimulation, square to rectangular in shape, 1,500–3,000 ft long, and 400–1,000 ft wide. The Viola-Simpson Formations have a higher fracture gradient than the Barnett and serve as a fracture barrier to water in the underlying Ellenburger Group. Likewise the Marble Falls Formation prevents water encroachment from the overlying Bend Formation. The middle Forestburg Limestone Member may also serve as a frac barrier, effectively separating the upper and lower shale members. Where frac barriers are absent, wells are drilled horizontally and with smaller, multiple treatments.	A typical slickwater frac consists of 100,000–850,000 to as much as 4,000,000 gal water (higher volumes in horizontal wells), 250,000–750,000 lbs sand proppant, and pumping rate of 30–100 bbl/min. Artificial-fracture fairways may reach a length of 2,500 ft. Underlying frac barriers include the Onondaga Limestone and Selinsgrove Limestone tongue. Possible fracture barriers above are the Tully Limestone and siltstone and limestone members of the Mahantango Formation. The Purcell Limestone and Cherry Valley Limestone Members may also serve as a frac barrier within the formation.
Horizontal drilling	Wells are turned through 90° over an interval of 500 ft or less and drilled in the direction normal to the expected orientation of induced fractures. Horizontal laterals reach from 1,000 to 5,000 ft although the optimum length is 2,500–3,500 ft. Shorter laterals require single stimulation and the casing is generally uncemented, whereas longer laterals require multi-stage stimulation and the casing is cemented. Perforations are placed in zones that are easiest to break, that is, silica-rich shale with low clay/carbonate content and shale with naturally occurring fractures. An optimal spacing of perforation clusters in the lateral can lead to fewer required fracture stages. If the spacing is too close, a stress shadow may restrict fracture growth in the middle cluster. If the spacing of perforation clusters is ideal, fracture growth will be enhanced in the orthogonal direction. To reduce the probability of creating multiple competing fractures, the cluster length should be less than 4 times the wellbore diameter. Cementing isolates the annulus between perforation clusters, enabling the creation of independent hydraulic fractures at each perforation cluster. The use of a cross-linked gel and 100-mesh sand in the pad stage of treatment improves the ability to disperse the proppant around the borehole.	Wells are usually drilled vertically with air to the kick-off point where the operator switches to an inhibited, water-based mud to drill to TD. Some operators use oil-based mud for its compatibility with the shale and/or to enhance the penetration rate. Laterals extend for 2,000 to 6,000 ft. Cemented production casing is most commonly used whereby each zone is isolated, perforated, and fractured in stages. A common variation involves an open hole with isolation by mechanical packer in conjunction with fracture-stimulation-initiation sleeve. Simultaneous fracs may yield a significantly higher initial potential, and zipper fracs can prevent induced fractures from intersecting one another. Horizontal wells are generally stimulated in four to eight stages. Stimulation consists of: acid treatment, slickwater pad, fine-proppant sequences, coarse-proppant sequences, and fresh-water flushing.
Well performance	IP = 700–1,000 Mcfg/d (vertical) and 1,600–2,500 Mcfg/d (horizontal). EUR = 0.7–1.0 bcfg (vertical) and 2.4–3.5 bcfg (horizontal). Recovery efficiency 10%, up to 20% with refrac. Well cost = $1,000,000 (vertical) and $2,000,000 (horizontal).	IP = 1,000 Mcfg/d (vertical) and 1,400–9,000 Mcfg/d (horizontal. EUR = 0.2–0.4 bcfg (vertical) and 0.6–3.5 bcfg (horizontal). Recovery efficiency 10%, up to 20% with refrac. Well cost = $1,000,000–$2,000,000 (vertical) and $3,000,000–$4,000,000 (horizontal).

7.0 REFERENCES

Advani, S.H., GangaRao, H.V.S., Chang, H.Y., Dean, C.S., and Overbey, W.K., 1977, Stress trajectory simulations across the Appalachian plateau province in West Virginia, Eastern Gas Shale Project 28.

Algeo, T.J., and Scheckler, S.E., 1998, Terrestrial-marine teleconnections in the Devonian: links between the evolution of land plants, weathering processes, and marine anoxic events: Philosophical Transactions Royal Society London, v. 353, p. 113–130.

Arbenz, J.K., 1989, The Ouachita system, *in* Bally, A.W., and Palmer, A.R., eds., The Geology of North America: an overview: Geological Society America, p. 371–396.

Arthur, J.D., Bohm, B., and Layne, M., 2008a, Hydraulic fracturing considerations for natural gas wells of the Marcellus Shale: presented at the Ground Water Protection Council 2008 annual forum, September 21–24, 2008, Cincinnati, OH, 16 p.: *http://www.dec.ny.gov/docs/materials_minerals_pdf/GWPCMarcellus.pdf*, accessed November 2009.

Arthur, J.D., Bohm, B., Coughlin, B.J., and Layne, M., 2008b, Evaluating the environmental implications of hydraulic fracturing in shale gas reservoirs: ALL Consulting, 21 p.

Arthur, J.D., Bohm, B., and Layne, M., 2009, Considerations for development of Marcellus Shale gas: World Oil, July 2009, p. 65–69.

Atlas Energy Resources LLC, 2008, Atlas Energy enhances Marcellus Shale production results with new technique: company news release: November 24, 2008.

Avary, K.L., and Lewis, J.E., 2008, New interest in cores taken thirty years ago: the Devonian Marcellus Shale in northern West Virginia: *http://www.papgrocks.org/avary_pp.pdf*, accessed July 2009.

Barnett Shale bibliography, no date: *http://www.beg.utexas.edu/pttc/BSR/barnettshalebiblography.xls*, accessed June 2009.

Barnett Shale Maps, 2007: *http://blumtexas.blogspot.com*, accessed May 2009.

Barrett, R., no date, The depositional setting of the Marcellus black shale: Appalachian Producers Issues Seminar. Independent Oil and Gas Association of West Virginia: *http://www.iogawv.com/RamsayBarrett-Shale.pdf*, accessed July 2009.

Berman, A., 2009, Shale plays and lower natural gas prices: a time for critical thinking: World Oil, January 2009, p. 15.

Billman, D. and 7 others, 2000, Reservoir characterization of the upper Devonian Elk sands in the Appalachian basin: Petroleum Technology Transfer Council, *http://www.pttc.org/workshop_summaries/401.htm*, accessed September 2009.

Blakey, R. 2005, Paleogeography and geologic evolution of North America: *http://jan.ucc.nau.edu/~rcb7/RCB.html*, accessed May 2009.

Boswell, R., 1996, Play USs: Upper Devonian black shales, *in* Roen, J.B., and Walker, B.J., eds., The atlas of major Appalachian gas plays: West Virginia Geological and Economic Survey Publication V-25, p. 93–99.

Bowker, K.A., 2002, Recent developments of the Barnett shale play, Fort Worth basin, *in* Law, B.E., and Wilson, M., eds., Innovative gas exploration concepts symposium: Rocky Mountain Association Geologists and Petroleum Technology Transfer Council, Oct 2002, 16 p.

Bowker, K.A., 2003, Recent developments of the Barnett shale play, Fort Worth basin: West Texas Geological Society Bulletin, v. 42, p. 8–10.

Bowker, K.A., 2007a, Barnett Shale gas production, Fort Worth basin: issues and discussion: American Association Petroleum Geologists Bulletin, v. 91, p. 523–533.

Bowker, K.A., 2007b, Development of the Barnett Shale Play, Fort Worth Basin: Search and Discovery Article #10126: *http://www.searchanddiscovery.net/documents/2007/07023bowker/index.htm*, accessed June 2009.

Boyce, M., 2009, Subsurface stratigraphy and petrophysical analysis of the Middle Devonian interval of central Appalachian basin: West Virginia and southwest Pennsylvania: PhD thesis proposal, West Virginia University, 23 p.

Brechtel, C.E., 1978, *In situ* stress measurements at the MERC well: EGSP Open File No. 116, May 1978, 19 p.

Broadhead, R.F. and Potter, P.E., 1980, Petrology of the Devonian gas-bearing shale along Lake Erie helps explain gas shows: DOE/METC/12140-29, November 1980, 49 p.

Brown, D. 2007, From sea to shining sea: if it's shale, it's probably in play: AAPG Explorer: *http://www.aapg.org/explorer/2007/04apr/beyond_barnett.cfm*, accessed May 2009.

Browning, D.W., and Martin, C.A., 1982, Geology of North Caddo Area, Stephens County, Texas: *in* Martin, C.A., ed., Petroleum Geology of the Fort Worth Basin and Bend Arch Area, Dallas Geological Society, p. 315–330.

Busch, Andreas, Alles, Sascha, Krooss, Bernhard M., Stanjek, Helge and Dewhurst, David 2009, Effects of physical sorption and chemical reactions of CO_2 in shaly caprocks: Energy Procedia, vol.1, p. 3,229–3,235 *www.elsevier.com/locate/procedia*.

Byrer, C.W., Trumbo, D.B., and Roades, S.J., 1976, Lithologic description of cored wells #11940 and #12041 in the Devonian shale in the Cottageville, West Virginia area: MERC/TPR-76/7, October 1976, 22 p.

Byrer, C.W., Vickers, M.K., Rhoades, S.J., and Easterday, B.G., 1976, Lithologic description of cored wells #20402 and #20403 in the Devonian shale in Lincoln County, West Virginia: MERC/TPR-76/9, October 1976, 58 p.

Castle, J.W., 2000, Recognition of facies, bundling surfaces and stratigraphic patterns in foreland-ramp successions: an example from the Upper Devonian Appalachian basin, USA: Journal Sedimentary Research, v. 70, p. 896–912.

Cheney, M.G., 1929, Stratigraphic and structural studies in North Central Texas: University of Texas Bulletin 291, 27 p.

Clarkson, G.R., 1980, Devonian conodont biostratigraphy in the subsurface of Mason County, West Virginia: West Virginia University, Unpublished Master's Thesis, 82 p.

Conway, M., and Hall, C., 2008, Shale gas evaluation: 2008 International Coalbed and Shale Gas Symposium Short Course #2, University of Alabama, 95 p.

Curtis, J.B., 2002, Fractured shale-gas systems: American Association Petroleum Geologists Bulletin, v. 86, p. 1921–1938. Daniels, J., Delay, K., Waters, G., LeCalvez, L., Lassek, J., and Bentley, D., 2007, Contacting more of the Barnett Shale through an integration of real-time microseismic monitoring, petrophysics, and hydraulic fracture design: Society Petroleum Engineers Paper 11562, 12 p.

Deacon, R., 2009, The size of the prize, *in* Marcellus Playbook: Hart Energy Publishing, p. 84–85.

Dennison, J.M., 1961, Stratigraphy of Onesquethaw stage of Devonian in West Virginia and bordering states: West Virginia Geological Survey Bulletin 22, 87 p.

Dennison, J.M., 1985, Catskill delta shallow marine strata, *in* Woodrow, D.L., and Sevon, W.D., eds., The Catskill Delta: Geological Society America Special paper 201, p. 91–106.

Dennison, J.M., and Hasson, K.O., 1976, Stratigraphic cross section of Hamilton Group (Devonian) and adjacent strata along south border of Pennsylvania: American Association Petroleum Geologists Bulletin, v. 60, p. 278–298.

Department of Energy, 1979, Eastern Gas Shales Project West Virginia #5 well, Mason County Phase II Report: Preliminary laboratory results, October 1979, 28 p.

Department of Energy, 1980a, Eastern Gas Shales Project West Virginia #6 well, Monongalia County Phase II Report: Preliminary laboratory results, March 1980, 21 p.

Department of Energy, 1980b, Eastern gas shales project planning document for FY 81, September 1980, 107 p.

Department of Energy, 1981a, Evaluation of Devonian shale potential in Pennsylvania: DOE/METC-119, January 1981, 103 p.

Department of Energy, 1981b, Eastern Gas Shales Project West Virginia #6 well, Monongalia County Phase III Report: Summary of laboratory analyses and mechanical characterization results, Cliffs Minerals, Inc., February 1981, 31 p.

Department of Energy, 1981c, Unconventional gas recovery program: Information file accession list, METC/82/1, October 1981, 152 p.

Department of Energy, 1982, Geologic analysis of Devonian shale cores, Cliffs Minerals, Inc., DOE/METC/08199-1130, February 1982, p. 46.

de Witt, W., Roen, J.B., and Wallace, L.G., 1993, Stratigraphy of Devonian black shales and associated rocks in the Appalachian basin, *in* Petroleum Geology of the Devonian and Mississippian black shale of eastern North America: USGS Bulletin 1909, p. B1–B57.

Donaldson, A.C., and Shumaker, R.C., 1981, Late Paleozoic molasse of central Appalachians, *in* Miall, A.D., ed., Sedimentation and tectonics in alluvial basins: Geological Society Canada Special Paper 23, p. 99–124.

Duffield, S.L., and Warshauer, S.M., 1981, Upper Devonian (Frasnian) conodonts and ostracodes from the subsurface of western West Virginia: Journal of Paleontology, v. 35, p. 72–83.

Durham, L.S., 2005, Barnett Shale play still going strong: American Association Petroleum Geologists Bulletin, v. 86, p. 1,921–1,938.

Durham, L.S., 2008, Appalachian basin's Marcellus—the new target: AAPG Explorer, March 2008: *http://www.aapg.org/explorer/2008/03mar/marcellus.cfm*, accessed July 2009.

Energy Information Administration, 2008, Annual Energy Outlook 2008: *http://www.eia.doe.gov/oiaf/aeo/production.html*, accessed May 2009.

Engelder, T., 1994, Brittle crack propagation, *in* Hancock, P. ed., Continental Tectonics: Oxford, Pergamon Press, p. 43–52.

Engelder, T., 2008a, Structural geology of the Marcellus and other Devonian gas shales: geological conundrums involving joints, layer-parallel shortening strain, and the contemporary tectonic stress field: Pittsburgh Association of Petroleum Geologists Field Trip (Sept. 12–13, 2008), 96 p.

Engelder, T., 2008b, Outcrops of the Middle Devonian Marcellus Formation: *http://www.geosc.psu.edu/~engelder/marcellus/marcellus.html*, accessed July 2009.

Engelder, T., 2009, Marcellus 2008: report card on the breakout year for gas production in the Appalachian Basin: Fort Worth Basin Oil & Gas Magazine, August 2008, p. 18–22.

Engelder, T., and Fischer, M.P., 1994, Influence of poroelastic behavior on the magnitude of minimum horizontal stress, S_h, in overpressured parts of sedimentary basins: Geology, v. 22, p. 949–952.

Engelder, T., and Lash, G.G., 2008, Marcellus Shale play's vast resource potential creating stir in Appalachia: The American Oil and Gas Reporter, May 2008, 7 p.

Engelder, T., Lash, G.G., and Uzcategui, R., 2009, Joint sets that enhance production from Middle and Upper Devonian gas shales of the Appalachian Basin: American Association of Petroleum Geologists Bulletin v. 93, p. 857–889.

Engelder, T., no date, A science briefing for Congressman John Peterson: *http://law.psu.edu/_file/aglaw/EngelderPresentation.pdf*.

Ettensohn, F.R., 1985, The Catskill Delta complex and the Acadian orogeny, *in* Woodrow, D.L., and Sevon, W.D., eds., The Catskill Delta: Geological Society America Special paper 201, p. 39–49.

Ettenhohn, F.R., 1994, Tectonic controls on formation and cyclicity of major Appalachian unconformities and associated stratigraphic sequences, *in* Dennison, J.M., and Ettensohn, F.R., eds., Tectonic and eustatic controls on sedimentary cycles: SEPM Concepts in Sedimentology and Paleontology #4, p. 217–242.

Ettensohn, F.R., 2008, Tectonism, estimated water depths, and the accumulation of organic matter in the Devonian-Mississippian black shales of the northern Appalachian basin: AAPG Eastern Section Meeting: *http://www.searchanddiscovery.net/abstracts/html/2008/eastern-pittsburgh/abstracts/ettensohn.htm*, accessed July 2009.

Ettensohn, F.R., and 8 others, 1988, Characteristics and implications of the Devonian-Mississippian black-shale sequence, eastern and central Kentucky, USA: pycnoclines, transgression, regression, and tectonism, *in* McMillan, N.J., Embry, A.F., and Glass, D.J., eds., Devonian of the World, Proceedings of Second International Symposium of Devonian System: Calgary, Canadian Society Petroleum Geologists Memoir 14, v. 2, p. 323–345.

Evans, M.A., 1980, Fractures in oriented Devonian shale cores from the Appalachian basin, Volume I: DOE/ET/12138-1341 (Vol.1) (DE83008494), January 1980, 64 p.

Fan, J., Frantz, J.H., and Gatens, J.M., 1993, Gas shales technology review, Volume 8, Number 2, October 1993, 111 p.

Fertl, W.H. and Rieke, H.H., 1979, Gamma ray spectral evaluation techniques identify fractured shale reservoirs and source rock characteristics: Society Petroleum Engineers, American Institute Mining, Metallurgical, Petroleum Engineers Paper SPE 8454, 14 p.

Filer, J.K., 1994, High frequency eustatic and siliciclastic sedimentation cycles in a foreland basin, Upper Devonian Appalachian basin, *in* Dennison, J.M., and Ettensohn, F.R., eds., Tectonic and eustatic controls on sedimentary cycles: SEPM Concepts in Sedimentology and Paleontology #4, p. 133–145.

Fischer, M.P., Gross, M.R., Engelder, T., and Greenfield, R.J., 1995, Finite-element analysis of the stress distribution around a pressurized crack in a layered elastic medium: implications for the spacing of fluid-driven joints in bedded sedimentary rock: Tectonophysics, v. 247, p. 49–64.

Fisher, M.K., Wright, C.A., Davidson, B.M., Goodwin, A.K., Fielder, E.O., Buckler, W.S., and Steinsberger, N.P., 2002, Integrating fracture mapping technologies to optimize stimulation in the Barnett Shale: Society Petroleum Engineers Paper 77441, 7 p.

Flaherty, K.J., 1996, Play Dho: fractured Middle Devonian Huntersville Chert and Lower Devonian Oriskany Sandstone: *in* Roen, J.B., and Walker, B.J., eds., The atlas of major Appalachian gas plays: West Virginia Geological and Economic Survey Publication V-25, p. 103–108.

Flawn, P.T., Goldstein, A., King, P.B., and Weaver, C.E., 1961, The Ouachita System: Texas Bureau of Economic Geology, Publication 6120, 401 p.

Flippin, J.W., 1982, The stratigraphy, structure, and economic aspects of the Paleozoic strata in Erath County, North-Central Texas, *in* Martin, C.A., ed., Petroleum geology of the Fort Worth Basin and Bend Arch area: Dallas Geological Society, p. 129–155.

Franz, J.H., and Jochen, V., 2005, Shale gas: Schlumberger White Paper, 9 p.

Gadde, P.B. and Sharma, M., 2006, Proppant placement/transport in fractures: *www.pge.utexas.edu/links/proppant.pdf*, accessed July 2009.

Gale, J.F.W., Reed, R.M., and Holder J., 2007, Natural fractures in the Barnett Shale and their importance for hydraulic fracture treatments: American Association Petroleum Geologists Bulletin, v 91, p. 603–622.

Garbutt, D., 2004, Unconventional gas: Schlumberter white paper: OF_03_056, *www.slb.com/media/services/solutions/reservoir/uncongas_whitepaper.pdf*.

Geology.com, 2008, June 18, Marcellus Shale—Appalachian basin natural gas play: *http://geology.com/articles/marcellus-shale.shtml*, accessed July 2009.

Ghiselin, D., 2009, Technology + experience: a winning combination, *in* Marcellus Playbook: Hart Energy Publishing, p. 68–77.

Givens, N., and Zhao, H., 2009, The Barnett shale: not so simple after all: *https://www.republicenergy.com/Articles/Barnett_Shale/Barnett.aspx*, accessed June 2009.Gottschling, J., 2007, Appalachian Basin black shale exploitation: past, present, and future: presentation IOGA of PA annual meeting, May, 2007, 49 p.

Gottschling, J., 2007, Appalachian Basin black shale exploitation: past, present, and future: Presentation IOGA of PA annual meeting, May 2007, 49 p., *http://www.wvsoro.org/resources/marcellus/John_Gott_Marcellus%20Shale.pdf*.

Gutschick, R.C., and Sandberg, C.A., 1983, Mississippian continental margins of the conterminous United States, *in* Stanley, D.J., and Moore, G.T., eds., The shelfbreak margin—critical interface on continental margins,: Society of Economic Paleontologists and Mineralogists, Special Publication 33, p. 79–96.

Harper, J.A., 1999, Devonian, *in* Shultz, C.H., ed., The geology of Pennsylvania: Pennsylvania Geological Survey and Pittsburgh Geological Society, p. 108–127.

Harper, J.A., 2008, The Marcellus Shale—an old "new" gas reservoir in Pennsylvania: Pennsylvania Geology, v. 38, p. 2–13: *http://www.dcnr.state.pa.us/topogeo/pub/pageolmag/pdfs/v38n1.pdf*, accessed July 2009.

Harper, J.A., and Patchen, D.G., 1996, Play Do: Lower Devonian Oriskany Sandstone structural play, *in* Roen, J.B., and Walker, B.J., eds., The atlas of major Appalachian gas plays: West Virginia Geological and Economic Survey Publication V-25, p. 109–117.

Hayden, J., and Pursell, D., 2005, The Barnett Shale, visitors guide to the hottest gas play in the US: Pickering Energy Partners, Inc.: *http://www.tudorpickering.com/pdfs/TheBarnettShaleReport.pdf*, accessed June 2009.

Henry, J.D., 1982, Stratigraphy of the Barnett Shale (Mississippian) and associated reefs in the northern Fort Worth basin, *in* Martin, C.A., ed., Petroleum geology of the Fort Worth basin and Bend Arch area: Dallas Geological Society, p. 157–178.

Hentz, T.F., Kane, J.A., Ambrose, W.A., and Potter, E.C., 2006, Depositional facies, reservoir distribution, and infield potential of the Lower Atoka Group (Bend Conglomerate) in Boonsville Field, Fort Worth basin, Texas: New Look at an Old Play, [abs]: American Association Petroleum Geologists annual convention abstracts, v. 15, p 46.

Hickey, J.J. and Henk, B., 2007, Lithofacies summary of the Mississippian Barnett Shale, Mitchell 2 T.P. Sims well, Wise County, Texas: American Association Petroleum Geologists Bulletin, v. 91, p. 437–443.

Hill, D.G., Lombardi, T.E. and Martin, J.P., 2004, Fractured Shale Gas Potential in New York: Northeastern Geology And Environmental Sciences. v. 26, 49 p.: *http://www.pe.tamu.edu/wattenbarger/public_html/Selected_papers/—Shale%20Gas/fractured%20shale%20gas%20potential%20in%20new%20york.pdf*, accessed July 2009.

Hill, R.J., Jarvie, D.M., Zumberge, J., Henry, M., and Pollastro, R.M., 2007a, Oil and gas geochemistry and petroleum systems of the Fort Worth Basin: American Assocociation Petroleum Geologists Bulletin, v. 91, p. 445–473.

Hill, R.J., Zhang, E., Katz, B.J., and Tang, Y., 2007b, Modeling of gas generation from the Barnett Shale, Fort Worth Basin, Texas: American Association Petroleum Geologists Bulletin, v. 91, p. 501–521.

Horton, A.I., 1981, A comparative analysis of stimulations in the eastern gas shales: DOE/METC-145, 128 p.

Jarvie, D., 2004, Evaluation of hydrocarbon generation and storage in the Barnett shale, Fort Worth basin, Texas: *http://www.humble-inc.com/Humble%20Barnett%20Shale%20presentation%20for%20BEG-PTTC.pdf*, accessesd May 2009.

Jarvie, D.M., Claxton, B.L., Henk, F., and Breyer, J.T., 2001, Oil and shale gas from the Barnett Shale, Fort Worth Basin, Texas [abs.]: American Association Petroleum Geologists Annual Meeting, Program and Abstracts, p. A100.

Jarvie, D.M., Hill, R.J., Pollastro, R.M., Claxton, B.L., and Bowker, K.A., 2004, Evaluation of hydrocarbon generation and storage in the Barnett Shale, Fort Worth basin, *in* Barnett Shale and other Fort Worth basin plays, Ellison Miles Memorial Symposium, Ellison Miles Geotechnical Institute, Brookhaven College, TX, p. 2–5.

Jarvie, D.M., Hill, R.J., Ruble, T.E., and Pollastro, R.M., 2007, Unconventional shale-gas systems: the Mississippian Barnett Shale of north-central Texas as one model for thermogenic shale-gas assessment: American Association Petroleum Geologists Bulletin, v. 91, p. 475–499.

Johnston, D. 2004a, Technological advances expand potential play: Oil and Gas Journal: *http://www.ogj.com/display_article/196507/7/7/ARCHI/none/none/1/Technological-advances-expand-potential-pay/*, accessed June 2009.

Johnston, D. 2004b, Reservoir characterization improves stimulation, completion practices: Oil and Gas Journal: *http://www.smtpbackup.com/artikler/Frac-Article.pdf*, accessed June 2009.

Kalyoncu, R.S., Boyer, J.P., and Snyder, M.J., 1979a, Characterization and analysis of Devonian shales as related to release of gaseous hydrocarbons well V-7 Wetzel County, West Virginia: ORO-52-5-11-1, UGR File #211, August 1979, 93 p.

Kalyoncu, R.S., Boyer, J.P., and Snyder, M.J., 1979b, Characterization and analysis of Devonian shales as related to release of gaseous hydrocarbons well C-1 Lincoln County, West Virginia: ORO-5205-T2, March 10, 1979, 448 p.

Kalyoncu, R.S., and Snyder, M.J., 1979, Characterization and analysis of Devonian shales as related to release of gaseous hydrocarbons well C-2 Lincoln County, West Virginia: FE5205-T1, March 30, 1979, 104 p.

Keller, G.R., 2005, The classic southern Oklahoma and Dniepr-Donets aulacogen analogy revisited [abs.]: Geological Society America Abstracts with Program, 39th annual meeting, South-central section, v. 37, p. 38.

Ketter, A.A., Heinze, J.R., Daniels, J.L., and Waters, G., 2008, A field study in optimizing completion strategies for fracture initiation in Barnett Shale horizontal wells: Society Petroleum Engineers Production & Operations, p. 373–378.

Kinley, T.J., Cook, L.W., Breyer, J.A., Jarvie, D.M., and Busbey, A.B., 2008, Hydrocarbon potential of the Barnett Shale (Mississippian), Delaware Basin, west Texas and southeastern New Mexico: American Association Petroleum Geologists Bulletin, v. 92, p. 967–991.

Komar, C.A., and Kahn, S., 1978, Hydraulic fracture modeling: Eastern Gas Shale Project: EGS–66.

Kurtz, T., McBane, R.A., and Westcott, P.A., 1985, Eastern Devonian gas shales technology review, Volume 2 Number 1, May 1985, 36 p.

Kuuskraa, V.A., Koperna, G., Schmoker, J.W., and Quinn, J.C., 1998, Emerging U.S. Gas Resources-5: Oil and Gas Journal, v. 96, issue 21, p. 67–76.

Kuuskraa, V.A., Sedwick, K.B., Thompson, K.B., and Wicks, D.E., 1985, Technically recoverable Devonian shale gas in Kentucky: DOE/MC/19239-1834 (DE85008608), May 1985, 120 p.

Kuuskraa, V.A., and Wicks, D.E., 1984, Technically recoverable Devonian shale gas in West Virginia: DOE/MC/19239-1750 (DE85003367), December 1984, 119 p.

Kuuskraa, V.A., Wicks, D.E., Sawyer, W.K., and Esposito, P.R., 1983, Technically recoverable Devonian shale gas in Ohio: DOE/MC/19239-1525 (DE84003057), July 1983, 101 p.

Lancaster, D.E., McKetta, S., and Lowry, P.H., 1993, Research findings help characterize Fort Worth Basin's Barnett Shale: Oil & Gas Journal, v. 91, issue 10, p. 59–64.

Larese, R.D., and Heald, M.T., 1977, Petrography of Selected Devonian Shale Core Samples from the CGTC 20403 and CGSC 11940 Wells, Lincoln and Jackson Counties, West Virginia: MERC/CR-77/6, 27 p.

Lash, G.G., 2007, Influence of basin dynamics on Upper Devonian black shale deposition, western New York State and northwest Pennsylvania: Search and Discovery Article #30050: *http://www.searchanddiscovery.com/documents/2007/07022lash/index.htm*, accessed July 2009.

Lash, G.G., 2008, Stratigraphy and fracture history of Middle and Upper Devonian succession, western New York—significance to basin evolution and hydrocarbon potential: Pittsburgh Association Petroleum Geologists 2008 Spring Field Trip, 88 p.

Lash, G.G., and Blood, D.R., 2007, Origin of early overpressuring in the Upper Devonian Catskill delta complex, western New York state: *http://www.searchanddiscovery.com/documents/2007/07028lash_blood/images/p01.pdf*, accessed July 2009.

Lash, G.G., and Engelder, T., 2006, A switch in joint driving mechanism as evidence for passage of a Morrawan peripheral bulge at the onset of the Alleghanian orogeny: *http://www.searchanddiscovery.net/abstracts/html/2006/eastern/abstracts/lash02.htm*, accessed July 2009.

Lash, G.G., and Engelder, T., 2008, Marcellus Shale subsurface stratigraphy and thickness trends: eastern New York to northeastern West Virginia: abstract and presentation: American Association Petroleum Geologists Eastern Section Meeting, Pittsburgh, Pennsylvania Search and Discovery #90084: *http://www.searchanddiscovery.net/documents/2008/08167eastern_abs/abstracts/lash.htm*, accessed July 2009.

Leonard, R., Woodroof, R., and Bullard, K., 2007, Barnett shale completions: a method for assessing new completion strategies, Society Petroleum Engineers Paper 110809, 28 p.

Liberatore, A.J., and Wilson, M.W., 1983, Field-scale experiment in underground gasification of coal at Pricetown, West Virginia: DOE/METC-83-49 (DE83011052), April 1983, 215 p.

Loucks, R.G., 2003, Origin of Lower Ordovician Ellenburger Group brecciated and fractured reservoirs in West Texas: paleocave, thermobaric, tectonic, or all of the above?: *http://aapg.confex.com/aapg/sl2003/techprogram/paper_78591.htm*, accessed June 2009.

Loucks, R.G., and Ruppel, S.C., 2007, Mississippian Barnett Shale: lithofacies and depositional setting of a deep-water shale-gas succession in the Fort Worth Basin, Texas: American Association Petroleum Geologists Bulletin, v. 91, p. 579–601.

Lyle, D., 2009, Marcellus draws a crowd, *in* Marcellus Playbook: Hart Energy Publishing, p. 22–25.

Marcellus Formation: Wikipedia, the free encyclopedia: *http://en.wikipedia.org/wiki/Marcellus_Formation*, accessed July 2009.

Marcellus Playbook, 2009: Hart Energy Publishing, 92 p.

Marcellus Shale in New York, 2009: *http://oilshalegas.com/marcellusshalenewyork.html*, accessed November 2009.

Martin, J.P., 2006, The middle Devonian Hamilton group shale in the northern Appalachian basin: production and potential, AAPG Search and Discovery Article #90059©2006 AAPG Eastern Section Meeting, Buffalo, New York: *http://www.searchanddiscovery.com/abstracts/html/2006/eastern/abstracts/martin01.htm*, accessed July 2009.

Martineau, D.F., 2007, History of the Newark East field and the Barnett Shale as a gas reservoir, American Association Petroleum Geologists Bulletin, v. 91, p. 399–403.

Martini, A.M., Walter, L.M., Budai, J.M., Ku, T.C.W., Kaiser, C.J., and Schoell, M., 1998, Genetic and temporal relations between formation waters and biogenic methane—Upper Devonian Antrim Shale, Michigan basin, USA: Geochimica et Cosmochimica Acta, v. 62, p. 1,699–1,720.

McHugh, S.L., Murri, W.J., Seaman, L., Curran, D.R., and Keough, D.D., 1978, Fracture of Devonian shale by tailored pulse-loading: Final report covering the period August 15, 1977 through August 15, 1978: DOE/ET/12074-T1, December 1978, 94 p.

McIver, R.D., and Zielinski, R.E., 1978, Geochemical evaluation of the eastern gas shales—part 1: MLM-2563 (UC-92), September 29, 1978, 33 p.

Milici, R.C., 1996, Stratigraphic history of the Appalachian basin, *in* Roen, J.B., and Walker, B.J., eds., The atlas of major Appalachian gas plays: West Virginia Geological and Economic Survey Publication V-25, p. 4–7.

Milici, R.C., 2005, Assessment of undiscovered natural gas resources in Devonian black shales, Appalachian Basin, Eastern U.S.A., U.S. Geological Survey Open-File Report 2005-1268, 31 p.: *http://pubs.usgs.gov/of/2005/1268/2005-1268.pdf*, accessed July 2009.

Milici, R.C., Ryder, R.T., Swezey, C.S., Charpentier, R.R., Cook, T.A., Crovelli, R.A., Klett, T.R., Pollastro, R.M., and Schenk, C.J., 2003, Assessment of undiscovered oil and gas resources of the Applachian Basin province, 2002: U.S. Geological Survey Fact Sheet FS-009-03. 2 p.: *http://pubs.usgs.gov/fs/fs-009-03/FS-009-03-508.pdf*, accessed July 2009.

Milici, R.C., and Swezey, C.S., 2006, Assessment of Appalachian basin oil and gas resources: Devonian shale—Middle and Upper Paleozoic Total Petroleum System: U.S. Geological Survey Open-File Report 2006–1237: *http://pubs.usgs.gov/of/2006/1237/*, accessed July 2009.

Miller, P.R., and Murphy, T.M., 1981, Devonian shale core characterization data summary: Appalachian basin, June 1981, p. 104.

Montgomery, S.L., Jarvie, D.M., Bowker, K.A., and Pollastro, R.M., 2005, Mississippian Barnett Shale, Fort Worth basin, north-central Texas: Gas-shale play with multi-million cubic foot potential: American Association Petroleum Geologists Bulletin, v. 89, p. 155–175.

Naik, G.C., 2007, Tight gas reservoirs—an unconventional natural energy source for the future: *http://www.sublette-se.org/files/tight_gas.pdf*, accessed November 2009.

Nuhfer, E.B., Vinopal, R.J., and Klanderman, D.S., 1979, X-radiograph atlas of lithotypes and other structures in the Devonian shale sequence of West Virginia and Virginia: U.S. Department of Energy METC/CR-79/27, 45 p.

Nyahay, R., Leone, J., Smith, L., Martin, J., and Jarvie, D., 2007, Update on the regional assessment of gas potential in the Devonian Marcellus and Ordovician Utica Shales in New York: abstract and presentation Association Petroleum Geologists Eastern Section Meeting, Lexington, KY Search and Discovery Article #10136(2007): *http://www.searchanddiscovery.net/documents/2007/07101nyahay/index.htm?q=%2Btext%3Anyahay*, accessed July 2009.

Overbey, W.K., and Carden, R.S., 1991, Report of drilling operations CNGD well 3997 Lee District Calhoun County West Virginia, January 15, 1991, 111 p.

Overbey, W.K., Carden, R.S., Locke, C.D., and Salamy, S.P. 1982, Final report drilling, completion, stimulation and testing of Hardy HW#1 Well Putnam County, West Virginia, March 24, 1992, 102 p.

Papazis, P.K., 2005, Petrographic characterization of the Barnett Shale, Fort Worth basin, Texas: Master's thesis, University of Texas at Austin, 142 p.

Parshall, J., 2008, Barnett shale showcases tight-gas development: Journal Petroleum Technology, September 2008, p 48–55.

Patchen, D.G., 1977, Subsurface stratigraphy in the Devonian shale in West Virginia: U.S. Energy Research and Development Administration, MERC/CR-77-5, March 1977, 39 p.

Peng, S.S., and Okubo, S., 1978, Prediction of *in-situ* stresses from directional properties of rock cores for field development of Devonian shales, final report: DOE/MC/08705-T1, July 1978, 82 p.

Pennsylvania Department of Conservation and Natural Resources, no date. Net feet of organic-rich shale in the Middle Devonian Marcellus Formation in Pennsylvania: *http://www.dcnr.state.pa.us/topogeo/oilandgas/images/Marcellus_Isolith.pdf*, accessed November 2009.

PennStateLive, 2008, Unconventional natural gas reservoir could boost U.S. supply: News release 07 January 2008: *http://live.psu.edu/story/28116*, accessed July 2009.

Perkins, R.B., Piper, D.Z., and Mason, C.E., 2008, Trace-element budgets in the Ohio/Sunbury shales of Kentucky: Constraints on ocean circulation and primary productivity in the Devonian–Mississippian Appalachian Basin: Palaeogeography, Palaeoclimatology, Palaeoecology, v. 265, p. 14–29.

Peters, K.E., and Cassa, M.R., 1994. Applied source-rock geochemistry, *in* Magoon, L.B., and Dow, W.G., eds., The petroleum system—from source rock to trap: American Association Petroleum Geologists Memoir 60, p. 93–120.

Petroleum Technology Transfer Council, 2009, Pennsylvania puts high value on Marcellus Development: PTTC Network News, v. 15, No. 3 (August), p. 10.

Petsch, S.T., Berner, R.A., and Eglinton, T.I., 2000, A field study of the chemical weathering of ancient organic matter: Organic Geochemistry, v. 31, p. 475–487.

Petzet, A., 2009, Seneca third largest Marcellus shale player: Oil and Gas Journal, January 2009, *alanp@ogonline.com*.

Pietrowski, R.G., and Harper, J.A., 1979, Black shale and sandstone facies of the Devonian "Catskill" clastic wedge in the subsurface of western Pennsylvania: U.S. Department of Energy, EGSP Series No. 13, 40 p.

Pollastro, R.M., 2007, Total petroleum system assessment of undiscovered resources in the giant Barnett Shale continuous (unconventional) gas accumulation, Fort Worth Basin, Texas: American Association Petroleum Geologists Bulletin, v. 91, p. 551–578.

Pollastro, R.M., Hill, R.J., Jarvie, D.M., and Henry, M.E., 2003, Assessing undiscovered resources of the Barnett-Paleozoic total petroleum system, Bend Arch-Fort Worth basin province, Texas: *http://www.searchanddiscovery.net/documents/pollastro/images/article.pdf*, assessed June 2009.

Potter, P.E., Maynard, J., and Pryor, W.A., 1980, Special geological, geochemical, and petrological studies of the Devonian shales in the Appalachian basin: U.S. Department of Energy Unconventional Gas Resource Programs 1976–1995, 86 p.

Powell, G., 2008, The Barnett Shale in the Fort Worth basin—a growing giant: Powell Barnett Shale Newsletter, issue of February 25, 2008: *http://www.barnettshalenews.com*, accessed June 2009.

Quinby-Hunt, M.S., and Wilde, P., 1996, Chemical depositional environments of calcic marine black shales: Economic Geology, v. 91, p. 4–13.

Quinlan, G.C., and Beaumont, C., 1984, Appalachian thrusting, lithospheric flexure, and the Paleozoic stratigraphy of the eastern interior of North America: Canadian Journal Earth Sciences, v. 31, p. 973–996.

Repetski, J.E., Ryder, R.T., Avary, K.L., and Trippi, M.H., 2005, Thermal maturity patterns (CAI and $\%R_o$) in the Ordovician and Devonian rocks of the Appalachian basin in West Virginia: U.S. Geological Survey Open-File Report 2005–1078, 72 p.

Rimmer, S.M., Thompson, J.A., Goodnight, S.A., and Robl, T.L., 2004, Multiple controls on the preservation of organic matter in Devonian–Mississippian marine black shales: geochemical and petrographic evidence: Palaeogeography, Palaeoclimatology, Palaeoecology, v. 215, p. 125–154.

Roen, J.B., 1984, Geology of the Devonian black shales of the Appalachian basin: Organic Geochemistry, v. 5, p. 241–254: *http://www.eesi.psu.edu/news_events/EarthTalks/2009Spring/materials2009spr/Roen84BlkShDevorggeoch.pdf*, accessed July 2009.

Roen, J.B., 1993, Introductory review—Devonian and Mississippian black shale, eastern North America, *in* Roen, J.B., and Kepferle, R.C., eds, Petroleum geology of the Devonian and Mississippian black shale of eastern North America: U.S. Geological Survey Bulletin 1909, p. A1–A8.

Roen, J.B., and Kepferle, R.C., 1993, Petroleum geology of the Devonian and Mississippian black shale of eastern North America: U.S. Geological Survey Bulletin 1909, 434 p.

Ross, C.A., and Ross, J.R.P., 1987, Late Paleozoic sea levels and depositional sequences, *in* Ross, C.A., and Haman, D., eds., Timing and deposition of eustatic sequences: constraints on seismic stratigraphy: Cushman Foundation for Foraminiferal Research Special Publication 24, p. 137–149.

Schettler, P.D., and Parmely, C.R., 1990, The measurement of gas desorption isotherms for Devonian shale: Gas Shales Technology Review, v. 7, no. 1, p. 4–9.

Schlumberger, 2007, Fracture Anisotropy modeling: *http://www.slb.com/media/services/consulting/dcs/fracture_anisotropy_modeling_ps.pdf*, accessed June 2009.

Schmoker, J.W., 1977, A borehole gravity survey to determine density variations in the Devonian shale sequence of Lincoln County, West Virginia: MERC/CR-77/7, May 1977, 19 p.

Schott, G.L., Overbey, W.K., Hunt, A.E., and Komar, C.A., 1977, Proceedings of first eastern gas shales symposium: MERC/SP-77/5, October 17–19, 1977, 783 p.

Schwietering, J.F., 1978, Preliminary model of Catskill delta in West Virginia, *in* Schott, G.L., Overbey, W.K., Hunt, A.E., and Komar, C.A., eds., Proceedings First Eastern Gas Shale Symposium: U.S. Department of Energy Morgantown Energy Research Center, Report MERC/SP-77/5, p. 195–205.

Seskus, A.P., 1981, The relationship between photolineaments and Devonian shale gas well productivity; with application to testing of Dupont EL-836 explosive: DOE/MC/08216-140, April 1981, 39 p.

Shumaker, R.C., 1996, Structural history of the Appalachian basin, *in* Roen, J.B., and Walker, B.J., eds., The atlas of major Appalachian gas plays: West Virginia Geological and Economic Survey Publication V-25, p. 8–21.

Shumaker, R.C., and Overbey, W.K., 1976, Devonian Shale Production and Potential: Proceedings of the Seventh Appalachian Petroleum Geology Symposium held at Morgantown, W.Va., March 1–4, 1976, MERC/SP-76/2, 270 p.

Shumaker, R.C., Rauch, H., Williams, R., Wheeler, R., Bebee, B., Berger, P., Dixon, J.M., Evans, M., Jones, D., Kirk, K., Lee, K., Long, B., Negus-de Wys, J., Nuckols, E.B., and Wilson, T., 1982, An analysis of the parameters of structural geology that affect gas production from the Devonian shale: DOE/MC/16360-1236 (DE82020096), March 1982, p. 125.

Shumaker, R.C., and Wilson, T.H., 1996, Basement structure of Appalachian foreland in West Virginia: its style and effects on sedimentation, *in* van der Pluijm, B.A., and Catacosinos, P.A., eds., Basement and basins of eastern North America: Geological Society America Special Paper 308, p. 139–156.

Slatt, R., Singh, P., Borges, G., Perez, R., Portas, R., Vellejo, J., Ammerman, M., Coffey, W., and Eslinger, E., 2009, Reservoir characterization of unconventional gas shales: example from the Barnett Shale, Texas, U.S.A.: Search and Discovery Article #30075, *http://www.searchanddiscovery.net/documents/2009/30075slatt/ndx_slatt.pdf*, accessed June 2009.

Soeder, D.J., 1988, Porosity and permeability of eastern Devonian gas shale: SPE Formation Evaluation, March 1988, p. 116–124.

Soeder, D.J., and Kappel, W.M., 2009, Water resources and natural gas production from the Marcellus Shale: U.S. Geological Survey Fact Sheet 2009–3032, 6 p.

Speight, J.G., 2006, The chemistry and technology of petroleum: CRC Press, 945 p.

Steward, D.B., 2007, The Barnett Shale play: phoenix of the Fort Worth basin, a history: Fort Worth Geological Society and North Texas Geological Society, 202 p.

Streib, D.L., 1980, Eastern gas shales project outgassing analysis—special report: METC/CR-80/2, February 1980, 102 p.

Streib, D.L., 1981, Distribution of gas, organic carbon and vitrinite reflectance in the eastern Devonian gas shales and their relationship to the geologic framework: DOE/MC/08216-1276, February 1981, 273 p.

Sumi, L., 2008, Shale Gas: Focus on the Marcellus Shale, for the Oil and Gas Accountability Project/ Earthworks: *http://www.earthworksaction.org/marcellusshale08.cfm*, accessed July 2009.

Tetra Tech, Inc., 1979, Geologic screening report for evaluation of the eastern gas shale in Pennsylvania: DOE contract DE-AC21-79MC10389.

Thompson, D.M. 1982, Atoka Group, Northern Fort Worth basin, Texas: terrigenous depositional systems, diagenesis, and reservoir distribution and quality: Texas Bureau of Economic Geology, Report of Investigations 125, 62 p.

Van Tyne, A.M., 1996, Play Dol: Middle Devonian Onondaga reef play, *in* Roen, J.B., and Walker, B.J., eds., The atlas of major Appalachian gas plays: West Virginia Geological and Economic Survey Publication V-25, p. 100–102.

Van Tyne, A.M., and Peterson, J.C., 1978, Thickness, extent of and gas occurrences in Upper and Middle Devonian black shales of New York, *in* Proceedings of Second Eastern Gas Shales Symposium, U.S. Department of Energy, Morgantown Energy Technology Center, METC/SP-76/6, v. 1, Morgantown, West Virginia, p. 99–128.

Ver Straeten, C.A., 2007, Basinwide stratigraphic synthesis and sequence stratigraphy, Upper Pragian, Emsian, and Eifelin stages (Lower to Middle Devonian), Appalachian basin, *in* Becker, R.T., and Kirchgasser, W.T., eds., Devonian events and correlations: Geological Society America Special Publication 278, p. 39–82.

Walper, J.L., 1982, Plate tectonic evolution of the Fort Worth basin, *in* Martin, C.A., ed., Petroleum geology of the Fort Worth basin and Bend Arch area: Dallas Geological Society, p 237–251.

Ward, J., 2007, Rock properties of the Marcellus Shale—a regional gas resource in southern New York, Pennsylvania, and West Virginia: *http://www.papgrocks.org/Sept%2007%20PAPG%20%20Flyer.pdf*, accessed July 2009.

Warshauer, S.M., no date, Report on phase III of the multivariate statistical characterization of geochemical data generated by the EGSP for cores 20403, 11940, 12041, GG5 and 7239: U.S. Department of Energy EGSP Open File No. 124, p. 38.

Wells, R.B., and Gognat, T.A., 2009, The Marcellus marches out, *in* Marcellus Playbook: Hart Energy Publishing, p. 5–12.

Werne, J.P., Sageman, B.B., Lyons, T.W., and Hollander, D.J., 2002, An integrated assessment of a "type euxinic" deposit: evidence for multiple controls on black shale deposition in the middle Devonian Oatka Creek Formation: American Journal Science, v. 302, p. 110–143.

West Virginia Geological and Economic Survey, 1979, Report of petrologic characterization of Lincoln 1637 (Columbia Gas Transmission Co. Well #20403): U.S. Department of Energy EGSP Open File No. 138, 203 p.

West Virginia Geological and Economic Survey, 1980a, Petrologic characterization of Mason 146, (Reel Energy D&K #3 Well), Mason Co., W.Va., March 1980, p. 178.

West Virginia Geological and Economic Survey, 1980b, Petrology of the Upper Devonian clastic sequence in Lincoln and Jackson Counties, West Virginia and Wise County, Virginia: UGR File #159, June 1980, 80 p.

West Virginia Geological Survey, 1997, Enhancement of the Appalachian Basin Devonian Shale resource base in the GRI hydrocarbon model: GRI contract no. 5095-890-3478, 57 p.

Wickstrom, L., and Carter, K., 2008, An update on the Marcellus Shale play—a primer: Presentation, Fall Technical Meeting, Ohio Oil Gas Association and Ohio Society Petroleum Engineers, p. 35.

Wrightstone, G., 2008, Marcellus Shale geologic controls on production: Presentation, American Association Petroleum Geologists Eastern Section meeting, Pittsburgh, PA, 49 p.

Zielinski, R.E., 1977, Physical and chemical characterization of Devonian gas shale: Mound Laboratories, MLM-M-ML-79-43-0004, 325 p.

Zielinski, R.E., and McIver, R.D., 1981, Resource and exploration assessment of the oil and gas potential in the Devonian gas shales in the Appalachian Basin: DOE/DP-0053-1125; MLM-MU-86-61-0002, 397 p.

Zielinski, R.E., and McIver, R.D., 1982, Resource and exploration assessment of the oil and gas potential in the Devonian gas shales of the Appalachian Basin: MLM-MU-82-61-0002, DOE/DP/0053-1125, 1982, 326 p.

Zielinski, R.E., and Nance, S.W., 1979, Physical and chemical characterization of Devonian gas shale, quarterly status report (January 1–March 31, 1970): MLM-ML-79-43-0004, MLM-EGSP-TPR-Q-009, 166 p.

1450 Queen Avenue SW
Albany, OR 97321-2198
541-967-5892

2175 University Avenue South
Suite 201
Fairbanks, AK 99709
907-452-2559

3610 Collins Ferry Road
P.O. Box 880
Morgantown, WV 26507-0880
304-285-4764

626 Cochrans Mill Road
P.O. Box 10940
Pittsburgh, PA 15236-0940
412-386-4687

13131 Dairy Ashford
Suite 225
Sugar Land, TX 77478
281-494-2516

WEBSITE: **www.netl.doe.gov**

CUSTOMER SERVICE: **1-800-553-7681**

April 2011